

**An Implantable Hydrogel for the Delivery of Cisplatin and
the *Ex Vivo* Neurotoxic, Neuromyopathic and Cardiotoxic
Activity of Platinum-Based Anticancer Drugs and
Macrocyclic Drug Delivery Systems**



By Rabbab Hadi Oun

2015

A thesis presented in fulfilment of the requirements for the degree of
Doctor of Philosophy

Copyright Statement

This thesis is the result of the author's original research. It has been composed by the author and has not been previously submitted for examination which has led to the award of a degree.

The copyright of this thesis belongs to the author under the terms of the United Kingdom Copyright Act as qualified by University of Strathclyde Regulation 3.50. Due acknowledgement must always be made of the use of any material contained in, or derived from, this thesis.

وَقُلْ رَبِّ زِدْنِي عِلْمًا

“And say: My Lord, increase me in knowledge”

Holy Quran 20:114

Contents

Acknowledgments.....	X
Publications.....	XI
Journal Articles and Book Chapters.....	XI
Journal Front Cover Images.....	XIII
Conference presentations.....	XIV
Achievements/Awards.....	XV
Animal License number.....	XVI
Abstract.....	XVII
List of Abbreviations.....	XX
List of Figures.....	XXIV
List of Tables.....	XXXIII
1 General Introduction.....	1
1.1 Cancer Statistics.....	2
1.1.1 What is Cancer?.....	2
1.1.2 The Development of Cancer: Oncogenes and Tumour Suppressor genes.....	3
1.1.2.1 Oncogenes in Cancer.....	4
1.1.2.2 Tumour Suppressor genes in Cancer.....	5
1.1.2.2.1 Cancer and the Two Hit Hypothesis.....	6
1.1.3 The Hallmarks of Cancer.....	8
1.1.3.1 Evasion of Apoptosis.....	9
1.1.3.2 Limitless Replicative Potential.....	9
1.1.3.3. Metastasis and Sustained Angiogenesis.....	10
1.1.4 Carcinogens.....	11
1.1.4.1 Physical Carcinogens: Ultraviolet Radiation.....	11
1.1.4.2 Chemical Carcinogens: Cigarette Smoke.....	12

1.1.4.3 Biological Carcinogens: Viruses and Infections	14
1.1.5 Cancer Diagnosis	16
1.1.6 Cancer Therapy	17
1.1.6.1 Surgery in Cancer Treatment	17
1.1.6.2 Radiation Therapy in Cancer Treatment	18
1.1.6.2.1 External Beam Radiation Therapy	18
1.1.6.2.2 Internal Radiation Therapy	19
1.1.6.2.3 Systemic Radiation Therapy	19
1.1.6.3 Hormonal Therapy in Cancer Treatment	19
1.1.6.4 Chemotherapy	20
1.1.7 Platinum Based Drugs in Cancer Therapy	20
1.1.7.1 Cisplatin in Cancer Therapy.....	21
1.1.7.1.1 Discovery of Cisplatin	22
1.1.7.1.2 Physical and Chemical Properties of Cisplatin	23
1.1.7.1.3 Administration, Formulation and Pharmacokinetics.....	23
1.1.7.1.4 Mechanism of Cisplatin Cell Entry.....	24
1.1.7.1.5 Mechanism of Action of Cisplatin	25
1.1.7.1.6 Non-DNA Targets of Cisplatin	27
1.1.7.1.7 Tumour Resistance to Cisplatin	27
1.1.7.1.7.1 Acquired Cisplatin Resistance	28
1.1.8 Circumvention of Platinum Resistance: Second and Third Generation Platinum-based Drugs	29
1.1.8.1 Carboplatin in Cancer Therapy	30
1.1.8.2 Oxaliplatin in Cancer Therapy	31
1.1.9 Drug Delivery in Cancer Therapy.....	32
1.1.9.1 Physio-Pathological Characteristics of Tumour Tissue	32

1.1.9.2 The Enhanced Permeability and Retention Effect	33
1.1.10.1 Liposomes	35
1.1.10.1.2 Liposomes for the Delivery of Cisplatin.....	36
1.1.10.2 Hydrogels	38
1.1.10.2.1 Hydrogels for the Delivery of Cisplatin.....	40
1.1.10.3 Macrocyclic Cucurbit[<i>n</i>]urils.....	41
1.1.10.3.1 Cucurbit[7]uril as a Cisplatin Drug Delivery System.....	44
1.1.10.3.1.1 Binding of Cisplatin@CB[7]	45
1.1.11 Aim of The Thesis.....	46
2.0 Implantable Hydrogels	50
2.1 Hydrogel Drug Loading	51
2.1.1 Drug Loading by Permeation, Entrapment and Covalent Interactions	51
2.1.2 Importance of Hydrogel Polymer Composition on the Rate of Drug Release..	52
2.1.3 Focus of This Study: An Implantable Hydrogel for the Delivery of Cisplatin.	53
2.1.4 The Use of Nude Mice in Cancer Research	54
2.1.4.1 Human Tumour Xenografts as Predictive Models for Anticancer Drug Activity.....	55
2.1.5 Aims of This Chapter	56
2.2 Materials and Methods.....	57
2.2.1.1 Materials used in the preparation of hydrogels	57
2.2.1.2 Materials used in the <i>In Vitro</i> Hydrogel Toxicity Studies	57
2.2.1.3 Materials used in the <i>In Vivo</i> Hydrogel Anti-tumour Efficacy Study.....	57
2.2.2 Methods.....	58
2.2.2.1 Synthesis of cisplatin@CB[7].....	58
2.2.2.2 Hydrogel Synthesis	58
2.2.2.3 <i>In Vitro</i> Hydrogel Swelling.....	59

2.2.2.4 Hydrogel Surface Imaging	59
2.2.2.5 <i>In Vitro</i> Drug Release.....	59
2.2.2.6 Effect of Hydrogel on <i>In Vitro</i> Cytotoxicity	60
2.2.2.7 <i>In Vivo</i> Effectiveness of Hydrogels.....	60
2.2.2.8 Statistics	61
2.3 Results	62
2.3.1 Cisplatin@CB[7] Binding.....	62
2.3.2 Hydrogel Synthesis	63
2.3.3 Hydrogel Swelling	64
2.3.4 Hydrogel Drug Release	65
2.3.5 Hydrogel Surface Features.....	66
2.3.6 <i>In Vitro</i> Efficacy of Cisplatin and Cisplatin@CB[7] Loaded Hydrogels	67
2.3.7 <i>In Vivo</i> Anticancer Efficacy of Cisplatin and Cisplatin@CB[7] Loaded Hydrogels	70
2.4 Discussion	74
3. Toxicology	79
3.1 General Introduction	79
3.1.1.1 <i>In Vitro</i> Assays in Toxicological Studies.....	79
3.1.1.2 <i>In Vivo</i> Toxicological Studies	80
3.1.1.3 <i>Ex Vivo</i> Assays in Toxicological Studies.....	80
3.1.1.4 Organ Baths in <i>Ex Vivo</i> Toxicity Studies.....	81
3.1.2 Neurotoxicity.....	82
3.1.2.1 The Nervous System	82
3.1.2.3. Action Potential.....	86
3.1.2.4 The Sciatic Nerve	89
3.1.2.5 Chemotherapy Induced Neurotoxicity	90

3.1.2.5.1 Etiology and Pathophysiology of Platinum Based Drugs Induced Neurotoxicity.....	92
3.1.2.5.2 Development of Neuroprotective Agents.....	93
3.1.2.5.2.1 Calcium and Magnesium Infusions.....	94
3.1.2.5.2.2 Vitamin E	94
3.1.2.5.2.3 Anti-epileptic Agents	95
3.1.2.5.2.4 Insulin Like Growth Factor	95
3.1.3 Neuromyopathy (Neuromuscular Toxicity).....	95
3.1.3.1 The Neuromuscular Junction	96
3.1.3.2 Neuromyopathy Induced by Chemotherapy	98
3.1.4 Cardiotoxicity.....	99
3.1.4.1 The Heart.....	99
3.1.4.2 Chemotherapy Induced Cardiotoxicity	100
3.1.4.2.1 Cardiotoxicity Induced by Platinum Based Drugs.....	101
3.1.5 Aims of This Chapter:.....	103
3.2 Materials and Methods.....	105
3.2.1 Materials.....	105
3.2.2 Methods.....	105
3.2.2.1 Electrophysiological Recordings from Mouse Sciatic Nerve	105
3.2.2.2 Isolated Chick Biventer Cervicis Nerve Muscle Preparation	107
3.2.2.3 Contractile Recordings from Rat Atria	109
3.2.2.4 Statistics	111
3.3 Results.....	112
3.3.1 Neurotoxicity.....	112
3.3.1.1 Viability of the <i>Ex Vivo</i> Sciatic Nerve Preparation.....	112
3.3.1.2 Neurotoxic Activity of Platinum-Based Drugs	113

3.3.1.3 Neurotoxic Activity of Macrocycles	116
3.3.1.4 Effect of CB[7] on the Neurotoxicity of Cisplatin.....	119
3.3.2 Neuromyopathy.....	120
3.3.2.1. Viability of the <i>Ex Vivo</i> Chick Biventer Cervicis Nerve Muscle Preparation	121
3.3.2.2 Neuromyopathic Activity of Platinum Based Drugs	122
3.3.2.3 Neuromyopathic Activity of Drug Delivery Macrocycles.....	126
3.3.2.4 Effect of CB[7] on the Neuromyopathy of Cisplatin.....	129
3.3.3. Cardiotoxicity.....	131
3.3.3.1 Viability of the <i>Ex Vivo</i> Atria Preparation	131
3.3.3.2 Cardiotoxic Activity of Platinum-Based Drugs	132
3.3.3.3 Cardiotoxic Activity of Macrocyclic Drug Delivery Systems.....	137
3.3.3.4 Effect of CB[7] on the Cardiotoxicity of Cisplatin.....	141
3.4. Discussion	143
4. Conclusion	151
4.1 Future Studies	153
References	156

Acknowledgments

AlhamduAllah; thanks to God Almighty for providing me with the opportunity to fulfill a career in the world of science.

Throughout my entire PhD I have had immense help and motivation from a number of people and I would like to take this opportunity to express my deepest gratitude.

I would like to thank Dr Nial Wheate for his ongoing support and motivation, not just as a supervisor, but also as a friend. His help, patience and direction during my PhD have been invaluable.

I would also like to thank Dr Edward Rowan for his tremendous help and for introducing a new era of science to me.

Many thanks to Dr Jane Plumb for allowing me to take my first PhD steps within her lab at the Beatson Institute of Cancer and for her invaluable guidance and support.

I would like to extend my deepest gratitude to my family and especially my parents for their encouragement and support, and for the many fundamental years they spent home schooling me.

Thanks to all of the PhD students and staff at the University of Strathclyde and the Beatson Institute of Cancer that put a smile on my face.

Lastly but not least, thanks to Professor Lyle Isaacs for providing me with valuable material and for his collaboration in parts of this study.

Publications

Work from this thesis has been published in the following forms:

Journal Articles and Book Chapters

- **Rabbab Oun**, Rafael S. Floriano, Lyle Isaacs, Edward G. Rowan and Nial J. Wheate, *The ex-vivo neurotoxic, myotoxic and cardiotoxic activity of cucurbituril-based macrocyclic drug delivery systems*. *Toxicol.Res.*, 2014, DOI: 10.1039/c4tx00082j.
- **Rabbab Oun**, Jane A. Plumb and Nial J. Wheate, *A cisplatin slow-release drug delivery system based on a formulation of the macrocycle cucurbit[7]uril, gelatin and polyvinyl alcohol in hydrogels*. *Journal of Inorganic Biochemistry*, 2014, 134, 100-105. DOI: 10.1016/j.jinorgbio.2014.02.004
- **Rabbab Oun** and Nial J. Wheate, *Platinum anticancer drugs* in *Encyclopedia of Metalloproteins*, Robert H. Kretsinger, Vladimir N. Uversky and Eugene A. Permyakov (Eds), Springer, 2012, ISBN 978-1-4614-1532-9.
- Jane A. Plumb, Balaji Venugopal, **Rabbab Oun**, Natividad Gomez-Roman, Yoshiyuki Kawazoe, Natarajan Sathiyamoorthy Venkataramanan and Nial J. Wheate, *Cucurbit[7]uril encapsulated cisplatin overcomes cisplatin resistance via a pharmacokinetic effect*, *Metallomics*, 2012, 4, 561-567. DOI:10.1039/C2MT20054F.
- Shonagh Walker, **Rabbab Oun**, Fiona J. McInnes and Nial J. Wheate, *The potential of cucurbit[n]urils in drug delivery*, *Israel Journal of Chemistry*, 2011, 51, 616-624. DOI: 10.1002/ijch.201100033. (Invited article in the special themed issue coinciding with the 2nd International Conference on Cucurbiturils).

- Nial J. Wheate, Shonagh Walker, Gemma E. Craig and **Rabbab Oun**, *The status of platinum anticancer drugs in the clinic and in clinical trials*, [Dalton Transactions](#), 2010, 39, 8113-8127. DOI: 10.1039/c0dt00292e.

Journal Front Cover Images

- **Rabbab Oun**, Rafael S. Floriano, Lyle Isaacs, Edward G. Rowan and Nial J. Wheate, *The ex-vivo neurotoxic, myotoxic and cardiotoxic activity of cucurbituril-based macrocyclic drug delivery systems*. *Toxicol.Res.*, 2014, DOI: 10.1039/c4tx00082j.
- Nial J. Wheate, Shonagh Walker, Gemma E. Craig and **Rabbab Oun**, *The status of platinum anticancer drugs in the clinic and in clinical trials*, [Dalton Transactions](#), 2010, 39, 8113-8127. DOI: 10.1039/c0dt00292e.



Conference presentations

- **Rabbab Oun**, Jane Plumb, Edward Rowan and Nial Wheate. *Encapsulation of cisplatin by cucurbit[7]uril decreases the neurotoxic and cardiotoxic side effects of cisplatin*. Abstract for poster presentation at 49th congress of the European Societies of Toxicology Eurotox Conference. Interlaken, Switzerland, September 2013.
- **Rabbab Oun**, Jane Plumb and Nial Wheate. *An implantable based hydrogel for the treatment of cancer*. Abstract for poster presentation at the XI International Symposium on Platinum Coordination Compounds in Cancer Chemotherapy stem cells, DNA repair mechanisms and DNA damaging agents conference. Verona, Italy, October 2012.
- **Rabbab Oun**. *An implantable platinum based hydrogel for the treatment of cancer*. Oral presentation at the FEBS Advanced Lecture Course on Translational Cancer Research. Algarve, Portugal, October 2011.
- **Rabbab Oun**, Jane Plumb, Natividad Gomez-Roman, Balaji Venugopal and Nial Wheate. *Orally active cisplatin that overcomes its own acquired resistance*. Abstract for poster presentation at the 10th European Biological Inorganic Chemistry Conference. Thessaloniki, Greece, June 2010.

Achievements/Awards

- Received 2nd best poster award at the XI ISPCC conference (XI International Symposium on Platinum Coordination Compounds in Cancer Chemotherapy Stem cells, DNA repair mechanisms, DNA-damaging agents. Verona, Italy, 2012.
- My scientific image entry (below) was accepted into Strathclyde's Images of Research competition 2012 and was showcased at venues across Glasgow to engage with the public.



Drug loaded hydrogels in the treatment of cancer

These hydrogel implants are currently under investigation as drug delivery systems, they are made from natural polymers and can be formulated into a variety of sizes and shapes. Cancer patients that undergo chemotherapy endure long hours of intravenous hydration before drugs such as the anticancer drug cisplatin is administered. Drug administration is a long procedure and can take between 2-8 hours over a number of days weekly. This method of administration results in 90% of cisplatin not reaching its target site and this causes toxic side effects. A hydrogel implant can act as a slow drug delivery system and can be tuned to release drugs over hours, days or weeks. Therefore patients will no longer need to spend long hours at the hospital. Also a slower drug release mechanism may ensure that more drug reaches the tumour. Other advantages of hydrogels include good biocompatibility and degradation of the gel into non-toxic by products. (<http://www.flipsnack.com/586EAB97C6F/fztm6njt.html>).

- Together with four other colleagues, I helped set up the “Women sharing a chemical moment in time” Conference. This was a networking session with presentations to celebrate the life and achievements of Marie Curie and to promote contemporary women in science. Glasgow, Scotland, 2011.

Animal License number: SAB/SCT/W10/055.

Abstract

Cisplatin is currently a leading anticancer drug used in the treatment of various cancers. Its clinical use, however, is limited by its poor bioavailability, its undesirable toxic side effects profile and by the ability of certain tumours to develop cisplatin resistance. A method that may overcome these problems is the reversible encapsulation of cisplatin within the cavity of a macro cyclic container such as cucurbit[7]uril; a macrocycle formed by the acid condensation of glycoluril and formaldehyde, which has been shown to overcome acquired resistance in an *in vivo* human tumour xenograft model via a pharmacokinetic effect.

In the first section of this thesis an implantable hydrogel based system was developed for the delivery of cisplatin and cisplatin@CB[7]. First, cisplatin was encapsulated within cucurbit[7]uril (CB[7]) to form the host-guest complex: cisplatin@CB[7]. This was then incorporated into gelatin and 0-4% w/v polyvinyl alcohol (PVA)-based hydrogels as slow release drug delivery systems. *In vitro* studies of the hydrogels demonstrated predictable yet not significant swelling and disintegration dependent on their PVA concentration. The hydrogel with the highest PVA content was slower to swell and release drug compared with hydrogels containing lower concentrations of PVA. The effect of the hydrogel's PVA concentration on *in vitro* cytotoxicity was examined using A2780/CP70 ovarian cancer cells with results showing a significant reduction in cytotoxicity as the hydrogel's PVA concentration increased which indicated that a slow release system was achieved. Over the 24 hours of drug exposure time used, hydrogels containing 4% PVA loaded with 1mM of cisplatin@CB[7] showed a $19 \pm 0.01\%$ ($p = 0.004$) decrease in viable cells compared to the control,

whereas hydrogels containing 0% and 2% PVA induced an $81.2 \pm 0.003\%$ ($p = 0.0005$) and $42 \pm 0.02\%$ ($p = 0.0002$) inhibition of cell growth, respectively. Finally, the *in vivo* efficacy of a 2% PVA hydrogel implanted under the skin of nude mice bearing A2780/CP70 xenografts showed that low dose hydrogels containing cisplatin@CB[7] (30 μg equivalent of drug) was just as effective as an intraperitoneal high dose administration of free cisplatin (150 μg) at inhibiting tumour growth. Overall, the results suggest an ability of implantable hydrogels to treat cancers with much lower doses of drug, thereby reducing the severity of the toxic side effects induced.

In the second section of this thesis, cisplatin, CB[7] and cisplatin@CB[7] were tested and compared for their *ex vivo* neurotoxic, neuromyopathic and cardiotoxic activity amongst other platinum-based drugs (K_2PtCl_4 , 56MESS and PHENEN) and macrocyclic drug delivery systems (CB[6], β -cyclodextrin, Motor2 and pentamer) using electrophysiological methods.

The neurotoxic activity of the drugs was studied using mouse desheathed sciatic nerve preparations. Both cisplatin and CB[7] administered at a concentration of 300 μM decreased the amplitude of the nerve compound action potential (nCAP) by $13 \pm 4.7\%$ ($p = 0.3$) and $4 \pm 0.2\%$ ($p = 0.8$), respectively over an 80 minute period. Neuromyopathic activity was studied using the chick biventer cervicis nerve muscle preparation. Results showed that incubation of the nerve-muscle tissue with 300 μM of cisplatin caused statistically significant muscle paralysis to occur by decreasing the electrically stimulated muscle twitch response by $96 \pm 4\%$ ($p = 0.001$), through

interference in the presynaptic neuron. Whereas, CB[7] caused a statistically significant muscle paralysis by decreasing the electrically stimulated muscle twitch response by $84 \pm 9\%$ ($p = 0.001$) through interference with the postsynaptic muscle membrane.

Cardiotoxic activity was examined using the rat right and left heart atria. Results show that incubation of the atria tissue with $300 \mu\text{M}$ of cisplatin reduced the contraction rate of the right atria by $68.8 \pm 1\%$ ($p = 0.001$) and in the left atria by $1 \pm 1\%$ ($p = 0.4$) by the end of the two hour period study. When incubated with $300 \mu\text{M}$ of CB[7], the contraction rate in the right atria increased by $31 \pm 13.6\%$ ($p = 0.3$) and decreased in the left atria by $10 \pm 3.5\%$ ($p = 0.3$)

Finally, the effect of the encapsulation of cisplatin by CB[7] on its neurotoxic, neuromyopathic and cardiotoxic activity was investigated. Results show that while the encapsulation had no effect on the neurotoxic activity of cisplatin, the encapsulated complex reduced the extent of cisplatin's neuromyopathic activity by reducing the muscle paralysis induced by cisplatin by 60%. When encapsulated by CB[7], the cardiotoxicity of cisplatin on the contraction rate of the right atria was also significantly decreased from 65.8% to 11%. In conclusion, these results suggest that CB[7] could exhibit neuromyopathy and cardio protective properties as it reduced the neuromyopathic and cardiotoxic activity of the encapsulated cisplatin.

List of Abbreviations

The following abbreviations are used in this work:

5-FU	5-Fluorouracil
56MESS	5,6-dimethyl-1,10-phenanthroline)(1 <i>S</i> ,2 <i>S</i> - diaminocyclohexane)platinum(II)] dichloride
A	Adenine
AAS	Atomic Absorption Spectrophotometry
ACh	Acetylcholine
ANOVA	Analysis of Variance
AV node	Atrioventricular node
bFGF	basic Fibroblast Growth Factor
BER	Base Excision Repair
CB[<i>n</i>]	Cucurbit[<i>n</i>]uril
CHF	Congestive Heart Failure
CML	Chronic Myelogenous Leukemia
cMOAT	canalicular Multi-Specific Organic Anion Transporters
CNS	Central Nervous System
CTR1	Copper Transporter Protein 1
DACH	Diaminocyclohexane
DMSO	Dimethylsulfoxide
DNA	Deoxyribonucleic Acid
DPPG	Dipalmitoyl Phosphatidyl Glycerol
ECG	Electrocardiogram

E. Coli	Escherichia Coli
EPR	Enhanced Permeability and Retention
FDA	Food and Drug Administration
FOXN1	Forkhead Box Protein N1
G	Guanine
GAPs	GTPase-activating Proteins
GDP	Guanosine Diphosphate
GEFs	Guanine Nucleotide Exchange Factors
G phase	Gap Phase
GTP	Guanine Triphosphate
HBEGF	Heparin-Binding Epidermal Growth Factor
HMG	High Mobility Group
H. Pylori	Helicobacter Pylori
HPV	Human Papilloma Virus
IARC	International Agency for Research on Cancer
ICP-MS	Inductively Coupled Plasma-Mass Spectrometry
ICP-OES	Inductively Coupled Plasma-Optical Emission Spectrometry
IUPAC	International Union of Pure and Applied Chemistry
KRAS	Kristen-ras
MMR	Mismatch Repair
MRI	Magnetic Resonance Imaging
MRP1	Multi-Drug Resistance Protein 1
MTD	Maximum Tolerated Dose

nAChRs	Nicotinic Acetylcholine Receptors
nCAP	Nerve Compound Action Potential
NCS	Neocarzinostatin
NER	Nucleotide Excision Repair
NDA	New Drug Application
NMR	Nuclear Magnetic Resonance
NSCLC	Non-Small Cell Lung Carcinoma
PBS	Phosphate Buffered Saline
Pegylated	polyethylene glycol coated
PHENEN	[Pt(1,10-phenanthroline)(1,2-diaminoethane)]Cl ₂
PNS	Peripheral Nervous System
pRb	Retinoblastoma Protein
Pt	Platinum
PVA	Polyvinyl Alcohol
Ras	Rat Sarcoma
RNA	Ribonucleic Acid
SA node	SinoAtrial Node
SCLC	Small Cell Lung Carcinoma
SEM	Standard Error Mean
SLC	Solute Carrier Transporters
SMA	Styrene Maleic Acid Polymer
SMANCS	Styrene Maleic Acid Neocarzinostatin
SPC-3	Soy Phosphatidyl Choline
T	Thymine

TGF- α	Transforming Growth Factor Alfa
TTX	Tetrodotoxin
UKCCR	United Kingdom Coordinating Committee on Cancer Research
UV	Ultraviolet
VEGF	Vascular Endothelial Growth Factor
WHO	World Health Organization

List of Figures

Figure 1.1. Normal cell division compared to cancer cell division. Healthy cells divide at a controlled steady rate before they ultimately undergo apoptosis. Cancer cells divide quicker than normal cells and do not undergo apoptosis thus resulting in large numbers of cancer cells that eventually form a tumour. Figure taken from <http://rise.duke.edu/seek/pages/page.html?0205>..... 3

Figure 1.1.1. The recessive nature of tumour suppressor genes. For cancer to occur, both genes of a tumour suppressor gene must be mutated..... 7

Figure 1.2. Image of a magnetic resonance imaging scanner. The MRI machine use radio waves to create pictures of all tissues in the body. Image taken from <http://pancreaticcanceraction.org/pancreatic-cancer/diagnosis/mri-scan/>. 16

Figure 1.3. The chemical structure of cisplatin..... 21

Figure 1.3.1. A scanning electron microphotograph of a) normal *E. Coli* bacteria and b) *E. Coli* grown in medium containing cisplatin. Image taken from <http://chemcases.com/cisplat/cisplat01.htm>..... 22

Figure 1.3.2. Mechanism of cisplatin cell entry and its mechanism of action. Once cisplatin enters cells either by passive diffusion or active transport it is aquated within the cytoplasm. This aquation allows it to attach to DNA causing a structural distortion in the double helix which prevents further DNA transcription and replication. Adapted from <http://pubs.rsc.org/en/content/articlehtml/2014/mt/c4mt00238e>. 25

Figure 1.3.3. A diagram showing the different binding modes of cisplatin with DNA nucleobases including: 1,2-(GG) intra-strand crosslinks, 1,3-(GG) inter-strand crosslinks, 1,2-(AG) intra-strand crosslinks, protein-DNA crosslinks and 1,3 and 1,4-(GG) intrastrand crosslinks. Image taken from <http://pubs.rsc.org/en/content/articlehtml/2010/mt/b911438f>..... 26

Figure 1.4. The chemical structure of carboplatin.	30
Figure 1.5. The chemical structure of oxaliplatin.	31
Figure 1.6. A diagram demonstrating the EPR effect. The endothelial cells that line tumour blood vessels have large gaps between them compared to normal vessels allowing the large molecules to be taken into the tumour.	33
Figure 1.7. A schematic diagram of a drug encapsulated by a liposome. Image taken from http://www.hindawi.com/journals/jdd/2012/581363/fig1/	35
Figure 1.8. An image of a gliadel wafer being implanted in the brain along the wall and floor of the cavity after a malignant glioma has been removed (left panel), as much as upto eight wafers can be placed where the tumour was located (right panel). Image taken from http://www.gliadel.com/about-gliadel/how-gliadel-used/	40
Figure 1.9. Image of an x-ray crystal structures of CB[5], CB[6], CB[7] and CB[8]. The top panel is a bird view image of the CB[n] cavity sizes and the bottom panel is a side view image. Colour codes; carbon (grey), nitrogen (blue), oxygen (red). Taken from http://en.wikipedia.org/wiki/Cucurbituril	43
Figure 1.10. Molecular model image of the preferred binding mode of cisplatin to CB[7]. A) molecular model showing the chloride ligands of cisplatin (green) are pointing into the cavity and b) the four hydrogen bonds (dashed lines) from cisplatin's ammine hydrogen atoms to the CB[7] carbonyl oxygen atoms. [108]	45
Figure 2.3.1. Confirmation of cisplatin binding within CB[7]. ¹ HNMR spectra of a) cisplatin@CB[7] and b) CB[7]. The CB[7] resonance spike at 5.66 ppm and 4.2 ppm is split into two spikes in the addition of cisplatin confirming binding of drug to macrocycle.	62

Figure 2.3.2. An example of a PVA and gelatin based hydrogel. Red dye was used for imaging purposes only (top panel) and the plastic tablet strip used in moulding the hydrogels (bottom panel). 63

Figure 2.3.3. The rate of hydrogel swelling in PBS. Hydrogels of different PVA content; 0% PVA (blue), 2% PVA (red) and 4% PVA (green) where immersed in PBS solution and their weight was monitored every 24 hours over a period of six days. Results are expressed as the means \pm SEM ($n = 3$). Statistical one way Anova with Bonferroni's multiple comparison post-tests was performed. 64

Figure 2.3.4. Rate of drug release from hydrogels with different PVA concentrations .The drug release rates from hydrogels containing different PVA content: 0% (blue), 2% (red) and 4% (green) PVA incubated in PBS over a period of 5 hours. The results are expressed as mean \pm SEM ($n = 3$). Statistical one way Anova with Bonferroni's multiple comparison post-tests was performed..... 65

Figure 2.3.5. Surface features of hydrogels. Optical microscope images of (a) 0% PVA, (b) 2% PVA and (c) 4% PVA demonstrating the differences in surface features between the hydrogels..... 67

Figure 2.3.6. Images of the hydrogel well inserts. Examples of the 24 well plates used to examine the *in vitro* cytotoxicity of the hydrogels showing the inserts with inlet channels containing a hydrogel (left panel) and the outer wells with just media in the first column and with fully submerged hydrogel containing inserts in the second, third and fourth columns of the plate (right panel)..... 68

Figure 2.3.6.1. Image of the crystal violet blue stained cells after treatment with various concentrations of PVA based hydrogels containing either 1 mM cisplatin or 1mM cisplatin@CB[7]..... 68

Figure 2.3.6.2. Rate of cell growth inhibition induced by hydrogels of different PVA concentrations. Graph showing the relative growth inhibition of ovarian A2780/CP70

cells by hydrogels of different PVA content (0%, 2% and 4%) containing either 1mM of cisplatin or 1mM cisplatin@CB[7] compared to untreated cells. Results are expressed as mean \pm SEM ($n = 4$). Statistical two way Anova with Bonferroni's multiple comparison tests was performed..... 69

Figure 2.3.7. The *in vivo* anti-tumour effect of hydrogels containing cisplatin and cisplatin@CB[7]. The graph represents the *in vivo* cytotoxicity of hydrogels against the human ovarian A2780/CP70 cisplatin resistant tumour xenograft, showing: saline control (dark blue, diamond), intraperitoneal free cisplatin 150 μ g (red, square), cisplatin in 2% PVA hydrogel 30 (purple, cross) μ g, cisplatin@CB[7] in 2% PVA hydrogel (light blue, cross). Results are expressed as mean \pm SEM ($n = 6$). Statistical two way Anova with Bonferroni's multiple comparison tests was performed..... 72

Figure 3.1.1. A schematic diagram showing a typical setup of an isolated tissue organ bath experiment. The animal tissue is incubated in a temperature controlled organ bath and attached to a transducer by a silk thread. The stimulator provides a means by which the rate of tissue contraction can be controlled; this is achieved if an electrode is placed in close proximity to the tissue. The analogue to digital converter (A/D converter) converts the physical quantity measured (usually in volts) into a digital number that can be displayed on a computer and used to generate a dose-response curve. Image taken from <http://link.springer.com/article/10.1007%2Fs00592-009-0156-x/fulltext.html>..... 82

Figure 3.1.2. A schematic diagram of a neuron showing the movement of an action potential from the axon hillock towards the axon terminal. Image taken from <http://classconnection.s3.amazonaws.com/1615/flashcards/596052/png/screen-shot-2011-01-19-at-8.27.56-pm.png>. 84

Figure 3.1.3. The flow of an action potential between cells through an electrical synapse compared to a chemical synapse. In an electrical synapse, the presynaptic and postsynaptic cell are connected by gap junctions that facilitate the direct transmission of an action potential between the cells. In a chemical synapse, the action potential is

transmitted from the presynaptic cell to the postsynaptic cell through the release of neurotransmitters from vesicles found in the presynaptic cell. These neurotransmitters bind to specific ion channels found on the membrane of the postsynaptic cell altering its membrane potential. Image taken from http://csls-text.c.u-tokyo.ac.jp/active/11_04.html. 85

Figure 3.1.4. Schematic diagram showing the various phases of an electrophysiological reading of an action potential that occurs as electrical impulses pass down a cell membrane. Image taken from <http://cs.brown.edu/people/tld/note/blog/13/04/19/>. 87

Figure 3.1.5. A schematic diagram showing the flow of a membrane potential as it moves down the length of an axon. Image taken from <http://mikeclaffey.com/psyc170/notes/notes-neurons.html>. 88

Figure 3.1.6. Picture of a mouse sciatic nerve. 89

Figure 3.1.7. Histology slide of the sciatic nerve showing the fascicles of nerve fibers, the connective tissue, and the axon and myelin. Image taken from http://missinglink.ucsf.edu/lm/ids_101_histo_resource/nerves_muscle.html. 90

Figure 3.1.8. A schematic diagram of a motor neuron and the neuromuscular junction where the neuron connects with a muscle fiber. Image taken from <http://classconnection.s3.amazonaws.com/334/flashcards/1645334/jpg/nmj1340211926722.jpg>. 97

Figure 3.1.9. A schematic diagram of a neuromuscular junction showing the flow of an action potential down the axon, the influx of calcium cations into the axonal terminus followed by the release of acetylcholine (ACh) from the presynaptic neuron and its binding to sodium channels located on the postsynaptic muscular membrane which generates an action potential and ultimately causes muscle contraction. Image

taken from http://www.collegepaeds.ac.za/past%20papers/2010-10/FCP1_2010-10.htm. 98

Figure 3.2.1. A schematic diagram of the sciatic nerve bath setup. The sciatic nerve (purple) is laid across three inter-connecting chambers, with each chamber connected to either a stimulator or an amplifier via metal electrodes..... 106

Figure 3.2.2. A schematic diagram showing the biventer cervicis muscle attached to a steel rod via a hoop (tied onto the end of the muscle by silk thread) and an electrode placed around the nerve of the muscle for direct stimulation. Image taken and adapted from <http://www.ncbi.nlm.nih.gov/pmc/articles/PMC1481857/?page=1>..... 108

Figure 3.2.3. A schematic diagram showing the setup of the organ bath used for both heart atria preparations. For tissues that were directly stimulated, an electrode was inserted into the organ bath and placed in close proximity to the tissue (not shown). Image taken and adapted from <http://www.intechopen.com/books/artery-bypass/pharmacology-of-arterial-grafts-for-coronary-artery-bypass-surgery>. 110

Figure 3.3.1.1. The nCAP amplitude of untreated nerves. Graph showing the change in the amplitude of the nCAP of untreated sciatic nerves over a period of two hours. Results are expressed as the means \pm SEM ($n = 3$)..... 112

Figure 3.3.1.2. The change in nCAP amplitude of the sciatic nerve after treatment with platinum-based drugs. Graph showing the changes induced in nCAP after treatment with cisplatin, K_2PtCl_4 , 56MESS and PHENEN after 80 minutes. Results are expressed as the means \pm SEM ($n = 3$). Statistical students paired t-test was performed and significant differences compared to time match control are indicated by * when $p < 0.05$ 115

Figure 3.3.1.3. The change in nCAP amplitude of the sciatic nerve after treatment with macrocycles. Graph showing the changes induced in nCAP after treatment with CB[6], CB[7], Motor2 and β -cyclodextrin after 80 minutes. Results are expressed as

the means \pm SEM ($n = 3$). Statistical students paired t-test was performed and significant differences compared to time match control are indicated by * when $p < 0.05$ 118

Figure 3.3.1.4. The difference in the change of the nCAP amplitude of the sciatic nerve after treatment with 1 mM of (blue) free cisplatin and (red) cisplatin@CB[7]. Results are expressed as the means \pm SEM ($n = 3$). Statistical students paired t-test was performed ($n = 3$) and significant differences are indicated by * when $p < 0.05$ 119

Figure 3.3.2. The percentage change in the response of untreated (control) chick biventer cervicis nerve-muscle to ACh, KCl and to the amplitude of electrically stimulated contraction after two hours incubation. Results are expressed as the means \pm SEM ($n = 3$). Statistical students paired t-test was performed..... 121

Figure 3.3.2.1. The responses of nerve-muscle to ACh (1 mM, 30 s) KCl (30 mM, 30 s) and electrically stimulated contraction at two hours after exposure to 300 μ M of platinum-based drugs. Results are expressed as mean \pm SEM. For cisplatin; $n = 4$, K₂PtCl₄; $n = 4$, PHENEN; $n = 3$ and 56MESS; $n = 3$. Statistical students paired t-test was performed and significant differences are indicated by * when $p < 0.05$ 125

Figure 3.3.2.2. The responses of nerve-muscle to ACh (1 mM, 30 s) KCl (30 mM, 30 s) and electrically stimulated contraction at two hours after exposure to 300 μ M of macrocycle. Results are expressed as mean \pm SEM. For untreated nerves; $n = 3$, CB[6]; $n = 3$, CB[7]; $n = 4$, Motor2; $n = 3$, and β -cyclodextrin; $n = 3$. Statistical students paired t-test was performed and significant differences are indicated by * when $p < 0.05$ 128

Figure 3.3.2.3. The effect of cisplatin ($n = 4$), CB[7] ($n = 4$) and cisplatin@CB[7] ($n = 8$) on the nerve muscle's response to ACh (grey), KCl (green) and amplitude of its electrically stimulated contraction after two hours of exposure to drug. Results are expressed as mean \pm SEM..... 130

Figure 3.3.3. The change in atria contraction rate (top panel) and force of contraction (bottom panel) in untreated right (dark red, dark blue) and left atria (light red, light blue) over a period of two hours. Results are expressed as the means \pm SEM ($n = 3$). Statistical students paired t-test was performed and significant differences compared to time 0 min are indicated by * when $p < 0.05$ 131

Figure 3.3.3.2. The effect of the platinum-based drugs on atria contraction rate. Graph shows the effect of a) cisplatin, b) K2PtCl4, c) 56MESS and d) PHENEN on atria contraction rate. Results are expressed as the means \pm SEM ($n = 3$). Statistical students paired t-test was performed and significant differences compared to time match control are indicated by * when $p < 0.05$ 134

Figure 3.3.3.3. The effect of the platinum-based drugs on atria force of contraction. Graph shows a) cisplatin, b) K2PtCl4, c) 56MESS and d) PHENEN on the contraction rate of the right and left atria. Results are expressed as the means \pm SEM ($n = 3$). Statistical students paired t-test was performed and significant differences compared to time match control are indicated by * when $p < 0.05$ 135

Figure 3.3.3.5. The changes in the rate of atria contraction when treated with 300 μ M of macrocycles. Graph shows (a) CB[6], (b) CB[7], (c) Motor2 and (d) β -cyclodextrin . Results are expressed as the means \pm SEM ($n = 3$). Statistical students paired t-test was performed and significant differences compared to time match control are indicated by * when $p < 0.05$ 139

Figure 3.3.3.6. The changes in the force of atria contraction when treated with 300 μ M of macrocycle . Graph shows (a) CB[6], (b) CB[7], (c) Motor2 and (d) β -cyclodextrin. Results are expressed as the means \pm SEM ($n = 3$). Statistical students paired t-test was performed and significant differences compared to time match control are indicated by * when $p < 0.05$ 140

Figure 3.3.3.7. The difference in effects of cisplatin and cisplatin@CB[7] on the rate of contraction (top panel) and force of contraction (bottom panel) of the right atria at specific intervals over a two hour period. Results are expressed as the means \pm SEM

($n = 3$). Statistical students paired t-test was performed significant differences compared to time match control are indicated by * when $p < 0.05$ 141

Figure 3.3.3.8. Actual readings of rate and force of contraction of the right heart atria at different time points after treatment with 300 μM of cisplatin or 300 μM of cisplatin@CB[7]. 142

List of Tables

Table 2.1. A summary of the changes induced by each platinum-based drug on the nCAP amplitude of the mouse sciatic nerve after 80 min. The arrows indicate an increase (↑) or decrease (↓) in the nCAP amplitude. 114

Table 2.2. A summary of the changes induced by each macrocycle on the nCAP amplitude of the mouse sciatic nerve after 80 min. The arrows indicate an increase (↑) or decrease (↓) in the nCAP amplitude. 116

Table 3.1. A summary of the changes induced by each platinum-based drug on the amplitude of the nerve-muscle contraction induced by ACh, KCl and electrical stimulation after two hour incubation. The arrows indicate an increase (↑) or decrease (↓) in nerve-muscle contraction. 124

Table 3.2. A summary of the changes induced by each macrocycle on the amplitude of the nerve-muscle contraction induced by ACh, KCl and ES (electrical stimulation) after 120 min. The arrows indicate an increase (↑) or decrease (↓) in nerve-muscle contraction..... 127

Table 3.3. A summary of the changes induced by free drug and the encapsulated complex on the amplitude of the nerve-muscle contraction induced by ACh, KCl and ES (electrical stimulation) after 120 min. The arrows indicate an increase (↑) or decrease (↓) in nerve-muscle contraction..... 130

Table 4.1. A summary of the cardiotoxic changes induced by the platinum-based drugs on the rate and force of contraction in both the right and left atria. Results are expressed as means ± SEM. (*n* = 3)..... 136

Table 4.2. A summary of the cardiotoxic changes induced by various macrocycles on the rate and force of contraction in both the right and left atria..... 138

Chapter 1

Cancer, Chemotherapy and Drug Delivery Systems.

1 General Introduction

1.1 Cancer Statistics

In 2008, cancer accounted for 7.6 million deaths worldwide (around 13% of all deaths), with lung, stomach, liver, colon and breast cancer being the most predominant cancer [1]. The WHO (World Health Organization) predicts that the global incidence of cancer is increasing, and estimates that in 2030 over 13.1 million international deaths will occur as a result of cancer [1].

1.1.1 What is Cancer?

The origin of the word cancer is credited to the Greek physician Hippocrates (460-370 BC), who is considered the “Father of Medicine” [2]. Hippocrates used the words “carcinoma” and “carcinomas” to describe cancer and tumours respectively, which in Greek translate to “crab” and “crab swelling”. These terms were specifically chosen by Hippocrates as when he examined the surface of a breast cancer, it appeared to resemble the shape of a crab with legs stretching outwards [2].

In scientific terms, cancer is described as a complex genetic disease in which a group of cells exhibit three main characteristics that are not seen in normal cells, these are: uncontrolled growth (cells divide and proliferate beyond the normal limits), the ability to invade and destroy adjacent tissue and the ability to metastasise (spread to other parts of the body via either the lymphatic system or blood circulation system) [3-5].

There are over 200 different types of cancer, all of which can arise from the mutation of a single cell [3]. Normal cells grow, die and are replaced under a tightly regulated

and controlled manner (Figure 1.1). Damage or change to a cell's genetic material induced either by environmental or internal factors can result in cells that do not die and instead multiply and grow uncontrollably [3-5].

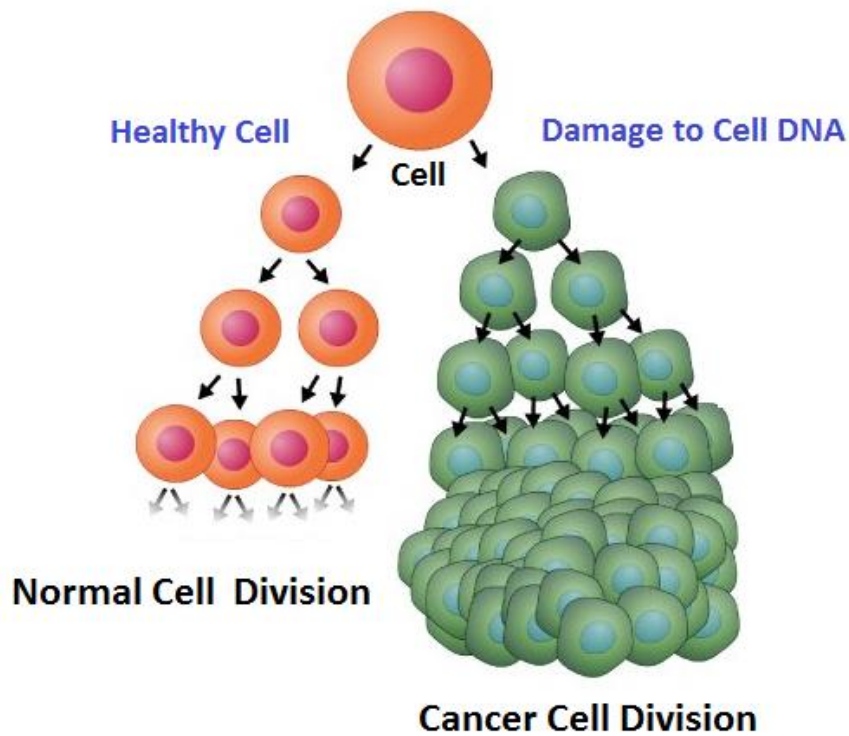


Figure 1.1. Normal cell division compared to cancer cell division. Healthy cells divide at a controlled steady rate before they ultimately undergo apoptosis. Cancer cells divide quicker than normal cells and do not undergo apoptosis thus resulting in large numbers of cancer cells that eventually form a tumour. Figure taken from <http://rise.duke.edu/seek/pages/page.html?0205>.

1.1.2 The Development of Cancer: Oncogenes and Tumour Suppressor genes

Cancer develops as a consequence of mutations which occur in genes that play important roles in the regulation of cell cycle and cell proliferation [4-8]. These mutations are predominantly found in genes called oncogenes and tumour suppressor

genes [9-11]. These genes code for proteins that control cell proliferation and cell apoptosis (programmed cell death), respectively. In normal cells, these pathways are under strict regulation and a balance is kept between cell division and cell death. If the control of one or more of these pathways is lost, due to mutations for example, this can lead to an uncontrolled cell proliferation with the loss of cell death function and therefore resulting in cells that accumulate forming a tumour [5, 9-11]. .

Tumours can be either benign, which are non-cancerous and remain localised, or they can be malignant which are cancerous and have the ability to metastasise.

1.1.2.1 Oncogenes in Cancer

Oncogenes are mutated versions of normal genes called proto-oncogenes. These genes code for proteins that are involved in promoting cell growth and proliferation. Mutations that convert proto-oncogenes to oncogenes increase the activity of the encoded protein or/and increase the expression of the normal gene [9-12].

The RAS gene is an oncogene that is most commonly activated in human tumours. It codes for four distinct yet highly homologous ~ 21 kDa RAS proteins: HRAS, NRAS, KRAS4A and KRAS4B [13]. All four proteins are involved in cell growth, differentiation and survival. Mutations in the RAS gene are very common and are found in 20-30% of all cancers including: ovary, pancreas, urinary tract, large intestine and liver with around 70-90% of pancreatic carcinomas containing a mutation in the RAS gene [10-13].

The RAS proteins cycle between “on” and “off” conformations that is determined by the binding of guanosine triphosphate (GTP) and guanosine diphosphate (GDP), respectively [13]. Under physiological conditions, the transition between the “on” and “off” state is regulated by guanine nucleotide exchange factors (GEFs) and by GTPase-activating proteins (GAPs) [13-15]. Studies have found that oncogenic mutations can impair the GTP hydrolysis reaction and that specific point mutations can prevent the formation of van der Waals bonds between RAS and GAP. The outcome of these mutations is the persistence of the “on” state of RAS, and as a consequence, there is a constant activation of a multitude of RAS downstream effector pathways (such as the MAP kinase pathway) that fuel cell proliferation. Various studies have also shown that the overexpression of RAS genes enhances the proliferation of cells by up-regulating cell transcription of growth factors such as the heparin-binding epidermal growth factor (HBEGF), transforming growth factor- α (TGF α). These affected cells show a greater growth advantage over normal cells and unlike normal cells, they lack cell repair mechanisms [10-15].

1.1.2.2 Tumour Suppressor genes in Cancer

In contrast to the cellular proliferating stimulation function of proto-oncogenes and oncogenes that drive cell cycle forward, tumour suppressor genes code for proteins that suppress cellular growth and division and promote apoptosis (programmed cell death) [9-11, 14].

The first tumour suppressor gene was identified in 1986 and named the RB1 gene. It codes for a protein known as the retinoblastoma protein (pRb) [10-14]. This protein

acts to stop the replication of damaged DNA by switching on the expression of genes that suppress the progression of cells from G phase (gap phase) of the cell cycle to S phase (synthesis) and therefore its inactivation allows for uncontrolled cell division. The types of genetic mutations that can lead to pRb inactivity most often involve frameshifts or deletions in the RB1 gene. Rb1 mutations have been found in various cancers including small cell lung, bladder, breast, cervical, thyroid and cancer of the eye (retina) [14-18].

The p53 tumour suppressor protein is the most common target for genetic alterations in tumours with more than 50% of human tumours containing a mutation in this gene. The p53 gene is a master regulator in inducing cell cycle arrest, DNA repair and apoptosis (amongst many more functions). The p53 protein activates expression of proteins that inhibit cell proliferation and those that promote apoptotic pathways in response to DNA damage. Any genetic alteration in the p53 gene will result in an inactivate p53 protein and therefore inhibiting the DNA damage responses that prevents cell cycle progression. Unlike the majority of tumour suppressor genes such as RB, APC and BRCA1 which are inactivated during cancer progression by deletions or truncating mutations, the p53 gene in human tumours is often mutated by a single nucleotide substitution [15, 18-19].

1.1.2.2.1 Cancer and the Two Hit Hypothesis

Mutations that occur in oncogenes are called “gain-of-function” mutations and are dominant which means that only one copy of the gene needs to be mutated in order to

promote cancer. In contrast, mutations that occur in tumour suppressor genes are recessive in nature (figure 1.1.1). Therefore, in order for a cell to become cancerous both of the tumour suppressor genes (both alleles) must be mutated, this is known as the two hit hypothesis [19, 20].

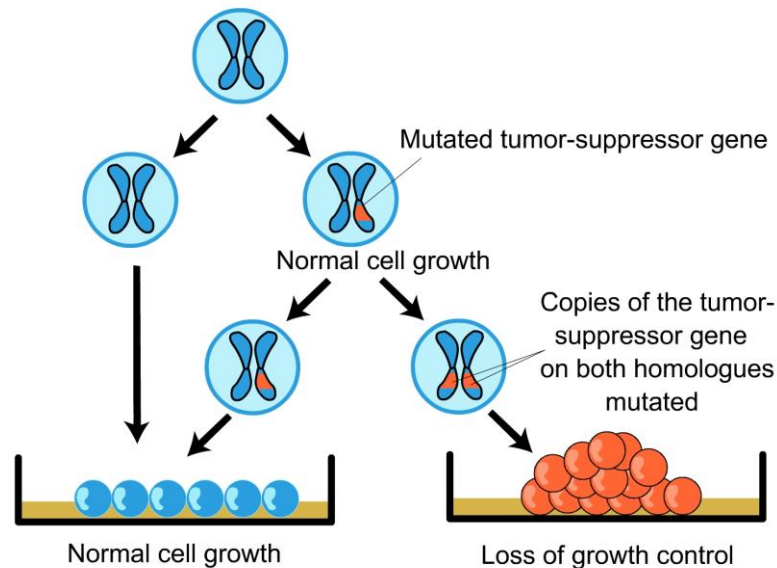


Figure 1.1.1. The recessive nature of tumour suppressor genes. For cancer to occur, both genes of a tumour suppressor gene must be mutated.

The two hit hypothesis was proposed by Dr Alfred Knudson in 1971 out of his interest in the genetic mechanisms underlying retinoblastoma, a childhood form of retinal cancer [11-21].

Retinoblasts are normal cells of the developing eye that stop growing and dividing during embryogenesis and differentiate into retinal photoreceptors and nerve cells. These differentiated cells do not divide, however in retinoblastoma, the retinoblasts

fail to differentiate and continue to divide forming tumours in the retina and if left untreated will metastasize to other parts of the body.

Between 1944 and 1959, Knudson had studied and compared the age at diagnosis, sex, family history, and whether the tumour occurred in one eye (unilaterally) or two eyes (bilaterally) in 48 patients with retinoblastoma. Knudson had observed that some children with an affected parent were disease-free, but that the offspring of these unaffected individuals developed retinoblastoma. Based on clinical and mathematical data, Knudson then concluded that retinoblastoma was caused by two mutations, one in each copy of a single tumour suppressor gene (RB1 gene) [20-21].

Today, this hypothesis serves as the basis for the understanding of how mutations in tumour suppressor genes drive cancer. This finding was crucial as it suggested that an individual could inherit a germ-line mutation but not be affected.

1.1.3 The Hallmarks of Cancer

There are six well defined biological steps that are required for the development of tumours [22-23]. These include the ability of cancer cells to evade apoptosis, their ability to replicate infinitely and their ability to metastasise to produce secondary tumours and produce new blood vessels [22-23].

1.1.3.1 Evasion of Apoptosis

Apoptosis, also known as programmed cell death, is a cellular suicide program that eliminates damaged or useless cells. It's a complex process that ultimately leads to the activation of a family of cysteine proteases called caspases. There are two routes to apoptosis; the extrinsic and intrinsic pathways [22-24].

In the extrinsic pathway, caspases are activated through the formation of a death inducing signal complex in response to the engagement of extracellular ligands to cell surface receptors [24]. Whereas the intrinsic pathway involves mitochondrial outer membrane permeabilization which in turn triggers the release of pro-apoptotic proteins that lead to the activation of caspases [24].

Cancer cells are under constant oncogenic stress such as genomic instability and hypoxia, in a normal cell, the intrinsic apoptosis pathway would normally be activated to induce apoptosis [22, 24, 25]. However, cancer cells are able to avoid the initiation of apoptosis by disabling apoptotic pathways. Studies have shown that cancer cells have an elevated expression of anti-apoptotic genes and an abnormally decreased expression of pro-apoptotic genes. Furthermore, they can inhibit apoptosis by post-translational modifications such as phosphorylation of pro-apoptotic proteins [24, 25].

1.1.3.2 Limitless Replicative Potential

Normal cells have a finite replicative ability that limits their multiplication to about 60-70 doubling (known as the Hayflick limit). During DNA replication, small segments of DNA at each end (known as telomeres) are unable to be copied and are

lost after each round of DNA duplication. The telomere region of DNA does not code for any protein. After a number of divisions the telomeres become depleted and the cell begins senescence [26].

Over the past two decades studies have shown that cancer cells have an unlimited replicative potential. This is due to cancer cells having an elevated expression of an enzyme called telomerase which maintains telomeres sequence at the end of DNA therefore giving cells an infinite replicative potential [22,23,26].

1.1.3.3. Metastasis and Sustained Angiogenesis

Metastasis is the process by which a tumour cell leaves its primary location and travels to a different site to establish a secondary tumour. For a cancer cell to metastasize it must penetrate a blood vessel or a lymphatic vessel by crossing the basal lamina and the endothelial lining of the vessel and then reverse again and grow at a new site. Cancer cells capable of metastasis are often more resistant to apoptosis and are less dependent on signals from other cells to grow and divide [22, 23,27]. Once a tumour surpasses 2 mm in size it must form new blood vessels to ensure tumour cells obtain sufficient oxygen and nutrients. Tumours attract the formation of new blood vessels from existing vessels by secreting angiogenic signals such as the vascular endothelial growth factor in response to hypoxic stress [22, 23, 28]. However, these new vessels are torturous and heterogenous in structure, leaky with dead ended branches. This results in irregular blood flow to the tumour helping to create additional regions of hypoxia.

1.1.4 Carcinogens

A carcinogen is defined as any substance that is able to cause cancer [29]. Carcinogens can be physical, such as ultraviolet (UV) light; chemical, such as those found in tobacco smoke; or biological, such as infections from certain viruses, parasites and bacteria [30-32]. The natural process of ageing is also a fundamental factor to the development of cancer as the incidence of cancer increases dramatically as age increases. This is believed to be due to the development of cell mutations over time [29]. The main risk factors of cancer worldwide have been identified to be due to the extensive use of tobacco and alcohol, unhealthy diets and physical inactivity [6].

1.1.4.1 Physical Carcinogens: Ultraviolet Radiation

Sunlight is the most ubiquitously occurring physical carcinogen that can induce melanocytic and non-melanocytic skin cancers [33].

The sun's UV spectrum is made up of three ultraviolet bands of different wavelengths; UVA (315-400 nm), UVB (280-315 nm) and UVC (< 280 nm). UVA and UVB are primarily responsible for the biological effects on human skin, as they are both capable of penetrating through the ozone layer, whereas UVC is nearly completely absorbed by the upper atmosphere [13]. UV light is absorbed by the human skin and does not penetrate the body any deeper than the skin. UVB is almost completely absorbed by the epidermis and UVA penetrates deeper into the dermis [33-35].

Epidemiological data has shown that recreational sun exposure and excessive or cumulative sunlight exposure can take place years and decades before skin cancer

arises [35,36]. There are three different types of skin cancer caused by exposure to ultraviolet light, these are: basal cell cancer, melanoma, and squamous cell cancer.

Experimental evidence has shown that DNA is the molecular target for most of the effects of UV light; this is because the bases that make up DNA all contain ring structures with an abundance of conjugated bonds that are known to absorb shortwave UV radiation [34]. UV light can induce mutations in several genes that are involved in tumour suppressive, oncogenic, and cell cycling pathways [35]. These pathways include mutations in the p16 and p53 tumour suppressor genes as well as the activation of Ras (Rat sarcoma) pathways, formation of specific mutagenic photoproducts and induction of reactive oxygen species [35, 36]. These ultimately result in the loss of induction of apoptosis and thus the loss of normal growth of keratinocytes and melanocytes [36].

1.1.4.2 Chemical Carcinogens: Cigarette Smoke

The link between cigarette smoking and lung cancer was first established in the early 1950s in a study that revealed a 26-fold increase of lung cancer in cigarette smokers compared with non-smokers [37]. Since then, several studies have directly linked cigarette smoking to various cancers, including: cancers of the oral cavity, oesophagus, larynx, lung, stomach, pancreas, kidney and leukaemia [37, 38].

In developed countries, cigarette smoking is responsible for 24% of all male deaths and 7% of all female deaths. Approximately 80-90% of all lung cancers and 30% of all cancers can be linked to the habit of cigarette smoking [39, 40].

There are more than 3,400 biologically active chemicals that have been identified in cigarette smoke, with sufficient evidence that 60 of them are carcinogenic in either laboratory animals or humans [37, 39]. These carcinogenic compounds belong to various classes including: aromatic amines, heterocyclic amines, aldehydes, volatile hydrocarbons, nitro compounds, organic compounds, inorganic compounds, metals, and nitrosamines. Of these polycyclic aromatic hydrocarbons, the tobacco specific nitrosamine 4-(methylnitrosamino)-1-(3-pyridyl)-1-buranone is likely to play a major carcinogenic role [37, 39].

The molecular mechanisms by which these chemicals induce cancer is diverse and depend on tissue type, however, the majority of cigarette carcinogens have shown to be capable of forming DNA site specific mutations specifically on tumour suppressive genes and by inducing oxidative damage [38].

The effect of cigarette carcinogens on tumour suppressor genes and specifically on the p53 tumour suppressor gene and the Kristen-ras (KRAS) oncogene have been widely documented [37]. The p53 protein which plays an essential role in cellular proliferation and cell death, is mutated in around 50% of all lung cancers. In a sample of 550 lung tumours with p53 mutations, 33% were shown to contain guanine (G) to thymine (T) DNA base transversions and 26% were shown to have guanine to adenine (A) transitions [37, 39]. These site specific mutations have also been found to occur in the KRAS gene which codes for proteins that play crucial roles in cellular growth. Around 24% - 50% of human lung adenocarcinomas have been shown to contain site specific mutations in the KRAS gene [37, 39].

The disturbance in oxidant-antioxidant cell balance has also been shown to cause cellular damage and trigger pro-inflammatory cytokines [40-43]. Studies have found that for every puff of cigarette smoke there is around 10^{14} - 10^{16} free radicals such as quinones, hydroquinones and semiquinones [40, 41]. All of these radicals are long lived and can generate further hydroxyl radicals and hydrogen peroxide in the presence of free iron which are capable of causing DNA nicking, and single strand breaks in DNA cultured rodent and human cells [43, 44].

1.1.4.3 Biological Carcinogens: Viruses and Infections

The International Agency for Research on Cancer (IARC) reported that biological carcinogens account for 18-20% of all human cancers [45]. Amongst these the most prominent carcinogenic infections are the human papillomavirus (HPV), hepatitis B and C viruses and the *Helicobacter pylori* bacteria.

The HPV is a small DNA virus that is associated with cervical cancer in women. Human papillomavirus types 16 and 18 have been implicated in 70% of all cases of cervical cancer, and in some cases of anogenital and oral carcinomas [4, 46, 47]. Cervical cancer is now the second most common cancer in women with an estimated 530,000 new cases each year [4]. Research into the mechanism by which the HPV virus induces its carcinogenic effect is still ongoing. Some studies have shown that the HPV is able to integrate itself into the host cell genome and use its transcription machinery to express viral proteins, of which two of them, named E6 and E7, are able to inactivate two essential tumour suppressor proteins; the p53 and pRb (retinoblastoma protein), respectively, disrupting cell cycle regulations [4, 46-48].

Helicobacter pylori (*H. pylori*), is a spiral shaped gram negative bacterium, that infects half of the world's population and is the major cause of gastric cancer; the second leading cause of death among all cancers [49, 50]. It is estimated that upto 85% of people infected with *H. pylori* show no symptoms of infection, and around only 1-2% of people infected with *H. pylori* develop stomach cancer [50].

The exact mechanism by which *H. pylori* causes gastric epithelial cells to become cancerous is still not fully understood, however, recent studies have shown that *H. Pylori* plays roles in causing impairment of the DNA mismatch repair system, induce oxidative stress as well as causing inflammatory stress and disruption of the cell cycle, as well as activating oncogenic pathways [49,51].

The hepatitis viruses affect several hundreds of millions of people worldwide and are a major cause of liver inflammation and cirrhosis [2,52]. Five main types of hepatitis viruses have been discovered and are referred to as hepatitis A,B,C,D and E [2]. Hepatitis B and C in particular can lead to chronic liver diseases including liver cirrhosis and cancer and it has been estimated that chronic infection with hepatitis B and C viruses are the cause of 75-80% of liver cancers worldwide [2,47].

The molecular basis by which hepatitis B and C cause cancer still remain incompletely understood. However, it is believed that malignant transformation occurs only after a long period of chronic liver disease. Chronic liver inflammation, continuous cell death and consequent cell proliferation are thought to increase the occurrence of genetic mutations and thus the risk of cancer [2, 45,45].

1.1.5 Cancer Diagnosis

Most cancers are recognised either through the appearance of lumps (depending on cancer type), or through routine screening. Various tests have been developed over the years to help determine whether cancer is present or not, including: blood and smear tests, as well as the use of several imaging techniques such as endoscopy, magnetic resonance imaging (MRI) (figure 1.2), scan and X-ray scans. Once suspected, diagnosis is usually made by a pathologist using tissue samples [2].

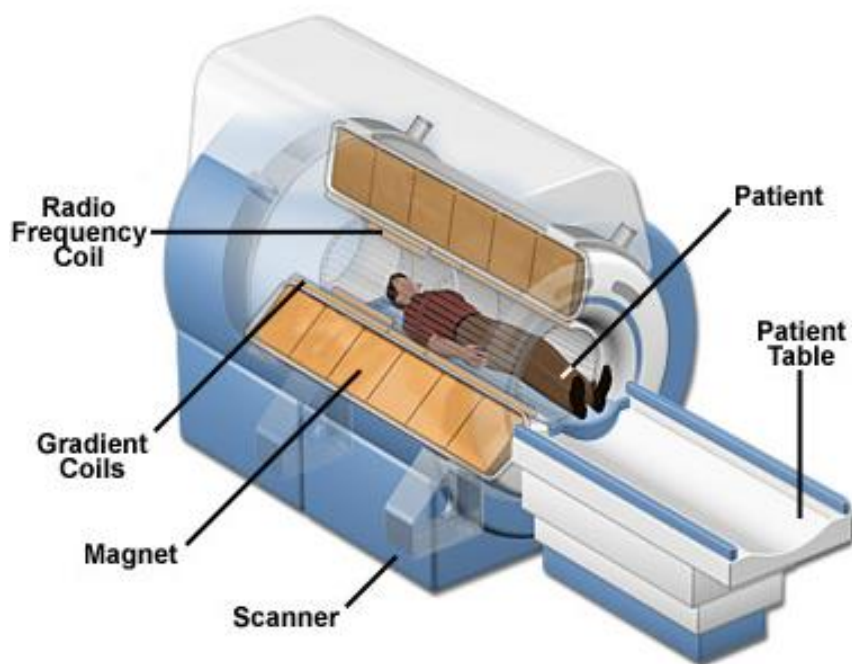


Figure 1.2. Image of a magnetic resonance imaging scanner. The MRI machine use radio waves to create pictures of all tissues in the body. Image taken from <http://pancreaticcanceraction.org/pancreatic-cancer/diagnosis/mri-scan/>.

1.1.6 Cancer Therapy

Cancer therapy encompasses a broad range of established clinical methods aimed at treating and curing patients of the disease. These established and innovative strategies include: surgery, radiation, hormonal therapy, and chemotherapy [56-58]. Hundreds of chemotherapeutic drugs have been developed and subsequently approved worldwide and many more are still undergoing clinical trials. In the period 2002-2012 the FDA (Food and Drug Administration, USA) has approved 85 new anticancer drugs for the treatment of various cancers [1].

1.1.6.1 Surgery in Cancer Treatment

Surgery is often the first line of treatment used to treat cancer. If detected early, the complete removal of the primary tumour can cure cancer with the use of adjuvant chemotherapy or radiotherapy. However, if the cancer has metastasized, it is more difficult to cure the cancer. In this case, surgery can still be used to remove parts or all of the tumour tissue to help reduce pressure on organs; a process called debulking [59].

There are two types of surgery currently used to treat cancer; traditional open surgery and the less invasive laparoscopic surgery. Several studies have shown advantages of laparoscopic surgery over open surgery, this includes: reduced pain and haemorrhaging, a quicker recovery period which means a shorter stay in the hospital. Laparoscopic surgery is a modern technique where small incisions (~ 0.5-1.5 cm) are made in locations far from the tumour. A telescopic rod lens system with cutting tools is then inserted into this incision and the surgeon directs this to the tumour location [59, 60].

1.1.6.2 Radiation Therapy in Cancer Treatment

Radiation therapy is used to treat around 50% of patients of various cancers such as skin, breast, lung, bladder, prostate and head and neck, either alone or in combination with surgery or chemotherapy, (in some cases all three forms of therapy are used together) [61]. The radiation used is in the form of high energy rays such as x-rays and photons which damage the cells genetic material (DNA) and thus prevent the cells from further division and proliferation. Damage to DNA by radiation is achieved through ionisation that can delete DNA segments, break the helical double strand, or form free radicals (ionisation of water molecules) that can ultimately induce cell apoptosis [61,62].

The goal of radiation therapy is to direct a high dose of radiation specifically to cancer cells while minimizing the exposure to adjacent non-cancerous cells. While normal cells that are adjacent to the cancer cells can be affected, they are more capable of repairing themselves at a fast rate and still retain their normal function, while cancer cells in general are not as efficient at repairing the damage caused by radiation treatment [61].

1.1.6.2.1 External Beam Radiation Therapy

This is the most common type of radiation therapy used. It involves directing a beam of high energy in the form of x-rays or photons from a machine to the site of the cancer while the patient lies still [62].

1.1.6.2.2 Internal Radiation Therapy

Also called brachytherapy, it involves the implantation of a sealed radioactive device such as tiny pellets containing radioactive isotopes inside or nearby tumour tissue such as the prostate. As the isotopes naturally decay overtime, they give off their radiation that damages the nearby cells [62].

1.1.6.2.3 Systemic Radiation Therapy

This technique involves the use of radioactive drugs that can be administered either orally or intravenously. Orally radioactive iodine (I-131) is currently used in the treatment of thyroid cancer (the thyroid gland absorbs most of the natural iodine in the body and therefore will selectively uptake the radioactive iodine) and injectable Strontium-89 is used in the treatment of bone cancer [62, 63].

1.1.6.3 Hormonal Therapy in Cancer Treatment

Hormones are biochemical compounds that are naturally produced by the endocrine glands within the human body. Their main function is to regulate essential physiological and behavioural activities that range from metabolism to reproduction, mood, movement, stress, and the growth and development of cells. Some cancers, namely breast, ovarian, prostate, thyroid and testicular are hormonal-related, that is their rate of cellular proliferation is dependent on the amount of hormones the body produces. Thus a strategy to treat these types of cancers is to inhibit the production of these hormones or block the uptake of hormones by the cancer cells [64].

Oestrogen and progesterone are female hormones that have shown to be strongly associated with the development of breast cancer in menopausal women when in high

concentrations. These cancers are referred to as oestrogen receptor positive (ER+), progesterone receptor positive (PR+) or both. These hormones have been found to stimulate epithelial breast cell mitosis, increasing the number of cell divisions and thus the opportunity for random genetic errors. Different hormonal therapies have been developed to treat and to prevent breast cancer, this includes drugs that inhibit the production of oestrogen such as the aromatase inhibitors, and drugs that work as antagonists to the oestrogen receptor on breast tissue, therefore decreasing the uptake of oestrogen by the cancer cell which ultimately induces cell death [64, 65].

1.1.6.4 Chemotherapy

Chemotherapy is defined as the use of chemical agents to destroy cancerous cells (although these agents can be non-cell specific). Over the years, various types of chemotherapeutic agents have been developed and are currently used in the clinic. These chemotherapeutic agents can be divided into several groups based on their structure and mechanism of action. The major classes include: the alkylating agents (e.g. the platinum-based drugs), antimetabolites (e.g. 5-fluorouracil (5-FU)), anthracyclines (e.g. doxorubicin), and the taxanes (e.g. paclitaxel) [66-73]. The platinum-based drugs will be given more focus in the next section as these are the drugs used in this thesis.

1.1.7 Platinum Based Drugs in Cancer Therapy

Platinum based drugs are amongst the most widely used anticancer drugs available. They are used to treat a wide spectrum of cancer types, including: testicular, colon, breast, brain, ovarian, bladder, lung, head and neck, stomach, prostate, cervical, small

and non-small cell lung, esophageal, as well as Hodgkin's and non-Hodgkin's lymphomas, neuroblastoma, sarcomas, multiple myeloma, melanoma, and mesothelioma, despite their dose limiting toxicity [74,75].

Cisplatin, carboplatin and oxaliplatin are the only platinum drugs approved for clinical use worldwide, while nedaplatin, lobaplatin and heptaplatin are only approved for use in certain countries (this will be discussed below) [75, 76].

1.1.7.1 Cisplatin in Cancer Therapy

Cisplatin (Figure 1.3), a square planar Pt^{2+} complex, was the first metal based drug to enter clinical trials in 1972 and the first to be used in the clinic in 1979 [76-78]. Platinum- based drugs are the most extensively used drugs in the treatment of cancer with cisplatin currently used in 32 of 78 treatment regimens listed in Martindale in 2010 [67].

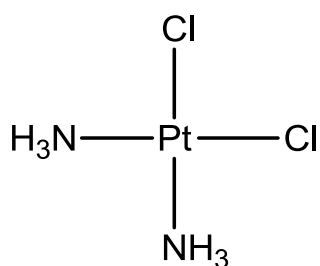


Figure 1.3. The chemical structure of cisplatin.

1.1.7.1.1 Discovery of Cisplatin

The antitumor properties of cisplatin were serendipitously discovered by Professor Barnett Rosenberg and his co-workers at Michigan State University in the 1960s [79, 80]. While investigating the effect of electrical fields on the growth of *E. Coli* bacteria, they observed that not only did the bacteria cease to divide, but that they also increased in size by 300-fold, losing their normal “sausage” like shape and becoming long “spaghetti” like rods (Figure 1.3.1) [81, 82].

Rosenberg and his co-workers had initially attributed this effect to the fact that somehow the current from the platinum-conducting plates were inhibiting cell division, but inducing cell growth. Sensing that they were observing something new and unusual, the investigators carried out a number of control experiments which showed that the electrical current was not the cause of inhibiting cell division, but a product that formed from the degradation of the platinum electrodes; cisplatin, a coordination complex that was synthesised and had been reported by Peyrone more than a hundred years earlier [80-84].

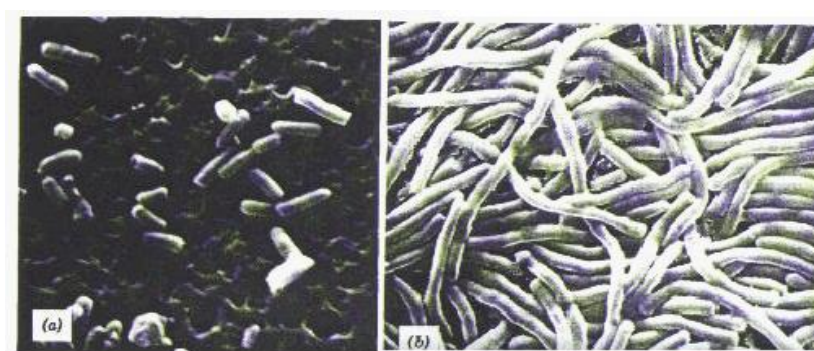


Figure 1.3.1. A scanning electron microphotograph of a) normal *E. Coli* bacteria and b) *E. Coli* grown in medium containing cisplatin. Image taken from <http://chemcases.com/cisplat/cisplat01.htm>.

Equipped with these results, Rosenberg then anticipated that because cisplatin inhibited bacterial cell division, it may also inhibit the proliferation of rapidly dividing cancer cells [81]. In 1968 cisplatin's anticancer effect was confirmed and further human clinical trials in 1971 showed cisplatin's value in testicular and bladder cancer which resulted in FDA approval in 1978 under the name Platinol [79].

1.1.7.1.2 Physical and Chemical Properties of Cisplatin

Cisplatin is a bright yellow crystalline solid with a molecular weight of 300.05 (g/mol) that is soluble in water and DMSO [2].

1.1.7.1.3 Administration, Formulation and Pharmacokinetics

Platinol-AQ, is a clinically ready to use aqueous formulation of cisplatin. Each 100 mL amber vial of infusion contains: 1 mg/mL cisplatin, 9 mg/mL sodium chloride (to prevent the premature aqation of the drug in solution), hydrochloric acid and sodium hydroxide to an approximate pH of 4.0. This is then diluted in 2 liters of 5% Dextrose in 1/2 or 1/3 normal saline [2].

Before commencing treatment, patients are pre-hydrated with 1-2 litres of fluid for 8-12 hours to minimise the risk of nephrotoxicity [83, 84]. Cisplatin is then intravenously administered over 6-8 hours in doses of up to 100 mg/m². Mannitol may be simultaneously given with the intravenous infusion to maximise patient urine flow [83]. Nausea and vomiting is typically severe and is treated with a 5-HT₃ antagonist (Granisetron) combined with a glucocorticoid steroid [85].

Following the intravenous administration of cisplatin, the drug is widely distributed through body fluids and tissue with the highest concentration of platinum found in the kidneys, liver and intestines. More than 90% of platinum remaining in the blood is bound (possibly irreversibly) to proteins including albumin, transferrin, and globulin [75].

1.1.7.1.4 Mechanism of Cisplatin Cell Entry

The exact mechanism(s) by which cisplatin enters cells is yet to be discovered. However, passive diffusion and active transport are believed to be equally likely [77, 86]. Passive diffusion relies solely on the difference of drug concentration outside and inside the cell. The dichloro and monohydroxo form of cisplatin are both neutral and carry no charge which would allow movement of drug across the cell membrane [84]. However, some studies have shown that cells with acquired resistance to cisplatin have few or no changes to the structure and function of the plasma membrane, suggesting that other mechanism(s) of cisplatin cell entry must exist [86, 87]. In 1981, cisplatin was proposed to be actively transported into the cell cytoplasm via various membrane embedded transporters. Over the years research has found that Na⁺, K-ATPase, solute carrier transporters (SLC) and in particular the copper transporter protein (CTR1) do play a role in the active uptake of cisplatin into cells [77, 88]. The CTR1 protein gained the most attention as a defect in this gene showed decreased cisplatin accumulation in yeast cells [88]. Once inside the cell, cisplatin has a range of targets including: RNA, sulphur containing peptides like glutathione, mitochondria and DNA, which is its primary biological target.

1.1.7.1.5 Mechanism of Action of Cisplatin

In the blood stream where the chloride concentration is high ~ 100 mM, cisplatin remains physically intact and non-reactive. However, once it enters the cytoplasm of a cell, where the chloride concentration is much lower ~ 4 -20 mM, its chloride ligands are spontaneously and sequentially replaced with water molecules [76, 81]. This results in the formation of a positively charged, bis-aquated platinum complex that is now able to bind its target; DNA (Figure 1.3.2) [75, 89, 90].

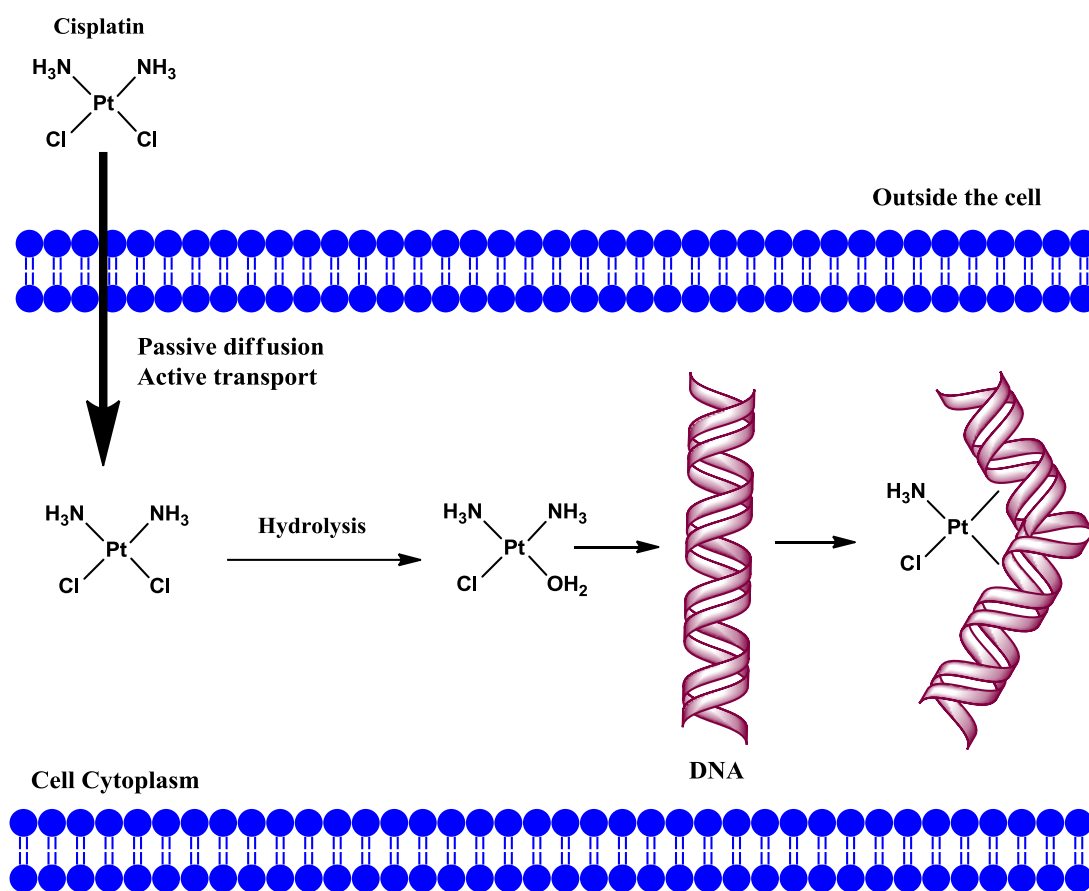


Figure 1.3.2. Mechanism of cisplatin cell entry and its mechanism of action. Once cisplatin enters cells either by passive diffusion or active transport it is aquated within the cytoplasm. This aquation allows it to attach to DNA causing a structural distortion in the double helix which prevents further DNA transcription and replication. Adapted from <http://pubs.rsc.org/en/content/articlehtml/2014/mt/c4mt00238e>.

Many studies have shown that cisplatin readily binds DNA at the N7 position of purine bases particularly guanine and adenine and to a lesser extent at the N1 of adenosine and O6 of guanosine [84, 89, 91, 92]. Cisplatin binds to two sequential bases on the same strand forming intrastrand adducts and to two bases on different DNA strands forming interstrand adducts. Studies have shown that the major DNA adducts formed by cisplatin are intrastrand adducts where 65% are between two adjacent guanines 1,2 GpG, 20% are between an adjacent guanine and adenine GpA, and 9% are 1,3 GNG or 1,4 GNG crosslinks where N indicates any nucleoside. Interstrand DNA adducts account for < 1% and occur between two guanines on opposite strands (Figure 1.3.3) [75,92].

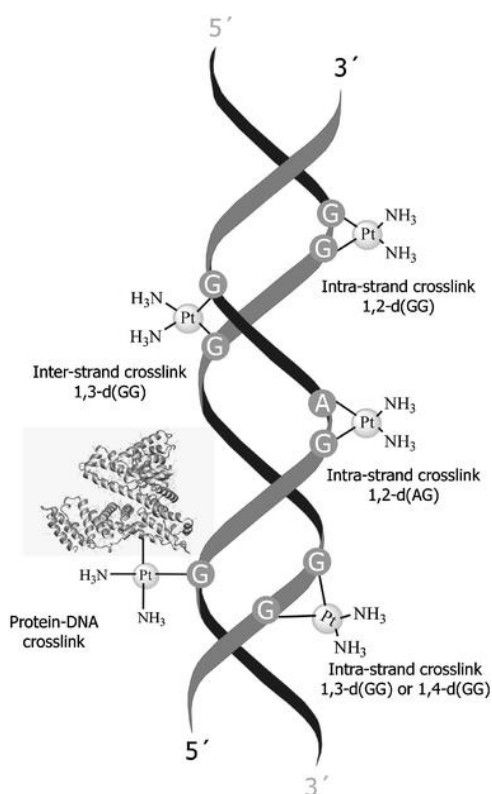


Figure 1.3.3. A diagram showing the different binding modes of cisplatin with DNA nucleobases including: 1,2-(GG) intra-strand crosslinks, 1,3-(GG) inter-strand crosslinks, 1,2-(AG) intra-strand crosslinks, protein-DNA crosslinks and 1,3 and 1,4-(GG) intrastrand crosslinks. Image taken from <http://pubs.rsc.org/en/content/articlehtml/2010/mt/b911438f>.

Distortions induced in the DNA by these adducts cause the hydrogen bonds between guanosine and cytosine to break leading to bending of the DNA helix by up to 60% towards the major groove and unwinding of the double helix by 23°. This Pt-DNA complex blocks RNA polymerase II at the lesion site and inhibits transcription. It has been suggested that Pt-DNA adducts can attract specific proteins containing a high mobility group (HMG) domain that bind to the site of platination and shield the nucleotide excision repair system from identifying and repairing the lesion and thus ultimately leading to cell death.

1.1.7.1.6 Non-DNA Targets of Cisplatin

Numerous studies over the years have shown that cisplatin binds to other components of the cell apart from DNA. Cisplatin has been shown to bind to and inhibit membrane proteins causing a lowering of the intracellular pH of the cell, promotion of lipid rafts in the membrane and inducing apoptosis by binding to death receptors found on the cell membrane [93-95].

1.1.7.1.7 Tumour Resistance to Cisplatin

A major obstacle to the success of cisplatin in cancer therapy is the emergence of cisplatin resistant cancers [94, 96]. When cells become resistant to cisplatin, the dose of drug given to the patient is increased, which in turn increases the level of its toxic side effects. Resistance of cancer cells to cisplatin can be either intrinsic or acquired [84]. Cisplatin is ineffective from the outset with cells that are intrinsically resistant, these cells are resistant through their inherent structural or functional characteristics. In comparison, cisplatin is initially beneficial against some cancers but becomes ineffective over time in cells with acquired cisplatin resistance.

1.1.7.1.7.1 Acquired Cisplatin Resistance

Various hypothesis have been developed over the years to explain methods by which cells become resistant to cisplatin. One of the most likely reasons is the insufficient accumulation of drug at the target site failing to cause cell death [95, 96]. High expression levels of sulphur-containing compounds such as glutathione and metallothionein are believed to play a role in cisplatin resistance [95, 96]. These proteins and peptides are abundant in mammalian cells such as ovarian cells and act as reducing agents by scavenging for free radicals. They have been shown to have a strong affinity for cisplatin, forming cisplatin-thiol conjugates which ultimately lead to depletion in the amount of intracellular cisplatin that can bind to DNA [89]. Studies have shown that cells containing high levels of glutathione such as the hepatic HepG2 and breast MCF7 cell lines were shown to be resistant to cisplatin [98, 97].

Damage to the CTR1 gene also plays a role in inducing cisplatin resistance, as deletion of the CTR1 gene decreases the intracellular accumulation of cisplatin [89]. Also an increased efflux of cisplatin from the cell by efflux proteins such as the ATP binding cassette subfamily which is also known as the multi-drug resistance protein 1 (MRP1) and canalicular multi-specific organic anion transporters (cMOAT) play a role in decreasing the intracellular accumulation of cisplatin by promoting its efflux from the cell and inducing resistance [97].

The development of cell resistance to cisplatin after it has bound to DNA is believed to occur through the cell's ability to repair DNA as well as its ability to remove cisplatin-DNA adducts [95, 96-97]. Many cisplatin resistant cell lines derived from

various types of human tumours have shown an increased capacity to repair DNA compared to their sensitive counterparts, and therefore drug resistance is believed to occur primarily by DNA repair [81, 89]. There are four major DNA-repair pathways that have been identified to play a role in inducing drug resistance, which include: nucleotide-excision repair (NER), base-excision repair (BER), mismatch repair (MMR) and double strand break repair. Both the NER and MMR pathways are believed to play major roles in the removal of cisplatin lesions [81, 89, 90].

1.1.8 Circumvention of Platinum Resistance: Second and Third Generation Platinum-based Drugs

In clinical practice, drug resistance constitutes the failure of a patient to achieve a complete or partial response to therapy. To circumvent chemo-resistance to cisplatin many analogues have been developed over the years including: satraplatin, ormaplatin, JM-11, BBR3464, and aroplatin amongst many more [67, 99]. To date, 14 platinum-based anticancer drugs have completed at least Phase I trials with only a few reaching Phase III [85, 99, 100]. These drugs were all discontinued due to lack of activity, high toxicity or for economic reasons [85].

Carboplatin and Oxaliplatin are the only successful second generation platinum-based drugs that are currently used in the clinic worldwide (these will be discussed in the next section) [91]. There are three other third generation platinum-based drugs that are approved for use in individual countries these are: nedaplatin which is approved for use in Japan, lobaplatin in China and heptaplatin in the Republic of Korea [67, 94-100].

1.1.8.1 Carboplatin in Cancer Therapy

Carboplatin, (Figure 1.4), was designed specifically to reduce the side effects associated with cisplatin at the London Institute of cancer research and approved by the US Food and Drug Administration (FDA) in 1989 under the brand name paraplatin [67, 85].

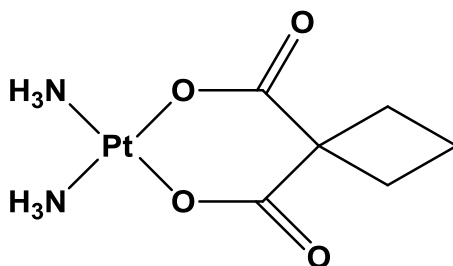


Figure 1.4. The chemical structure of carboplatin.

The key difference between the structure of carboplatin and cisplatin is that the former possesses a six membered dicarboxylate ring, which because of the chelate effect (slow aquation rate constant 10^{-8} s^{-1} compared with 10^{-5} s^{-1} for cisplatin), makes it much less reactive than cisplatin ([67,91]. Carboplatin is currently used alone or in combination with other drugs to treat various cancers including: ovarian, head and neck, bladder, testicular, small cell lung and brain cancers [67, 91-93]. Although carboplatin is essentially devoid of nephrotoxicity and is much less neurotoxic compared to cisplatin, it is extremely myelosuppressive, in which it reduces the number of white blood cells in the body, in particular thrombocytopenia rendering patients vulnerable to infection by various organisms [91,93].

1.1.8.2 Oxaliplatin in Cancer Therapy

Oxaliplatin, (Figure 1.5), was synthesised by Connors *et al* in 1972 by the substitution of the two ammine groups of cisplatin with a DACH (1*R*,2*R*-diaminocyclohexane) which showed anticancer effectiveness in cisplatin resistant cells through the formation of different DNA adducts compared to cisplatin (predominantly forms GpG intrastrand adducts with its bulky hydrophobic dach ligand pointing into the DNA major groove which prevents binding of DNA repair proteins) [93]. It was first approved for clinical use in France in 1996, the European Union in 1999 and the USA in 2002. Oxaliplatin in combination with 5-FU (fluorouracil) is the only platinum drug that exhibits clinical activity in colon carcinoma, in which cisplatin and carboplatin have essentially no activity [93-95]. Compared with cisplatin, oxaliplatin has a very good safety profile characterised by lower haematotoxicity and moderate and manageable gastrointestinal toxicity. Its limitation, however, is that it induces long term peripheral neuropathy (nerve damage), the mechanism by which oxaliplatin induces neuropathy is still not known [70, 93-95].

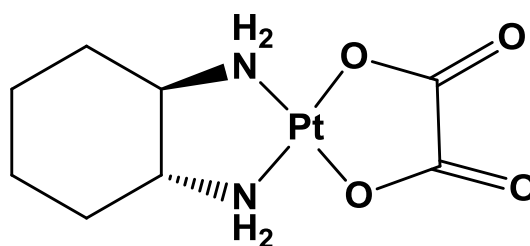


Figure 1.5. The chemical structure of oxaliplatin.

1.1.9 Drug Delivery in Cancer Therapy

As well as the continued search for new anti-cancer drugs with high efficacy and low side effects, there has been focus on improving delivery of drugs to cancer cells by means of drug delivery systems. Over the last 20 years, various drug delivery systems such as liposomes, hydrogels, nanoparticles, dendrimers, cyclodextrins and cucurbit[n]urils have been developed and studied with anticancer drugs at the molecular and biological level for the treatment of cancer. The use of drug delivery systems provides a strategy that not only shields drugs from premature deactivation, which in turn increases their circulation time in the bloodstream, but can also passively target drugs to tumour cells by exploiting the enhanced permeability and retention effect (EPR). This also reduces the drugs associated toxic side effects as it decreases the amount of drug reaching healthy tissue [101-105].

1.1.9.1 Physio-Pathological Characteristics of Tumour Tissue

Tumour cells divide at a rapid and uncontrollable rate compared to normal tissue. A tumour cell obtains a sufficient supply of nutrients and oxygen by passive diffusion until it reaches a size of 2 mm. Once they surpass 2 mm in size they require a different mechanism to fulfil their energy needs. To expand and continue to grow, the tumour forms new blood vessels (angiogenesis) from pre-existing ones by the over expression of pro-angiogenic growth factors including: vascular endothelial growth factor (VEGF), basic fibroblast growth factor (bFGF), bradykinins and prostaglandins [104-109]. However, this dramatic proliferation gives rise to abnormal and defective architecture of the blood vessels compared to that of normal cells. New tumour blood vessels are characterised by a disorganised structure with large gaps between the endothelial cells. This gives rise to a leaky and porous vasculature system that

increases the permeability of macromolecules (~ 40 kDa) into the tumour cells compared with normal healthy cells [106-110].

1.1.9.2 The Enhanced Permeability and Retention Effect

The EPR effect was first described by Matsumura and Maeda in 1986. Their investigations reported that the majority of human tumours produce extensive amounts of vascular permeability factors and that most tumours have blood vessels with defective architecture [104,105,109]. The size of the gaps between the endothelial cells range from 100-780 nm, depending on the tumour type, which greatly differs from the tight endothelial junctions of normal vessels which have gaps of 5-10 nm (Figure 1.6) [104, 109, 110].

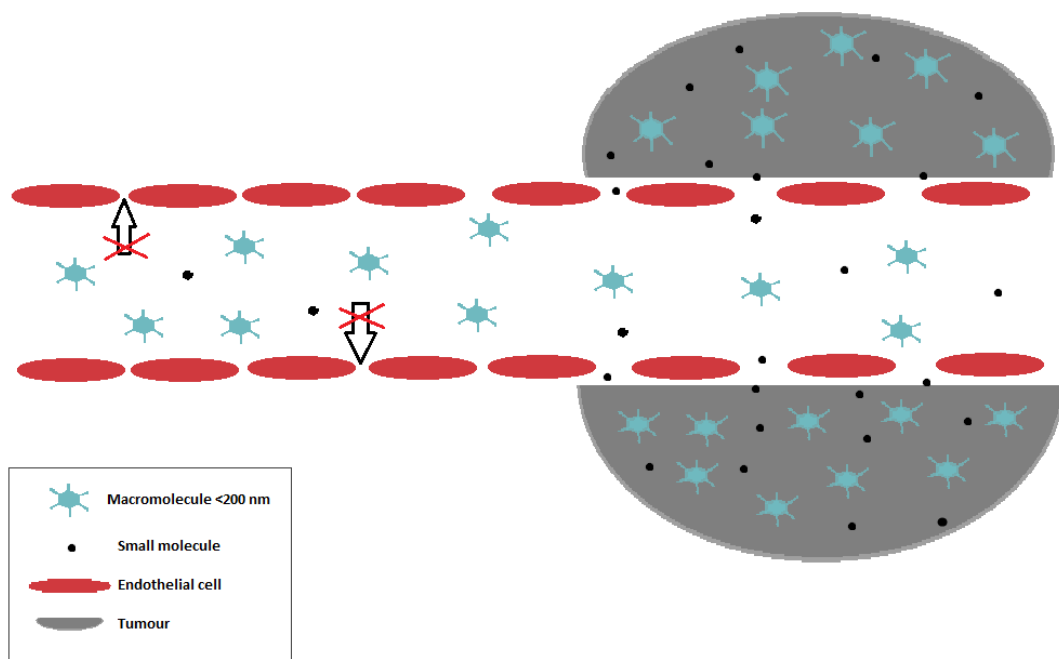


Figure 1.6. A diagram demonstrating the EPR effect. The endothelial cells that line tumour blood vessels have large gaps between them compared to normal vessels allowing the large molecules to be taken into the tumour.

In 1979 an anticancer protein named neocarzinostatin (NCS) was synthesised for the first time by Maeda *et al* and conjugated to a styrene maleic acid copolymer (SMA) (the drug-polymer complex was named SMANCS) [111]. Studies found that not only did SMANCS accumulate to a greater degree in tumour cells compared with the free drug NCS, but that the drug complex had a longer plasma half-life (up to 200 times more) than the free drug [111-113].

The unique phenomenon of the EPR effect is now considered a landmark principle in tumour targeting and a gold standard in anticancer drug design using macromolecular agents. Doxil, which is a PEGylated (polyethylene glycol-coated) liposomal formulation of the anthracycline drug doxorubicin is used routinely for the treatment of ovarian cancer and Kaposi sarcoma [105, 114-116]. There are also many other polymeric drugs that are currently under Phase I and Phase II clinical trials. However, regardless of the popularity of the EPR effect, there are some problems that exist with this strategy. Studies have shown that the central part of tumours do not exhibit the EPR effect and show much less accumulation of macromolecules than in other parts [105, 114,115].

1.1.10 Cisplatin Based Drug Delivery Systems

Over the past ten years, there has been a sharp increase in the number of drug delivery systems developed for the delivery of cisplatin. These systems include: gold nanoparticles, dendrimers, carbon nanotubes, liposomes, macrocycles, silica microparticles, nanoscale metal organic frameworks, polymer conjugations, nasal

inserts and hydrogels. Of these systems, the most promising have been liposomes, macrocycles and hydrogels as they have either shown promising pre-clinical results or are undergoing phase clinical trials [117-119].

The next section of this thesis will introduce these three systems and more importantly analyse the preclinical and clinical results of their formulation with cisplatin.

1.1.10.1 Liposomes

Liposomes are microscopic vesicles composed of natural or synthetic lipids that self-assemble into bilayers that surround an aqueous core upon hydration (Figure 1.7) [120-122]. The lipid layers are composed mainly of amphipilic phospholipids containing a hydrophilic head and hydrophobic tail, with other constituents being cholesterol and fatty acids. Both hydrophobic and hydrophilic drugs can be associated within liposomes, and since their discovery, a number of liposomal drug based formulations have been developed and this will be discussed below [120-122].

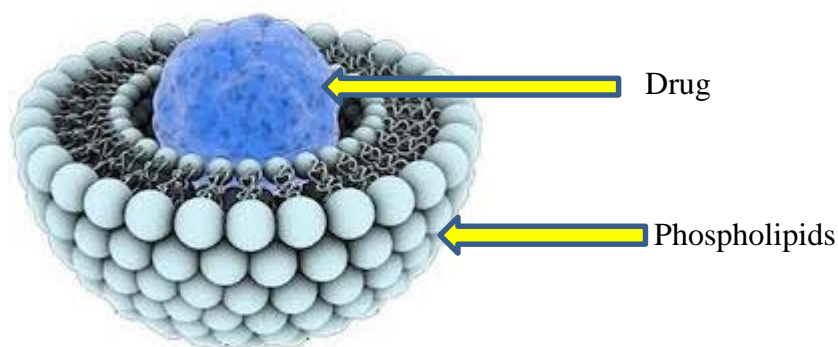


Figure 1.7. A schematic diagram of a drug encapsulated by a liposome. Image taken from <http://www.hindawi.com/journals/jdd/2012/581363/fig1/>

Doxil™, is the first liposomal drug product to be licensed for use in the USA. It is composed of a pegylated (polyethylene glycol coated) liposome-encapsulating the anthracycline drug doxorubicin. The use of Doxil™ is favoured over the use of free doxorubicin as it exhibits up to an 8-fold increase in circulation half-life compared to free drug and a significant decrease in the cardiotoxic side effects induced by doxorubicin [123,124].

1.1.10.1.2 Liposomes for the Delivery of Cisplatin

Lipoplatin is a liposomal formulation of cisplatin and three phospholipids (soy phosphatidyl choline (SPC-3), cholesterol, dipalmitoyl phosphatidyl glycerol (DPPG) and methoxypolyethylene glycol-disteaoryl phophatidylethanolamine (mPEG2000-DSPE) that has shown interesting and promising results in both preclinical and clinical trials [125,126].

Preclinical *in vitro* studies have shown that lipoplatin may have a higher therapeutic index compared to free cisplatin as it had superior cytotoxicity to cancer cells including: non-small cell lung cancer and renal cell carcinomas compared to normal non-cancerous cells [125]. Due to these results, it was hypothesized that because lipoplatin is a small nanoparticle of 110 nm in diameter, it may be able to passively target tumour cells through the compromised endothelium of the tumour vasculature system [125]. Furthermore, *in vivo* studies have shown that when administered intraperitoneally to rats at 30 mg/kg, lipoplatin demonstrated complete absence of nephrotoxicity, whereas animals injected with free cisplatin at the same dose developed renal insufficiency with clear evidence of tubular damage [125, 128].

These preclinical results amongst many more revealed that the reformulation of cisplatin through this particular liposome may be the answer to increasing the bioavailability of cisplatin [125]. Thus, over the last five years lipoplatin has undergone clinical trials and has recently finished all three phase clinical trials [125-128]. In these trials, lipoplatin was tested for tumour shrinking efficacy and general toxicity compared to free cisplatin in various cancers including: pancreatic cancer, head and neck cancer, mesothelioma, breast and gastric cancer, and NSCLC [125-128].

The overall results from the phase clinical trials have shown that although lipoplatin had an increased amount of platinum in tumour tissue and lesser side effects compared to free cisplatin, the response and survival rate of free cisplatin to lipoplatin in patients were not significantly different [126, 127].

In a randomized phase III clinical study comparing lipoplatin combined with 5-fluorouracil versus cisplatin combined with 5-fluorouracil, results showed that lipoplatin had a significantly shorter half-life and increased clearance than free cisplatin [126-128]. Toxicity results showed that renal toxicity was much lower in the lipoplatin arm compared to the cisplatin arm and that higher myelotoxicity was observed in the cisplatin arm (31.7% versus 12% in the lipoplatin arm). The response rate in this study was higher in the cisplatin arm, but stable disease was higher in the lipoplatin arm [126-128]. In a different phase III trial, patients with advanced non-small cell lung cancer were randomized to receive either lipoplatin plus paclitaxel (Arm A) or cisplatin plus paclitaxel (Arm B) administered intravenously every two

weeks [126,128]. The results of this study showed that the lipoplatin (Arm A) had significantly less toxicity than cisplatin namely; nephrotoxicity (6.1% in Arm A versus 40% in Arm B, $p < 0.001$), neutropaenia (33.3% in Arm A versus 45.2% in Arm B, $p = 0.017$) and nausea/vomiting (32.5% in Arm A versus 45.2% in Arm B, $p = 0.042$) [126,127,128]. Although the overall response rate was numerically higher in lipoplatin compared with cisplatin (58.8% versus 47.0%, $p = 0.073$), the median overall survival was similar in both groups of patients (9 versus 10 months, $p = 0.57$) [125-128].

The overall results from the phase clinical trials have shown that although lipoplatin had an increased plasma circulation time compared to free cisplatin as well as an increased amount of platinum in the tumour tissue and lesser side effects compared to free cisplatin, the response and survival rate of free cisplatin to lipoplatin were of no significant difference. Although no difference was seen in patient survival rate, the reduction in toxicity is important to improving patient quality of life.

This study has highlighted that although the use of liposomes may have no effect on the response and survival rate of patients, it has the ability to reduce toxic side effects (possibly through preventing the drug from unwanted protein/cell receptor binding) of the encapsulated drug and thereby improving the quality of patient life.

1.1.10.2 Hydrogels

Over the past few years, injectable and implantable hydrogels have been under investigation as a means to prolong the therapeutic dose of drugs in the bloodstream [129]. Various pre-clinical studies of hydrogels with different chemotherapeutic drugs

have shown that not only is a slow drug release system achievable, but more importantly that a slow release can also simultaneously increase the efficacy of a drug by increasing its bioavailability and decreasing its toxic side effects [130,131].

Hydrogels are three-dimensional polymeric water swollen matrices held together by physical or chemical bond [129-132]. They are suitable for biomedical applications because of their ability to simulate some aspects of biological tissue; fully swollen hydrogels share physical features that are common to that of living tissues, including: a soft and springy texture, a rubbery consistency which reduces interfacial tension with biological fluids, and an elastic nature that minimizes irritation to the surrounding tissues when implanted. The low interfacial tension has also been shown to minimise protein adsorption and cell adhesion, and therefore, reduces the chances of a negative immune response from the host [129-135].

Gliadel® is currently the only hydrogel that is approved for clinical use in the treatment of high grade glioma (approved for use only in the USA). It is composed of a biodegradable polymer called polifeprosan and the chemotherapeutic drug carmustine [136-138]. The wafer is the size of a British five pence coin (approximately 1.45 cm in diameter and 1 mm thick) and it is surgically implanted in the brain along the walls and floor of the cavity after a malignant glioma has been surgically removed (Figure 1.8) [139]. This is a local therapy designed to provide controlled release of carmustine over a period of two to three weeks. In theory this should reduce systemic toxicities and allow a greater dose to be provided to the residual tumour than injectable carmustine alone. Using this method to treat high-grade glioma also simplifies

subsequent management, as systemic chemotherapy is usually given over a prolonged course of around six months [136-144].

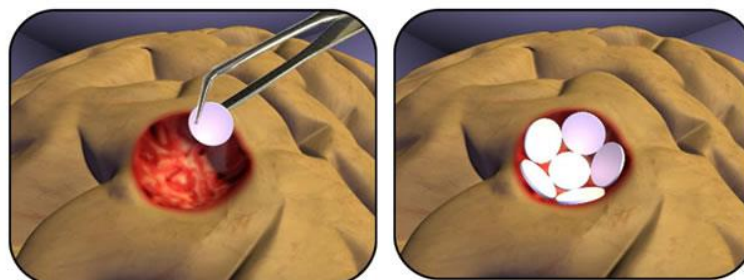


Figure 1.8. An image of a gliadel wafer being implanted in the brain along the wall and floor of the cavity after a malignant glioma has been removed (left panel), as much as upto eight wafers can be placed where the tumour was located (right panel). Image taken from <http://www.gliadel.com/about-gliadel/how-gliadel-used/>.

Phase two and three clinical trials have shown that Gliadel® can increase survival rate by 34% but only in patients with primary glioma and not for those with recurrent disease. The results of these trials also showed that although Gliadel® did not decrease side effects such as seizures, nausea, infection insomnia, depression and visual defects, this treatment strategy did not increase the number or the intensity of these side effects [137-140,143].

1.1.10.2.1 Hydrogels for the Delivery of Cisplatin

There is very few data published on the use of hydrogels for the delivery of cisplatin. Most hydrogel studies are still in their preliminary stage focused on the *in vitro* release of drugs over time using different types of hydrogels.

One study however has highlighted the possible benefits of using a hydrogel to deliver cisplatin [144]. In this study, Konishi *et al* developed an injectable gelatine-based

hydrogel and showed that when treating fibrosarcoma tumour bearing mice, the survival rate of mice treated with hydrogel containing 40 µg of cisplatin had significantly increased by 80% compared to those treated with free cisplatin at the same dose [144]. Furthermore, pharmacokinetic studies showed that after administration Pt levels in tumour were higher in the free cisplatin arm in the first 3 hours compared to the cisplatin-hydrogel arm, however, Pt levels were still detected in the cisplatin-hydrogel arm after 2 weeks compared to free cisplatin which was negligible for Pt content. Toxicity studies found no significant difference in weight loss and hematotoxicity between the groups of mice receiving the cisplatin-hydrogel and free cisplatin [144, 145]

Although research using hydrogels as a delivery system for cisplatin is still in its early stage, these results have highlighted some valuable benefits of using hydrogels and have set a platform for future studies.

1.1.10.3 Macrocyclic Cucurbit[*n*]urils

Macrocycles are currently under investigation as drug delivery systems. They are defined by the International Union of Pure and Applied Chemistry (IUPAC) as cyclic macromolecules, and unlike other types of drug delivery systems such as liposomes, dendrimers and carbon nanotubes, macrocycles show potential not only to sequester drugs within their cavity but to also control the rate of drug release [146,147]. A number of macrocycles have shown potential in drug delivery all of which protect the drug from degradation, increase the drug's solubility and shelf life, however, only three of them: cucurbit[*n*]urils (CB[*n*]), cyclodextrins and calixarenes, have been studied extensively [147].

Cucurbit[*n*]uril are a family of macrocyclic compounds that are capable of binding small molecules within their cavity [146, 148]. Over the past few years they have been studied in the laboratory as drug delivery systems and various drugs have been encapsulated within their cavity including: cisplatin, paracetamol, memantine, coumarin, prilocaine, and sanguinarine [148-151].

Cucurbit[*n*]uril was first synthesised by Behren *et al* in 1905 by the acid condensation reaction between glycoluril and formaldehyde, but it was not until the late 1980s that their structure was elucidated by Mock *et al.* [148-151]. The macrocycle was named cucurbit[*n*]uril for its physical resemblance to a pumpkin (which belongs to the cucurbitaceae family) (Figure 1.9) [151].

Structurally, CB[*n*]s contain two hydrophilic carbonyl-lined portals and a hydrophobic interior. The *n* in CB[*n*] represents the number of glycoluril repeats within the macrocycle. To date the CB[*n*] family consists of CB[5], CB[6], CB[7], CB[8], CB[10], and CB[14], a CB[*n*] composed of 9, 11 and 12 glycoluril repeat units have yet to be isolated [151, 152]. All cucurbit[*n*]urils share a common height of 9.1 Å, and their internal cavity volumes ranges are 82, 164, 279, 479 and 870 Å³ as the glycoluril units (*n*) increases respectively (CB[14] does not have a normal cavity like the other CB[*n*] and has the appearance of a folded, figure of eight conformation) [151].

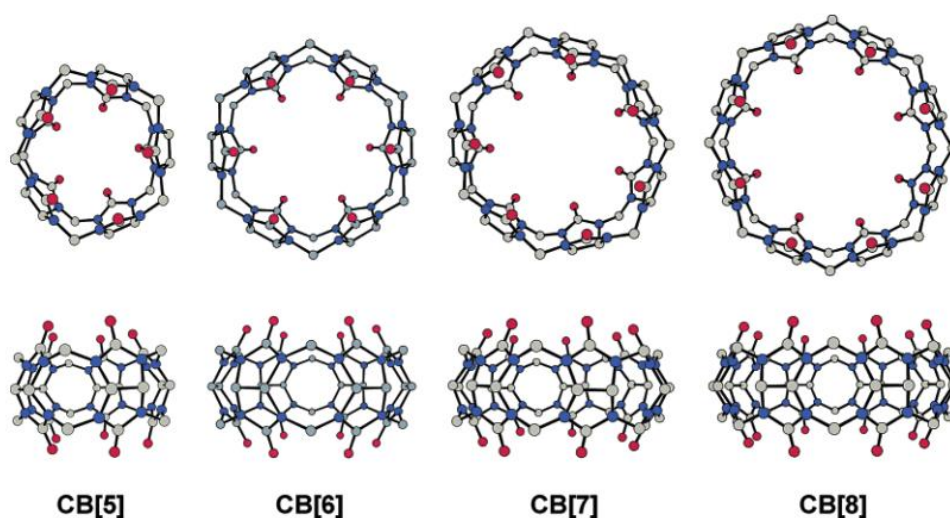


Figure 1.9. Image of an x-ray crystal structures of CB[5], CB[6], CB[7] and CB[8]. The top panel is a bird view image of the CB[n] cavity sizes and the bottom panel is a side view image. Colour codes; carbon (grey), nitrogen (blue), oxygen (red). Taken from <http://en.wikipedia.org/wiki/Cucurbituril>.

The most commonly used cucurbit[n]urils in drug delivery are CB[6], CB[7] and CB[8]. Studies have shown that the cavity of CB[5] is too small to incorporate drugs and the cavity of CB[10] is too large for prolonged drug encapsulation [153].

NMR, X-ray crystallography and molecular modelling studies have shown that guests can be fully or partially encapsulated within the CB[n] cavity. Drug encapsulation is achieved via ion-dipole interactions, formation of hydrogen bonds between the hydrogen atoms of the guest molecules and the oxygen atoms at the portals of the CB[n], or by hydrophobic interactions between guest molecule inside the cavity [148, 151, 154, 155, 160-162].

There are many advantages associated with using CB[n]s as drug delivery vehicles. Studies have shown that the encapsulation of a drug within the cavity of a CB[n] shields the drug from premature degradation, hydrolysis, sulfation and prevents the unwanted interaction of drug with proteins [145, 147, 151, 153]. Encapsulation has also been found to increase the drug's solubility and decrease its toxic side effects due to controlled drug release [147-153, 157] .

1.1.10.3.1 Cucurbit[7]uril as a Cisplatin Drug Delivery System

Cucurbit[7]uril has shown promising potential as a platinum drug delivery vehicle. Recent *in vivo* studies by Wheate *et al*, have shown that the encapsulation of the dinuclear platinum drug BBR3571 by CB[7] increased the drug's MTD (maximum tolerated dose) in mice by 70% from 0.1 mg/kg to 0.45 mg/kg and that the encapsulated complex was just as active as the free drug. In a separate study, although the encapsulation of cisplatin by CB[7] showed no change in cisplatin's *in vitro* cytotoxicity in the human ovarian carcinoma cell line A2780, it showed significant effect on *in vivo* cytotoxicity in a human tumour xenograft model where it overcame acquired resistance via a pharmacokinetic effect [154-156].

For any possible future use of CB[n], in the clinic as drug delivery vehicles, they must not only demonstrate that they are able to increase the efficacy of the encapsulated drug and/or decrease their associated side effects, but they must also demonstrate that they are themselves inert and non-toxic.

Fortunately, a number of studies have shown that CB[7] has no *in vitro* or *in vivo* toxicity. In a recent study at concentrations of up to 1 mM, CB[7] demonstrated no

toxicity in a range of human cell lines including: the human A549 non-small lung cancer, SKOV-3 ovarian cancer, SKMEL-2 melanoma, XF-498 brain cancer and HCT-15 human colon cancer [152, 153]. Also, when delivered intravenously at a dose of 250 mg/kg, CB[7] showed little sign of toxicity (only a body weight loss of 5%, four days after injection) [155-157]. In a separate study an *in vivo* intravenous administration of CB[7] showed no toxicity up to 200 mg/kg and when administered as a fast injection and at higher doses (200-250 mg/kg) mice went into a shock-like state [152]. These results highlight the potential use of CB[7] in cancer therapy as a method of increasing drug bioavailability and efficacy while not inducing any side effects.

1.1.10.3.1.1 Binding of Cisplatin@CB[7]

Molecular models of how cisplatin is encapsulated within CB[7] have been predicted from ^1H NMR and ^{195}Pt NMR spectrums. The most energetically favourable binding mode seems to occur with the platinum atom and the two chloride ligands of cisplatin located within the cavity of CB[7] (Figure 1.10 a).

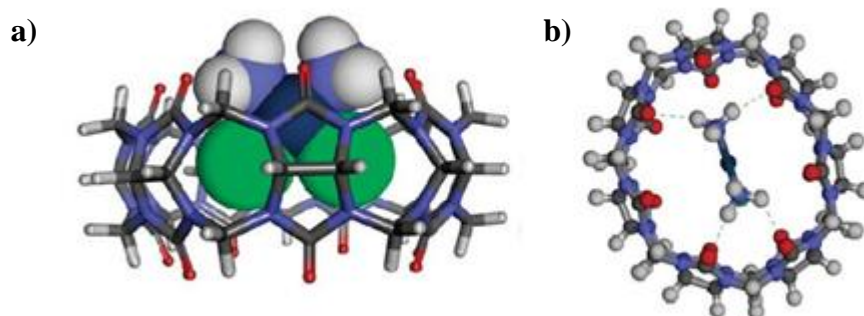


Figure 1.10. Molecular model image of the preferred binding mode of cisplatin to CB[7]. A) molecular model showing the chloride ligands of cisplatin (green) are pointing into the cavity and b) the four hydrogen bonds (dashed lines) from cisplatin's ammine hydrogen atoms to the CB[7] carbonyl oxygen atoms. [108]

In this manner of binding, four hydrogen bonds operate between the ammine hydrogens of cisplatin and the oxygen of the CB[7] portal carbonyl groups (Figure 1.10). These hydrogen bonds have been calculated to have lengths of 2.15, 2.22, 2.38 and 2.11 Å that stabilise the encapsulation [108, 153]

1.1.11 Aim of The Thesis

Cisplatin still remains the mainstay of cancer therapy despite its severe dose limiting side effects and the emergence of cisplatin resistant cancer cells. Over the years, scientists have been encouraged to develop methods that enhance the efficacy of cisplatin through increasing its bioavailability, decreasing its toxic side effects and circumventing drug resistance. One such approach which has shown some success is the reformulation of drugs by their encapsulation within drug delivery systems.

Various studies have shown the potential of using CB[*n*] as a drug delivery system for cisplatin in the treatment of cancer, however, more information is needed regarding the toxic side effects of CB[*n*] and cisplatin@CB[*n*] (cisplatin encapsulated by cucurbit[*n*]urils) before they can be used clinically. Furthermore, there are no published research that investigate the effect of a two layered drug delivery system for the delivery of cisplatin.

The practical work of this thesis is divided into two sections:

a) In the first section a novel implantable hydrogel has been developed for the delivery of cisplatin and cisplatin encapsulated by CB[7]. In this section titled “A gelatine and

PVA-based implantable hydrogel for the delivery of cisplatin and cisplatin encapsulated by cucurbit[7]uril” the focus is to:

- Design of a novel implantable polymer-based hydrogel for the delivery of cisplatin and cisplatin@CB[7].
- Study the swelling and drug release rates of hydrogels with different polymer content to find the optimal hydrogel for *in vivo* studies.
- Study the *in vitro* efficacy of cisplatin and cisplatin@CB[7] loaded hydrogels.
- Study the *in vivo* efficacy of cisplatin and cisplatin@CB[7] loaded hydrogels.

b) The second section of this thesis is titled “The neurotoxic, neuromyopathic and cardiotoxic effects of platinum –based drugs and macrocyclic delivery systems”, and the aims of this section includes:

- To Investigate the *ex vivo* neurotoxic, neuromyopathic and cardiotoxic activity of various platinum-based drugs using the mouse sciatic nerve, chick biventer cervicis muscle and rat heart atria preparations, respectively.
- To investigate the *ex vivo* neurotoxic, neuromyopathic and cardiotoxic activity of various macrocycles using the mouse sciatic nerve, chick biventer cervicis muscle and rat heart preparations, respectively.
- Study the effect of the encapsulation of cisplatin by CB[7] on cisplatin’s *ex*

vivo neurotoxic, neuromyopathic and cardiotoxic activity.

Chapter 2

A Gelatine and PVA-Based Implantable Hydrogel for the Delivery of Cisplatin and Cisplatin Encapsulated by Cucurbit[7]uril.

2.0 Implantable Hydrogels

The delivery of drugs for pharmaceutical and medical applications is usually achieved through the use of topical, intravenous or oral routes such as sprays, injections and tablets [165, 166]. These systems must deliver the correct therapeutic dose of the drug in an efficient manner; that is in a way that maintains the optimal concentration of drug within the bloodstream for a reasonable period of time [165, 166].

The intravenous route is by far the most common method of anticancer drug delivery [165]. However, drugs are prone to early proteolytic degradation at the injection site, therefore creating a short drug plasma circulation time [165]. In order to maintain drug effectiveness another dose of drug is usually required, however, multiple daily injections decrease patient compliance and an increased drug dose induces severe toxic side effects [165, 166].

Over the past few decades controlled drug delivery systems such as implantable hydrogels have emerged in which drug release can be controlled and maintained over a long period of time [167, 168]. Hydrogels were introduced in the late 1960s and since then have had many applications across various scientific fields ranging from food additives to tissue engineering and biomedical implants [168]. They can be easily formulated into a variety of physical forms such as; slabs, nanoparticles, microparticles, coatings and films, and are now under investigation as controlled drug delivery systems in the treatment of cancer [168].

2.1 Hydrogel Drug Loading

Hydrogels have a unique physical property of high porosity that can be easily tuned by controlling the density of polymer cross-links in the matrix [169-172]. This has labelled hydrogels as a class of “intelligent” drug delivery systems, because the porosity allows drug uptake and subsequent drug release at a rate dependent on the diffusion coefficient of the drug molecule through the gel matrix [169-172].

The ability to load and release drugs from the hydrogel matrix depends on a variety of factors. This includes the number and dimensional size of the hydrogel pores as well as the size and charge of the drug to be loaded [167, 174]. Hydrogels with higher polymer concentrations are physically stronger, stiffer, with smaller pore sizes and slower drug release as a result of the high cross-linking network produced [166, 169]. Drug release from hydrogels can be triggered by physical or chemical changes and complete drug release time can be anywhere from hours, to months, to years [166, 171, 175]. There are three main methods reported by which hydrogel drug encapsulation occurs; through permeation, entrapment and covalent attachment [165, 167, 172, 173].

2.1.1 Drug Loading by Permeation, Entrapment and Covalent Interactions

Drug permeation involves submerging a fully formed hydrogel into medium saturated with the drug. Depending on the type of hydrogel, the size of its pores, size and charge of drug, the therapeutic will slowly diffuse into the gel over a period of time. The drug release profile for this loading approach shows a rapid release of drug at the first stages of hydrogel swelling. This has been reported to be as high as a 70% drug loss [166, 167, 172, 176].

In the entrapment method the drug is mixed with the polymer solution before gelation takes place. Both hydrophilic and hydrophobic molecules can be loaded and a moderate drug release profile that lasts between days to months has been reported [166,167, 177].

Drugs that are covalently linked to hydrogel polymers require an enzymatic reaction to cleave the drug from the polymer or to degrade the hydrogel. In this case, the hydrogel must be chemically or enzymatically degraded before the drugs can be released [166,167,178].

2.1.2 Importance of Hydrogel Polymer Composition on the Rate of Drug Release

A major advantage that hydrogels possess is that drug release from their matrix can be controlled through tailoring the hydrogel's polymer concentration. Polymeric controlled release formulations offer a sustained release mechanism in which the rate of drug release can be controlled by substituting polymers with lower molecular weights with those that have higher molecular weights such as PLGA (Poly lactic glycolic acid) or by increasing the polymer concentration within the hydrogel. Various studies have shown that by modifying the polymer composition of the hydrogel, slower swelling and degradation rates can be achieved and thus subsequent slower drug release rates [179-181].

Both hydrophilic and hydrophobic polymers can be used to design hydrogels, however care must be taken when choosing these polymers as hydrophobic polymers can induce detrimental effects to the encapsulated drug/peptide/protein and may trigger host

immune responses. Whereas on the other hand, hydrophilic polymers provide mild network fabrication and can also trigger a host immune response [169, 171, 177, 179]

Hydrogels can be prepared from either natural or synthetic polymers. Although hydrogels made from natural polymers may not provide sufficient mechanical properties and may evoke immune or inflammatory responses as they can contain pathogens, they offer several advantages over synthetic polymers including biocompatibility, biodegradability and biologically recognisable moieties that support cellular activities [169, 171, 177-179].

2.1.3 Focus of This Study: An Implantable Hydrogel for the Delivery of Cisplatin

Due to the above reasons, and because there have been no previous investigations on implantable hydrogels for the delivery of cisplatin, two natural polymers were chosen to design an implantable hydrogel for the delivery of cisplatin. The effect of different polymer compositions on drug release was investigated *in vitro* in order to choose the optimal hydrogel for *in vivo* anti-tumour studies. Furthermore, a two layered drug delivery system consisting of cisplatin encapsulated by CB[7] and its further encapsulation within a hydrogel was developed and examined for its anti-tumour effect compared to cisplatin encapsulated by hydrogel. The effect of a two layered delivery system for cisplatin has not previously been examined and thus is of novel interest.

Nude mice bearing human tumour xenografts were used in this PhD research to investigate the anti-tumour efficacy of drug loaded hydrogels. In the following section

a brief overview of nude mice and why they are considered as good and predictive models for anticancer drug activity is explained.

2.1.4 The Use of Nude Mice in Cancer Research

Since its discovery in 1966, the mutant nude mouse has been an invaluable tool in both the study of the molecular mechanisms of cancer and in the development of new anticancer drugs [183-185].

The existence of the nude mouse is a result of a mutation in the FOXP1 (forkhead box protein N1) gene that leads to two major defects: abnormal hair growth and a defective thymus [185-187]. Although the mice appear hairless (hence the name “nude”), they are born with functional, but faulty hair follicles, and the development of a defective thymus results in a lack of cell mediated immunity [187]. Nude mice do not have T cells and are therefore unable to defend themselves against bacterial or viral infections, malignant cells, synthesise most antibodies or reject tissue grafts [186-190]. The adaptive immune response of the nude mice is so limited that they accept grafted tissue from other species (xenografts) [189-190]. This makes them an excellent host for cancer research, as they allow for the study of human tumours within them [186-190].

Various types of human tumours have been transplanted into nude mice over the past 15 years, including: brain, colon, skin, lung, ovarian, prostate and lung tumours, however, not all tumours can grow in nude mice [185, 190]. Tumour growth has been found to depend on the origin, type, inoculation site, and age of the mouse amongst other factors [190].

2.1.4.1 Human Tumour Xenografts as Predictive Models for Anticancer Drug Activity

Numerous murine models have been developed over the years to study human cancers and the factors involved in its malignant transformation, invasion and metastasis as well as the response to tumour cells to novel therapeutic agents [185, 191-194] . One of the most widely used methods is the human xenograft model. In this model human tumour cells are transplanted into nude mice [191]. Depending on the number of cells injected, or the size of the tumour transplanted into the mice, the tumour can take between a week to months to grow, and the response of the tumour to specific chemotherapeutic drugs can be studied [191, 194].

Several advantages are associated with the use of human tumour xenografts to study the therapeutic response of an agent; most importantly, the ability to use actual human tumour tissue which features the complex genetic and epigenetic abnormalities that exist in human tumour populations. In addition, multiple therapies can be tested from a single tumour biopsy and results can be obtained in a matter of days to weeks regarding response to therapy [195].

The main types of responses to therapy that are studied using a human tumour xenograft model include: effect of the therapy on the tumour growth rate, tumour shrinkage and overall survival rate [191-196].

2.1.5 Aims of This Chapter

- Design of a novel implantable gelatine and polyvinyl alcohol based hydrogels for the delivery of cisplatin and cisplatin@CB[7] (cisplatin encapsulated within CB[7]).
- Study the swelling and drug release rates of hydrogels with the same gelatine content but different polyvinyl alcohol content (0% to find the optimal hydrogel for *in vivo* studies).
- Study the *in vitro* efficacy of hydrogels with different polymer content on human ovarian A2780 cells and their cisplatin resistant A2780/CP70 sub-line.
- Study the *in vivo* efficacy of a hydrogel containing cisplatin@CB[7] compared to free cisplatin in nude mice containing A2780/CP70 xenografts.

2.2 Materials and Methods

2.2.1 Materials

2.2.1.1 Materials used in the preparation of hydrogels

Cisplatin, PVA (polyvinylalcohol) and gelatin were bought from Sigma-Aldrich. Cucurbit[7]uril was bought from Dr Anthony Day, University of New South Wales, Australia.

2.2.1.2 Materials used in the *In Vitro* Hydrogel Toxicity Studies

The human ovarian cell lines A2780 and CP70 and the colon HCT 116 cell line were obtained from Invitrogen® and the cisplatin resistant ovarian cell line A2780/CP70 was derived in house at the Beatson Cancer Institute, Glasgow from an A2780 line obtained from Dr R.F. Ozols (Fox Chase Cancer Centre, Philadelphia, PA). Cells were maintained in Roswell Park Memorial Institute medium (RPMI, invitrogen) supplemented with 10% heat inactivated fetal calf serum, and 1% L-glutamin. Cells were maintained in 5% CO₂ at 37°C and sub-cultured every 3-4 days to maintain growth.

2.2.1.3 Materials used in the *In Vivo* Hydrogel Anti-tumour Efficacy Study

CD-1 ® athymic nude mice were obtained from Charles River laboratories and were housed in a sterile environment in the biological services unit at the Beatson Institute of Cancer Research. Animal studies were carried out under an appropriate United Kingdom Home Office Project License, and all work was conformed to the UKCCR guidelines for the welfare of animals in experimental neoplasia.

2.2.2 Methods

2.2.2.1 Synthesis of cisplatin@CB[7]

Equimolar quantities of cisplatin and CB[7] were stirred in distilled water in a beaker at room temperature until fully dissolved. The resultant solution was then transferred into a round bottom flask and rotary evaporated to dryness. The remaining powder (cisplatin@CB[7]) was then scrapped off from the round bottom flask and transferred into a vial for future use. The binding of cisplatin to CB[7] was confirmed by nuclear magnetic resonance (NMR) and the molecular weight confirmed by mass spectrometry. This was done in collaboration with the chemistry department at Strathclyde University.

2.2.2.2 Hydrogel Synthesis

Polyvinyl alcohol (0, 2 and 4% w/v) was dissolved in 10 mL of water with stirring at 130 °C. When fully dissolved, 960 mg of gelatin was added and the mixture was allowed to stir for a further 2 h at 90 °C. The mixture was poured into molded plastic tablet strips and then cooled to room temperature, at which time the formulation turned semi-solid. Samples were stored at 4 °C until needed. To prepare cisplatin and cisplatin@CB[7] hydrogels, the PVA and gelatin mixtures were dissolved in water containing the desired concentration of drug then poured into molded plastic tablet strips that had dimensions of either 4 x 7 mm for *in vitro* studies or 5 x 10 mm for *in vivo* studies and then cooled to room temperature.

2.2.2.3 *In Vitro* Hydrogel Swelling

Hydrogel swelling was monitored over a 7 day period. Hydrogels of a homogenous volume containing 0, 2 and 4% PVA were placed in 200 mL phosphate buffered saline (PBS) in a beaker at room temperature. The extent of swelling was monitored by recording the weight of the hydrogels at specific hourly intervals until the hydrogels dissolved and could no longer be weighed (six days). Each hydrogel had an *n* of 4 and the average weight was calculated with SEM.

2.2.2.4 Hydrogel Surface Imaging

The hydrogels were placed on a glass strip and examined under a DXR Raman microscope at 100 times magnification. The pore sizes were analysed and measured using the μ View PC computer program. Only one hydrogel sample was used for each group.

2.2.2.5 *In Vitro* Drug Release

Hydrogels of 0, 2 and 4% PVA containing 3 mM cisplatin were incubated in 200 mL of PBS at room temperature in a closed glass container. At hourly intervals for a period of five hours, 5 mL of solution was extracted and its platinum content determined by inductively coupled plasma mass spectrometry (ICP-MS) in collaboration with the chemistry department at the University of Strathclyde. An Agilent 7700X instrument, with a micromist nebuliser and an octapole collision cell, was calibrated using solutions prepared from a Spex CertPrep platinum standard at concentrations ranging from 0 – 1000 ppb, containing 2% nitric acid. The platinum drug concentration was determined using the ^{195}Pt isotope. Instrument operating conditions used were 1,550 W RF forward power, 0.85 L min⁻¹ plasma carrier gas flow, 0.2 L min⁻¹ makeup gas

flow, 4.6 mL min⁻¹ helium gas flow in the collision cell and 0.1 rps for the nebulizer pump. Sample depth was 8 mm, sample period was 0.31 s and integration time was 0.1 s. A Calibration curve between the instrument response and actual known concentration of the analyte was produced. Quantitation was based on linear regression analysis. Correlation coefficient greater than 0.99 ($r > 0.99$) was accepted for each standard curve.

2.2.2.6 Effect of Hydrogel on *In Vitro* Cytotoxicity

Cisplatin resistant cells (A2780/CP70) were seeded into 24 well plates at a density of 900 cells per well and allowed to attach and grow for 48 h before drug treatment. Cells were then exposed to either 0, 2 and 4% PVA hydrogels containing either 1 mM cisplatin or 1 mM cisplatin@CB[7] for 24 h at 37°C under a 5% CO₂ atmosphere. The medium containing drug was then removed and fresh medium was supplied to the cells and re-incubated for a further 72 h. On the final day, dead cells were washed away with cold PBS, and the remaining cells fixed with methanol and stained with crystal violet blue. Cells were then dissolved in DMSO and the fluorescence reading of each plate was measured at 590 nm.

2.2.2.7 *In Vivo* Effectiveness of Hydrogels

For the A2780/CP70 xenografts, monolayer cultures cells were harvested with trypsin/EDTA (0.25%/1 mM in PBS), cells were then collected and centrifuged at 300g for 5 minutes. The supernatant was then discarded and the cell pellet was re-suspended in sterile PBS to achieve a concentration of 5-10 x 10⁷ cells per 100µL. Between 100-200µL of the cell suspension was then injected subcutaneously into the flank of immunodeficient nude mice using a 1 mL syringe with 23G needle. Mice were

inspected once every 2-3 days for general welfare and tumour growth. Once the mean diameter of the tumours had reached ≥ 0.5 cm mice were randomised into groups of six for experiments. Mice were then treated with either an intraperitoneal dose of saline, cisplatin (150 μg) or with a 2% PVA hydrogel containing either free cisplatin (30 μg) or cisplatin@CB[7] (30 μg). To implant the hydrogels a small incision was made in the skin of the mice near the tumour, the hydrogels were placed under the skin, which was then resealed with a clamp. Mice were weighed daily and tumour volumes were estimated by calliper measurements assuming spherical geometry (volume = $d^3 \times \pi/6$), where “d” is the mean of the two perpendicular diameters. This study was completed in collaboration with Dr Jane Plumb and this type of tumour measurement was performed as it was standard practice within the Beatson Institute of Cancer Research.

2.2.2.8 Statistics

Significant differences between groups were identified by ANOVA (analysis of variance) and Bonferroni’s multiple comparison post-tests. The significance level of individual differences was determined by Student’s- *t*- test. A statistical significant difference was deemed to be present when $p < 0.05$.

2.3 Results

2.3.1 Cisplatin@CB[7] Binding

The binding of cisplatin to CB[7] was confirmed by ^1H NMR. Results show that when cisplatin is added to CB[7] there is a division of the CB[7] peak resonance at 5.6 ppm (parts per million). This is split into two peaks; one peak is shifted at 5.63 ppm and one downfield at 5.55 ppm (Figure 2.3.1). Additionally, the CB[7] doublet peak at 4.2 ppm splits in a similar manner. These splitting of the CB[7] resonances indicate that cisplatin is encapsulated by CB[7] as previously reported by Collins *et al* [108].

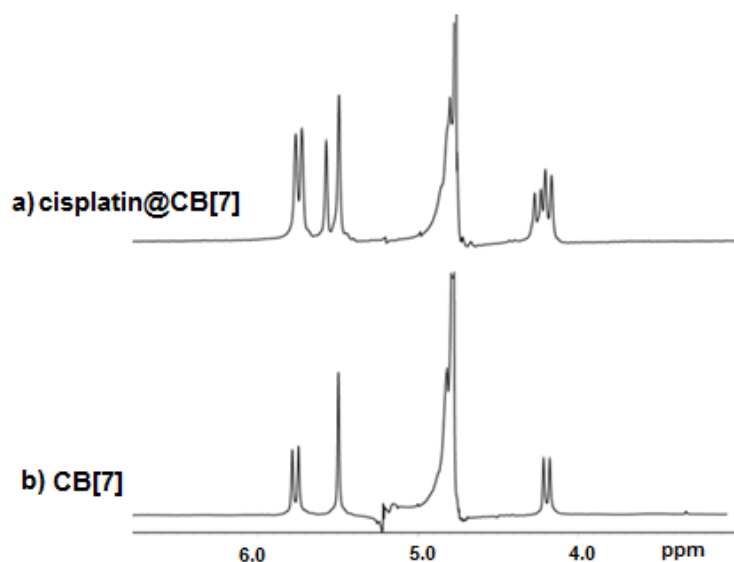


Figure 2.3.1. Confirmation of cisplatin binding within CB[7]. ^1H NMR spectra of a) cisplatin@CB[7] and b) CB[7]. The CB[7] resonance spike at 5.66 ppm and 4.2 ppm is split into two spikes in the addition of cisplatin confirming binding of drug to macrocycle.

2.3.2 Hydrogel Synthesis

Hydrogels were synthesized by dissolving PVA in hot water (130 °C) containing drug. Once fully dissolved, gelatin was then added to the mixture. The resultant solutions were then poured into plastic tablet strips and subsequently cooled to room temperature (bench top) which resulted in semi-solid, transparent hydrogels (Figure 2.3.2). Each hydrogel had either dimensions of 4 x 7 mm which were used for swelling, disintegration, drug release and for *in vitro* studies or 5 x 10 mm which were used for *in vivo* studies. Three types of hydrogels all containing gelatin but with varying concentrations of PVA: 0, 2 and 4% w/v, were synthesised. The hydrogels were stored in the freezer (4 °C) until required and then thawed for 2 hours before use.

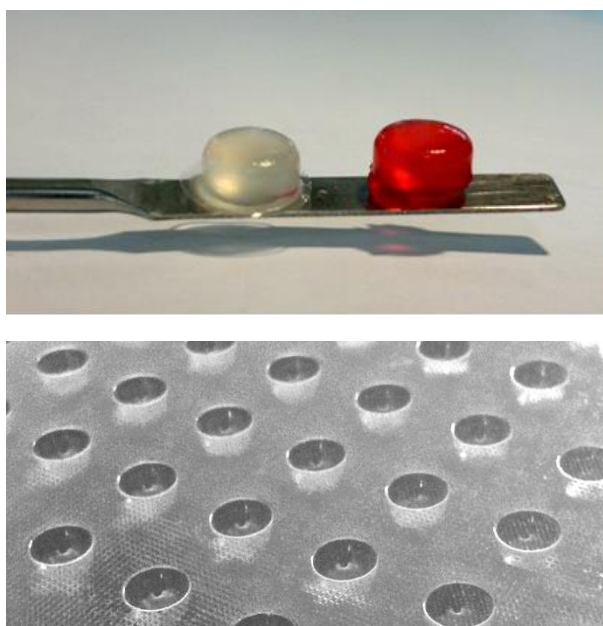


Figure 2.3.2. An example of a PVA and gelatin based hydrogel. Red dye was used for imaging purposes only (top panel) and the plastic tablet strip used in moulding the hydrogels (bottom panel).

2.3.3 Hydrogel Swelling

Hydrogel swelling was examined in PBS by measuring the mass of each individual hydrogel over a seven day period. The results (Figure 2.3.3) indicates two sequential events taking place. Initially the hydrogels swell with water growing up to 227% of their original size (0% PVA swelled by $227 \pm 13.6\%$ by 24 hr, 2% PVA swelled by $183.7 \pm 3.3\%$ by 48 hr and 4% PVA by $205 \pm 13.9\%$ by 96 hours). At their maximum size a tipping point is reached and the absorption of more water results in the gradual disintegration of the hydrogel until it loses all of its physical structure (the hydrogel slowly dissolved until it could not be lifted from solution using a spatula).

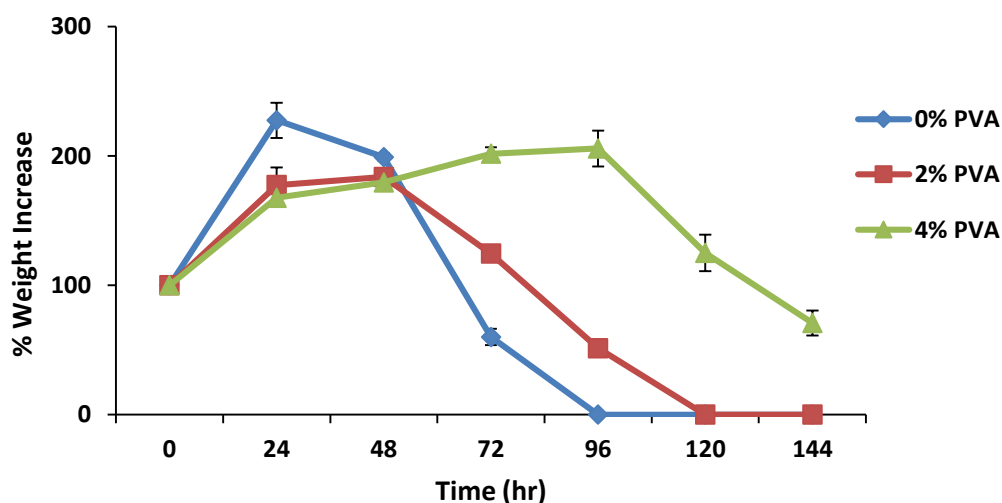


Figure 2.3.3. The rate of hydrogel swelling in PBS. Hydrogels of different PVA content; 0% PVA (blue), 2% PVA (red) and 4% PVA (green) where immersed in PBS solution and their weight was monitored every 24 hours over a period of six days. Results are expressed as the means \pm SEM ($n=3$). Statistical one way Anova with Bonferroni's multiple comparison post-tests was performed.

Even within the first three hours differences in the swelling rates between the three hydrogels can be observed (Figure 2.3.3). The gel with no PVA has a swelling peak time of 24 hours after which it disintegrates over the next three days. The gel with 2%

PVA swells for twice as long (48 hours) but disintegrates over the same length of time (three days). The gel which contains 4% PVA displays the longest peak swelling time of 3.5 days and has not fully disintegrated even by day six. The results show a clear correlation between the amount of PVA and the rate of its swelling and disintegration in that hydrogels with higher PVA content took the longest to swell and disintegrate. Bonferroni's multiple comparison post-tests was performed and showed that all hydrogels were statistically significant to each other $p < 0.05$ for (0% PVA vs 2% PVA, 0% PVA vs 4% PVA and 2% PVA vs 4% PVA).

2.3.4 Hydrogel Drug Release

Hydrogels with either 0, 2 or 4% w/v PVA and with an effective drug concentration of 3 mM were incubated in PBS at room temperature at intervals for up to 5 hours. Drug release is observed within 10 minutes and continues over the next 5 hours (Figure 2.3.4).

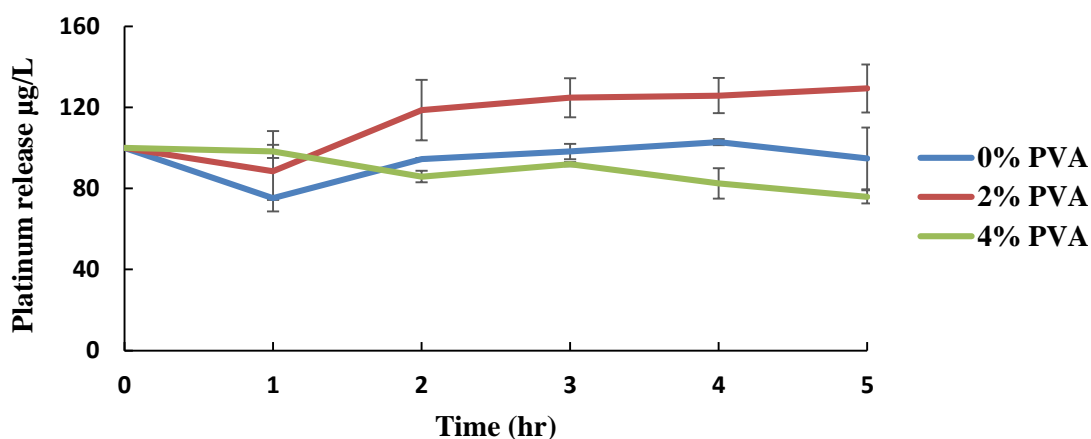


Figure 2.3.4. Rate of drug release from hydrogels with different PVA concentrations. The drug release rates from hydrogels containing different PVA content: 0% (blue), 2% (red) and 4% (green) PVA incubated in PBS over a period of 5 hours. The results are expressed as mean \pm SEM ($n = 3$). Statistical one way Anova with Bonferroni's multiple comparison post-tests was performed.

From figure 2.3.4 it can be seen that there was a statistically significant difference between the different gel compositions; by the end of the experiment hydrogels with 0% PVA released $94.8 \pm 15.3 \mu\text{g/l}$, 2% PVA hydrogel $129.4 \pm 11.9 \mu\text{g/l}$ and 4% PVA $76 \pm 3.27 \mu\text{g/l}$ of cisplatin. Bonferroni's multiple comparison post-tests was performed and showed statistical significance in the amount of drug released between 0% PVA and 2% PVA ($p < 0.05$) and 2% PVA vs 4% PVA ($p < 0.05$) while no significant difference was found between 0% PVA vs 4% PVA ($p > 0.05$).

Figure 2.3.3 also shows that the 4% PVA hydrogel followed the same trend as the 0% PVA and 2% PVA hydrogel in the first hour, in which there is a similar level of drug release; however, compared to the 0% and 2% PVA hydrogels which show a continued and gradual increase of cisplatin release, the 4% PVA hydrogel reaches its peak drug release at one hour after which drug release in the solution does not increase. This could be a result of the much slower swelling and disintegration of the 4% PVA hydrogel compared with the other hydrogels. No statistically significant difference is observed in the amount of drug that is released between the 0 and 4% PVA hydrogels over the 24 hour period.

2.3.5 Hydrogel Surface Features

The swelling, disintegration and drug release results may possibly also be explained in part by the varying porosity of the hydrogels with different PVA concentrations. From optical microscope images of intact hydrogels, significant surface differences are observed for each hydrogel with the average surface indentation size decreasing with increasing PVA content (Figure 2.3.5). The surface of the 0% PVA hydrogels is characterised by a small number of very large indentations with diameters between 38

- 45 μm . In contrast, the 2% PVA hydrogels have many more indentations but they are considerably smaller; 4 - 11 μm in diameter. The 4% PVA hydrogels show almost a perfectly smooth surface with few indentations which average less than 1 μm in size.

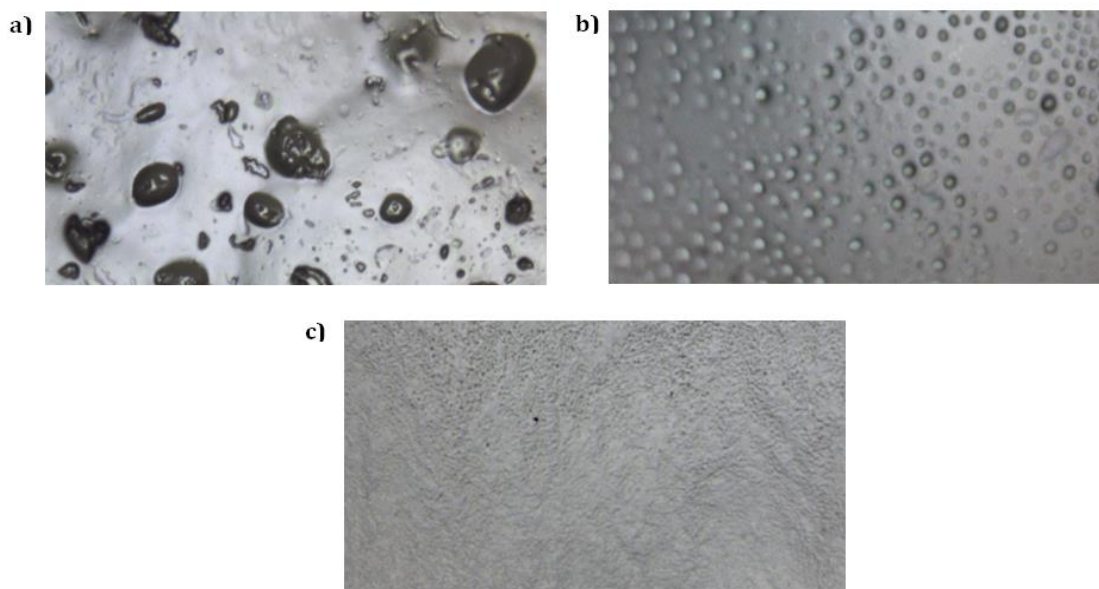


Figure 2.3.5. Surface features of hydrogels. Optical microscope images of (a) 0% PVA, (b) 2% PVA and (c) 4% PVA demonstrating the differences in surface features between the hydrogels.

2.3.6 *In Vitro* Efficacy of Cisplatin and Cisplatin@CB[7] Loaded Hydrogels

The effect of the hydrogels on the cytotoxicity of free cisplatin and cisplatin@CB[7] was determined using *in vitro* growth inhibition assays with A2780/CP70 cisplatin-resistant ovarian carcinoma cells. Unlike conventional *in vitro* assays which use 96 well plates, the hydrogels were examined using 24 well plates. For each plate, individual hydrogels were placed inside a permeable insert, which were then fully submerged into separate wells. Each well contained the cancer cells and media (Figure 2.3.6). As media is absorbed by the hydrogels within the insert, they slowly swell and

disintegrate, releasing the drug to the outer well where it could then be taken up by the cancer cells.



Figure 2.3.6. Images of the hydrogel well inserts. Examples of the 24 well plates used to examine the *in vitro* cytotoxicity of the hydrogels showing the inserts with inlet channels containing a hydrogel (left panel) and the outer wells with just media in the first column and with fully submerged hydrogel containing inserts in the second, third and fourth columns of the plate (right panel).

On the final day of the experiment, dead cells were washed away and the remaining cells fixed with methanol and stained with crystal violet blue (Figure 2.3.6.1). Cells were then dissolved in DMSO and the absorbance reading of each plate was recorded at 590 nm.

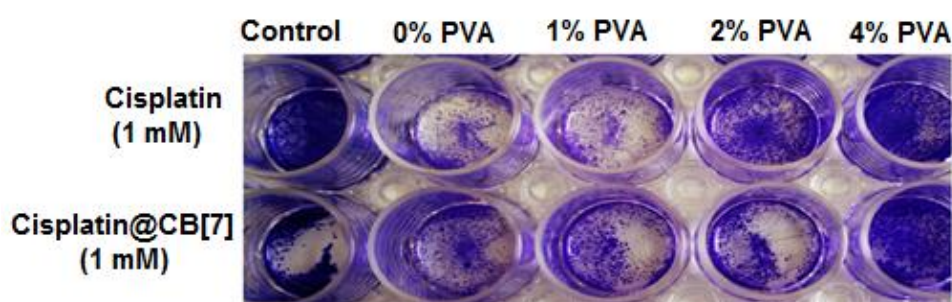


Figure 2.3.6.1. Image of the crystal violet blue stained cells after treatment with various concentrations of PVA based hydrogels containing either 1 mM cisplatin or 1mM cisplatin@CB[7].

Cytotoxicity is expressed as the cell viability as a percentage of growth inhibition compared with untreated cells (Figure 2.3.6.2).

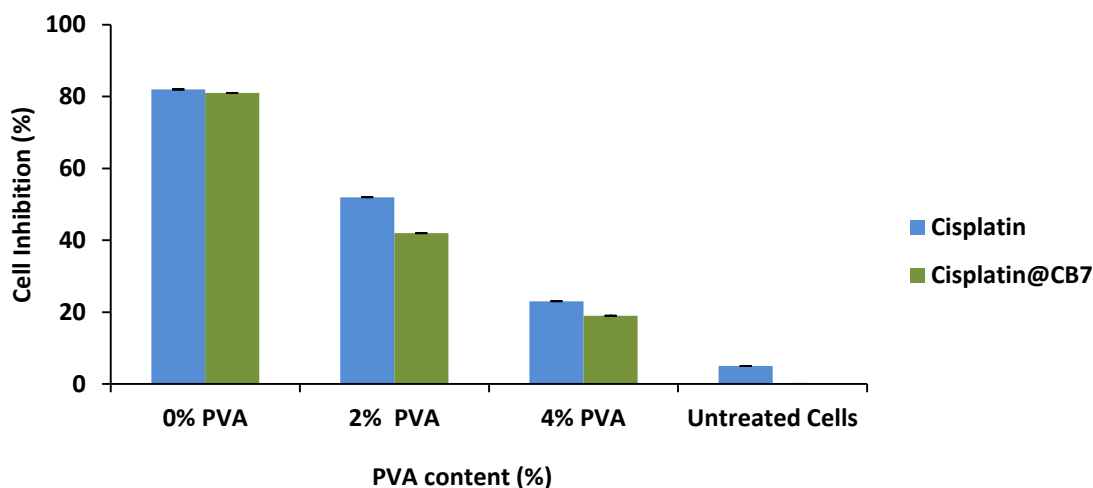


Figure 2.3.6.2. Rate of cell growth inhibition induced by hydrogels of different PVA concentrations. Graph showing the relative growth inhibition of ovarian A2780/CP70 cells by hydrogels of different PVA content (0%, 2% and 4%) containing either 1mM of cisplatin or 1mM cisplatin@CB[7] compared to untreated cells. Results are expressed as mean \pm SEM ($n = 4$). Statistical two way Anova with Bonferroni's multiple comparison tests was performed.

The results (Figure 2.3.6.2) show that as the PVA concentration increases the number of cells killed decreases. This could be the result of a slower drug release system developed; as the PVA concentration increases, the slower the swelling and disintegration of the hydrogel and thus the slower release of drugs.

Hydrogels containing 0% PVA induced the highest cytotoxicity by inhibiting cell growth by $82.1 \pm 0.01\%$ in the cisplatin arm and by $81.2 \pm 0.003\%$ in the cisplatin@CB[7] arm. In comparison, hydrogels containing 2% PVA showed a

moderate inhibition of cell growth by $51.7 \pm 0.04\%$ in the cisplatin arm and by $42 \pm 0.02\%$ in the cisplatin@CB[7] arm, whereas hydrogels containing 4% PVA released the smallest amount of drug and induced an inhibition of cell growth by $23 \pm 0.03\%$ in the cisplatin arm and $19 \pm 0.01\%$ in the cisplatin@CB[7] arm. Post Bonferroni's multiple comparison post-tests was performed and showed that hydrogels of 4% PVA containing either cisplatin or cisplatin@CB[7] were significantly more cytotoxic than hydrogels of 0% PVA and 2% PVA containing cisplatin or cisplatin@[CB7], respectively ($p < 0.05$). However, statistical analysis also showed that there was no significant difference between the cytotoxicity of cisplatin compared to cisplatin@CB[7] of the same hydrogel PVA content. For example 4% PVA hydrogels containing cisplatin showed no significant difference in cytotoxicity compared to 4% PVA hydrogels containing cisplatin@CB[7]. These results are consistent with earlier *in vitro* studies conducted by Dr Jame Plumb at the Beatson Institute that showed there was no comparable difference in the *in vitro* cytotoxicity of free cisplatin compared to cisplatin@CB[7]. In this study Plumb *et al* calculated that the IC_{50} of cisplatin in the A2780/CP70 cells was $0.11 \pm 0.01 \mu\text{M}$, and for cisplatin@CB[7] it was $0.09 \pm 0.01 \mu\text{M}$. Overall, the results in this study show that by increasing the hydrogel PVA content, fewer cells are killed as a result of a slow drug release system developed.

2.3.7 *In Vivo* Anticancer Efficacy of Cisplatin and Cisplatin@CB[7] Loaded Hydrogels

To examine the *in vivo* antitumour effectiveness of the hydrogels, nude mice bearing A2780/CP70 xenografts were treated with saline, intraperitoneal free cisplatin (150 μg) and two different implantable hydrogels which both contained 2% PVA and either

free cisplatin (30 μg) or cisplatin@CB[7] (equivalent to 30 μg of cisplatin). In order to limit the number of animals required for this study only hydrogels of 2% PVA were chosen. From the previous *in vitro* studies, 0% PVA hydrogels exhibited a too fast drug release system and 4% PVA a too slow release system, therefore a moderately slow system was chosen.

Due to the slow release nature of the hydrogels, their effect on tumour growth delay was monitored over a period of two weeks. Because the xenograft is highly cisplatin resistant a high intravenous dose of cisplatin (150 μg per animal) was needed to delay tumour growth significantly (tumour grew to only 42% size of the control tumours over the same time period). With an average body weight of 25 g per animal each hydrogel implant gives a total drug dose of ~ 1.2 mg/kg, which is well below the maximum tolerated dose of cisplatin in this bred of animal. As such, the hydrogels were well tolerated by the mice with no significant change in body weight in the first two days after implantation.

Figure 2.3.6 shows the anti-tumour effect of each arm of this study (control, free cisplatin, 2% PVA hydrogel containing cisplatin and 2% PVA hydrogel containing cisplatin@CB[7]) on the A2780/CP70 xenograft.

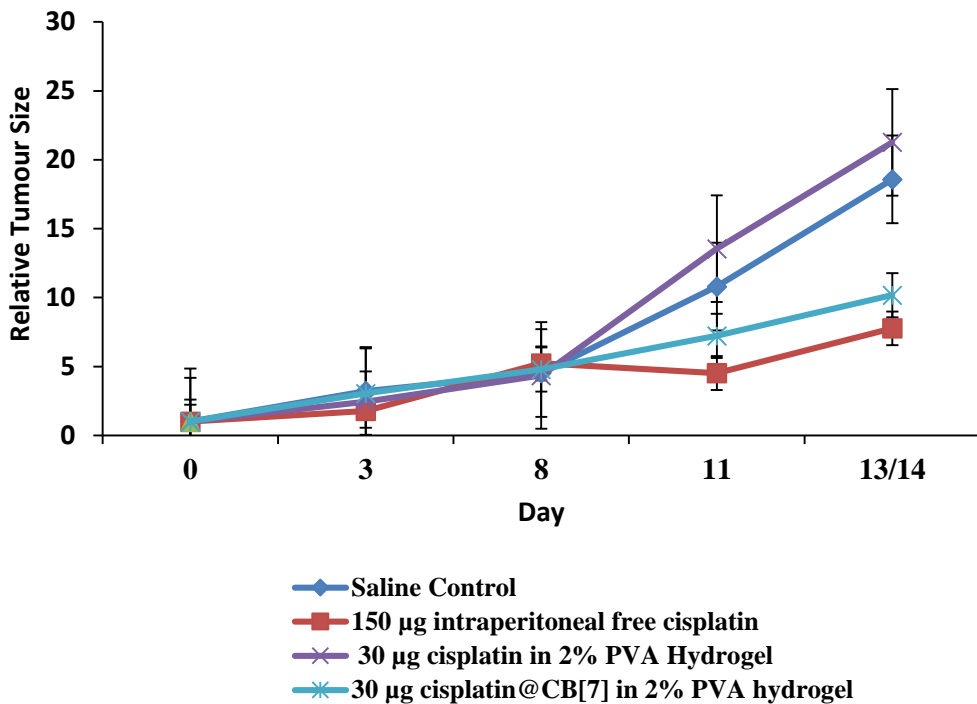


Figure 2.3.6. The *in vivo* anti-tumour effect of hydrogels containing cisplatin and cisplatin@CB[7]. The graph represents the *in vivo* cytotoxicity of hydrogels against the human ovarian A2780/CP70 cisplatin resistant tumour xenograft, showing: saline control (dark blue, diamond), intraperitoneal free cisplatin 150 µg (red, square), cisplatin in 2% PVA hydrogel 30 (purple, cross) µg, cisplatin@CB[7] in 2% PVA hydrogel (light blue, cross). Results are expressed as mean \pm SEM ($n = 6$). Statistical two way Anova with Bonferroni's multiple comparison tests was performed.

Figure 2.3.6 shows that when free cisplatin is administered via a 2% PVA hydrogel and at a dose of 30 µg per animal, there is no measurable delay in tumour growth compared with the saline control. In contrast, at the same 30 µg equivalent dose of cisplatin, the cisplatin@CB[7] hydrogel complex has the same effectiveness as a high dose of free cisplatin 150 µg. However, Bonferroni's multiple comparison post-tests showed that there was no significant difference in the tumour shrinkage efficacy of

each arm (control, free cisplatin, 2%PVA hydrogel containing cisplatin and 2% PVA hydrogel containing cisplatin@CB[7]) compared to each other ($p > 0.05$).

If the results were of statistical significance, this study would have demonstrated the benefit of the slow release of cisplatin from the hydrogel using CB[7], as the delivery of 30 μg of cisplatin@CB[7] by a 2% PVA implanted hydrogel is just as effective at decreasing/delaying tumour growth as an intraperitoneal dose of 150 μg of free cisplatin.

2.4 Discussion

The experimental methods in this section were designed to study whether the reformulation of cisplatin by using a two layered drug delivery system could increase the anti-tumour efficacy of cisplatin through a slow release mechanism provided by the implantable hydrogel and protection of drug from early degradation provided by cucurbit[7]uril.

The ovarian cancer cell line A2780 and the cisplatin resistant derivative (A2780/CP70) were chosen for these studies as they have been previously well characterised. The A2780 cell line are sensitive to cisplatin and show a clear dose response to treatment when grown as xenografts in nude mice. The cisplatin resistant cell line was established by Dr Jane Plumb at the Beatson cancer Institute of Glasgow, the mechanism of cell resistance to cisplatin was shown to be due to the loss of DNA mismatch repair by the loss of MLH1 (MutL Homolog 1) gene expression.

In this study, implantable hydrogels made from gelatine and varying concentrations of PVA (0%, 2% and 4% w/v) were synthesised as slow drug delivery systems for cisplatin and cisplatin@CB[7]. The results show that the hydrogel's rate of swelling and degradation is related to the hydrogel's PVA concentration with hydrogels containing the highest PVA concentration (4% w/v) displaying the slowest swelling, disintegration and release properties. When these hydrogels were loaded with cisplatin, or with cisplatin@CB[7], they displayed *in vitro* cytotoxicity towards human ovarian cisplatin-resistant cells A2780/CP70 dependent on their PVA content, with 0% PVA drug loaded hydrogels inducing the highest level of cytotoxicity because they

released the drug the fastest rate (in the short time of the *in vitro* assay) and 4% PVA hydrogels inducing the least cytotoxic effects as they released the drug the slowest. An interesting objective to these results that was not taking into account during the experimental procedure was whether cisplatin itself interacted with PVA and if this was the reason to the low cytotoxicity. If cisplatin does bind to PVA, then the drug would not be free to interact with the cell's DNA or may have not even been able to cross the cell membrane. Nuclear magnetic resonance would be an ideal technique to study whether cisplatin interacts with PVA, there are currently no published data on the interaction of cisplatin with PVA.

As a result of these *in vitro* results, hydrogels containing 2% PVA were selected for further *in vivo* studies as they displayed a moderate rate drug release system. The *in vivo* results demonstrated possible future success of using the hydrogel as a drug delivery system; as a low dose formulation of cisplatin@CB[7] in the 2% PVA hydrogel (30 µg per animal) was able to overcome resistance and was just as effective at inhibiting tumour growth as a high intraperitoneal dose of cisplatin (150 µg per animal). Overall these results suggest the possibility of using implantable gelatine and PVA based hydrogels in the treatment of cancer using a much lower dose of drug compared to the conventional treatment. The implications of this could lead to better quality of life for patients during treatment or potentially greater effectiveness of the drugs when administered at high doses.

Polymers such as PVA and gelatine have a long history of use in pharmaceuticals, cosmetics and food products. These polymers are attractive as they are cheap, readily

available, biocompatible, biodegradable, have low antigenicity and do not produce harmful byproducts upon enzymatic degradation [31]. Although their use as material for implantable hydrogels has not been studied in depth, PVA and gelatine have both been under intensive investigation as materials for the preparation of nanoparticles [31]. In a study by Chuoubi *et al*, nanoparticles made from gelatine and containing the anticancer drug cytarabine were prepared [31]. The rate of *in vitro* drug release was investigated and their results are similar with the results obtained in this chapter in that the cross linking density of the gelatine was shown to have a significant influence on drug release such that nanoparticles prepared with higher concentrations of gelatine had a slower swelling and drug release rate [31]. This trend is also seen in a different study in which gelatin nanoparticles containing 5-FU were prepared [32]. Naidu *et al* studied the *in vitro* release of 5-FU from nanoparticles containing different concentrations of gelatin. Their results showed that as the polymer concentration increased the drug release was slower due to the slower swelling of the nanoparticle [32]. Overall these studies show that drug release can be modified by tuning the number of polymer crosslinks within the drug delivery vehicle used.

The initial scope of this hydrogel study was wider than what has been provided in this thesis. It was planned that the pharmacokinetics and pharmacodynamics of cisplatin when administered by the implantable hydrogels would be studied and compared to free intraperitoneal cisplatin, as well as animal toxicity studies. However, due to unforeseen reasons which involved the change in both first and second PhD supervisors, this study could not be completed either at the Beatson Institute of Cancer Research or at Strathclyde University.

Therefore, in completion of this PhD, twitch tension experiments in collaboration with Dr Edward G Rowan at Strathclyde University was undertaken. This collaboration involved the novel study of the *ex-vivo* neurotoxic, neuromyopathic and cardiotoxic activity of various platinum-based drugs and macrocyclic drug delivery systems (introduced in the next chapter of this thesis). Although this research is not in direct correlation with cancer, the results derived show further benefits of using CB[7] as a delivery system for cisplatin in that it significantly reduced the neuromyo- and cardiotoxicity effects induced by free cisplatin. Due to the experimental design of these *ex-vivo* studies, hydrogels could not be incorporated in this study.

Chapter 3

The Neurotoxic, Neuromyopathic and Cardiotoxic effects of Platinum-Based Drugs and Macrocyclic Drug Delivery Systems.

3. Toxicology

3.1 General Introduction

The word toxicology comes from the Greek word “toxicos” meaning “poisonous” and is essentially the study of the adverse effects of chemicals on living organisms [197-200]. Today, the majority of countries have developed laws and regulations that control the marketing and licensing of new therapeutic drugs, which includes extensive testing of their toxicology [198].

In general, a toxicity test is designed to generate data concerning the toxic effects of a substance either in humans or animals [197-200]. Pre-clinical lab tests fall into three categories: *in vitro* tests which involve the use of components of an organism that have been isolated from their usual biological surrounding (most commonly cells), *in vivo* tests which involve testing a chemical in a living animal in their normal state, and *ex vivo* tests which are performed on functional organs that have been removed from the euthanised intact animal [200].

3.1.1.1 *In Vitro* Assays in Toxicological Studies

In vitro tests are also known as “test tube experiments” and in toxicology involve the analysis of the toxic effects of chemicals on cultured bacterial, mammalian and fungal cells as well as viruses. *In vitro* assays are popular and are used routinely by all industries in testing, risk evaluation and safety assessment, and they are usually the first set of experiments performed to analyse the toxicity of a substance [197-201]. The greatest advantages of using *in vitro* tests is for determining the biological processes that are involved in a toxic response to a substance at the molecular level [200-202].

They are cost and time effective, easy to handle, results are easily reproduced and there are not associated ethical problems [198, 200]. However, *in vitro* methods cannot duplicate the complex processes of a whole animal as the substance under examination can accumulate and interact throughout the whole body [200-202]. Thus, *in vitro* results cannot be fully relied upon to provide dependable results of the pharmacodynamics and pharmacokinetics of a substance in the animal's body and this is why whole animal studies are required.

3.1.1.2 *In Vivo* Toxicological Studies

“*In vivo*” is the Latin phrase for “within the living” and involves the administration of a substance to a living animal, such as a mouse or a rat, to observe the overall effects of the substance to the organism's body. Advantages of using *in vivo* studies is that it allows for specific details on drug pharmacokinetics and pharmacodynamics to be studied which cannot be conducted in *in vitro* or *ex vivo* studies [198, 200, 202]. Also, pharmacological effects in animals can be similar to that of humans, and thus *in vivo* studies, can be relied on for semi-accurate predictions of drug effects in humans. Disadvantages of *in vivo* testing include expensive costs of animals and their related ethical issues [198, 200, 201].

3.1.1.3 *Ex Vivo* Assays in Toxicological Studies

“*Ex vivo*” is the Latin phrase for “out of the living” and involves experiments performed on whole organs or tissues that have been extracted from an organism with minimum alterations to the tissues condition and studied in an environment that mimics its natural environment in an organ bath (this is usually achieved by incubating

the tissue or organ in oxygenated physiological salt solution buffer maintained at 37 ° C [199].

3.1.1.4 Organ Baths in *Ex Vivo* Toxicity Studies

Organ bath assays are classical pharmacological and toxicological screening tools used to assess the effect of various drug concentrations in contractile tissue. Compared to molecular assays, organ baths can be used to study the effect of compounds with unknown molecular targets while controlling several physiological parameters. Organ baths are most commonly used in cardiovascular research, using isolated aortic rings and ventricle or atrial tissue. It is also used for studying gastro-intestinal effects using the colon or ileum, and respiratory effects using isolated tracheal rings and diaphragm tissue. Other isolated tissue preparations include: urinary bladder, skeletal muscle and prostate tissue.

Isolated tissue experiments (Figure 3.1.1) can be run in groups of 2, 4, or 8 depending on the organ bath used, thereby enabling a high throughput of results. Tissues are usually prepared and cleaned (removal of outer membrane or of any extra tissue attached) before mounting into the organ bath in such a way that one end of the tissue is attached to a mounting hook and the other end to a transducer via thread. The water jacketed organ bath provides easy temperature control and the tissue can be electrically stimulated by placing an electrode in close proximity to the tissue. A transducer then records the force and rate of tissue contraction throughout the experiment, and this data is then used to generate dose-response curves.

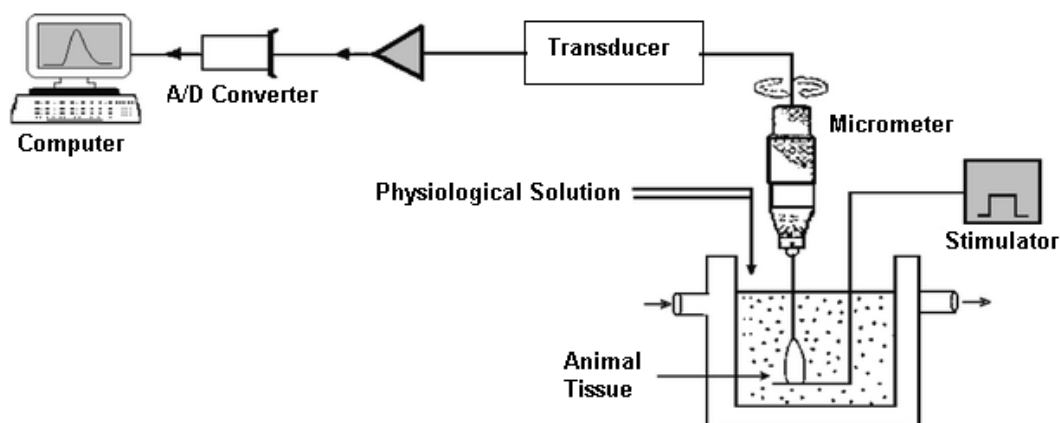


Figure 3.1.1. A schematic diagram showing a typical setup of an isolated tissue organ bath experiment. The animal tissue is incubated in a temperature controlled organ bath and attached to a transducer by a silk thread. The stimulator provides a means by which the rate of tissue contraction can be controlled; this is achieved if an electrode is placed in close proximity to the tissue. The analogue to digital converter (A/D converter) converts the physical quantity measured (usually in volts) into a digital number that can be displayed on a computer and used to generate a dose-response curve. Image taken from <http://link.springer.com/article/10.1007%2Fs00592-009-0156-x/fulltext.html>.

3.1.2 Neurotoxicity

Neurotoxicity is defined as a detrimental effect on the nervous system caused by a biological, chemical or physical agent. Neurotoxic agents are referred to as neurotoxins and they work by altering the normal activity of neurons (cells that make up the nervous system) [203].

3.1.2.1 The Nervous System

The nervous system is a highly complex system that regulates all aspects of bodily functions, including: movement, vision, thought and speech through an organised network of hormones, ion channels, receptors, and electrical and chemical signals

[204-206]. It can be divided into two intimately interconnected systems: the central nervous system (CNS), composed of the brain and spinal cord, and the peripheral nervous system (PNS), consisting of the nerves that connect the brain or spinal cord to the body's muscles, glands and sense organs [204-206].

The nerve cell, also known as the neuron, is the basic unit of the nervous system [204-206]. Neurons operate by generating signals that move from one part of the cell to the neighbouring cell by either electrical or chemical means depending on cell type [204-206].

3.1.2.2 The Structure and Function of Neurons

Neurons occur in a wide variety of sizes and shapes and are composed of three regions (Figure 3.1.2), all of which carry out different specialised functions: the cell body, dendrites and axons [204-206]. The cell body contains the nucleus and ribosomes and is the site at which neuronal protein and membrane synthesis occurs [205, 206]. The dendrites are a series of small branched outgrowths that extend outward from the cell body and are specialised in receiving signals from axons of other neuronal cells and then transmit them to the cell body [205, 206]. The axons are long fibers that conduct electrical and chemical impulses, known as action potentials, along their length away from the cell body [205, 206]. Axons can range from a few microns to over a meter in length. The region of the axon that arises from the cell body is called the axon hillock and this is where the electrical signals are generated [205, 206]. When an action potential is generated, it arises at the axon hillock and travels towards the axon terminal from which the electrical signal can pass either electrically or chemically to another

neuron in a nerve circuit, to a muscle at a neuromuscular junction, or to various other types of cells [205, 206].

Neurons can be divided into three classes dependent on their function: afferent, efferent and interneurons [205, 206]. Afferent neurons conduct impulses from the body's tissues and organs towards the CNS, whereas, efferent neurons conduct information away from the CNS towards effector cells such as muscles and glands, and interneurons connect neurons within the CNS [204-206].

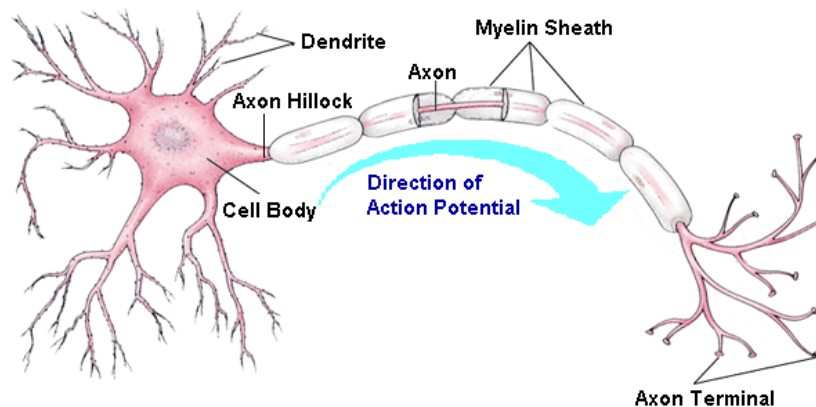


Figure 3.1.2. A schematic diagram of a neuron showing the movement of an action potential from the axon hillock towards the axon terminal. Image taken from <http://classconnection.s3.amazonaws.com/1615/flashcards/596052/png/screen-shot-2011-01-19-at-8.27.56-pm.png>.

Synapses (Figure 3.1.3) are specialised sites where neurons communicate. There are two types of synapses that exist: electrical and chemical, both of which transmit signals in different ways [204, 205]. In an electrical synapse, the plasma membrane of the presynaptic and postsynaptic cell are joined by gap junctions, this allows for the flow

of action potentials across the junction from one neuron to the next [205]. In a chemical synapse, the electrical activity in the presynaptic neuron causes it to release chemical neurotransmitters (such as acetylcholine) that bind to receptors located on the membrane of the postsynaptic cell (receiving cell) [205]. This binding causes a change in the ion permeability of the postsynaptic membrane inducing a new action potential in a neuronal cell or a twitch in a muscle cell [205, 206].

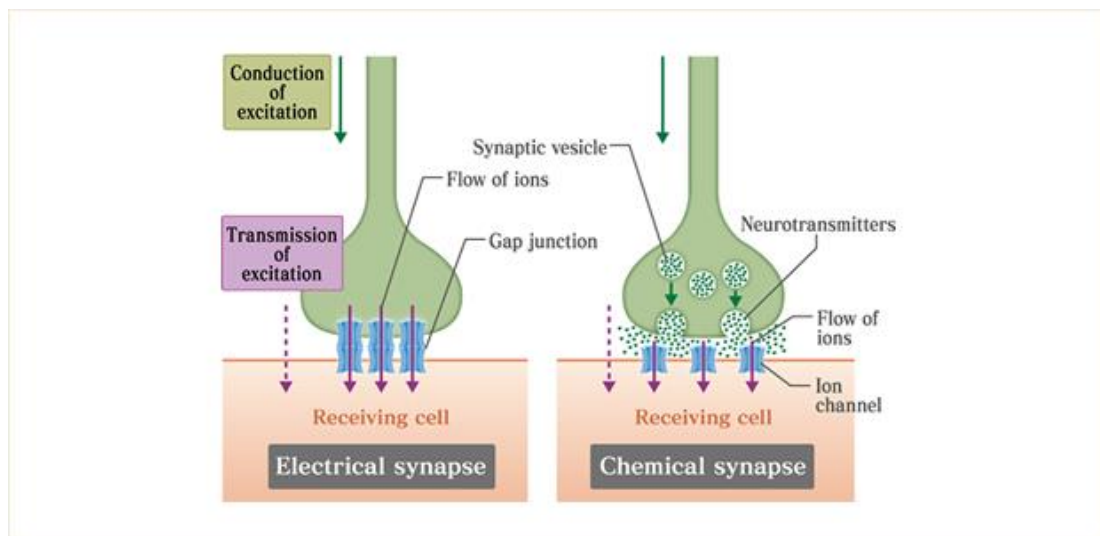


Figure 3.1.3. The flow of an action potential between cells through an electrical synapse compared to a chemical synapse. In an electrical synapse, the presynaptic and postsynaptic cell are connected by gap junctions that facilitate the direct transmission of an action potential between the cells. In a chemical synapse, the action potential is transmitted from the presynaptic cell to the postsynaptic cell through the release of neurotransmitters from vesicles found in the presynaptic cell. These neurotransmitters bind to specific ion channels found on the membrane of the postsynaptic cell altering its membrane potential. Image taken from http://csls-text.c.u-tokyo.ac.jp/active/11_04.html.

3.1.2.3. Action Potential

Each cell in the human body is surrounded by a thin membrane known as the plasma membrane [204, 205]. This membrane is selectively permeable to specific ions (charged molecules) which can move into and out of the cell through specific ion channels embedded in the plasma membrane [204, 205]. Due to this specific movement of ions, an electrical gradient is established across the cellular membrane, and an imbalance in its electrical charge is called the membrane potential. Every cell in the human body is more negative inside than outside and has a resting membrane potential of approximately ~ -60 to -90 mV (depending on the cell type) (Figure 3.1.4) [205, 207].

The resting membrane potential exists due to a tiny excess of negative ions inside the cell and an excess of positive ions outside [204, 205]. The excess negative charges inside are attracted to the positive charge outside the cell, and vice versa. Thus the excess ions collect in a thin tight shell against the inner and outer surfaces of the plasma membrane, whereas the bulk of the intracellular and extracellular fluids remain neutral [206, 207]]. The predominant diffusible solutes in the extracellular fluid are sodium and chloride ions, and the intracellular fluid contains high concentrations of potassium ions. Each of these ions has a 10- to 30-fold difference in concentration between the inside and outside of the cell (there are many other ions, including Mg^{2+} , Ca^{2+} , H^+ , HCO_3^- , SO_4^{2-} , amino acids and proteins in both compartments) [206, 207]. The concentration differences for Na^+ and K^+ are established by the action of the sodium-potassium ion pump (Na^+/K^+ -ATPase) that pumps Na^+ out of the cell and K^+ in, and the reason for Cl^- distribution varies among cell type [205, 207].

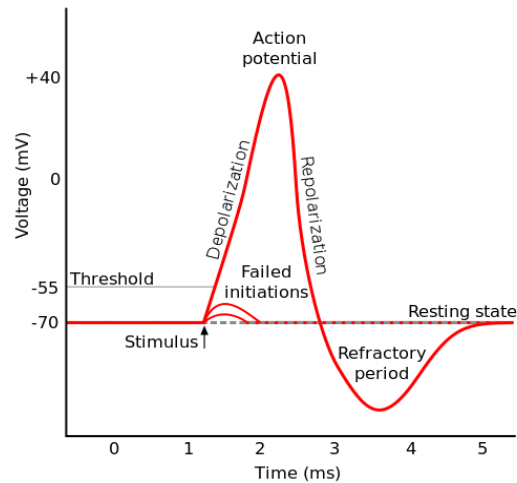


Figure 3.1.4. Schematic diagram showing the various phases of an electrophysiological reading of an action potential that occurs as electrical impulses pass down a cell membrane. Image taken from <http://cs.brown.edu/people/tld/note/blog/13/04/19/>.

Excitable cells (those that are able to generate or conduct electrical impulses such as nerve, cardiac, and muscle cells) are able to rapidly reverse their resting membrane potential from negative values to positive values; a phenomenon called an action potential (Figure 3.1.4) [205, 207].

When an electrical, chemical or mechanical stimulus disturbs a nerve cell, a few sodium channels in a small portion of the cell membrane open, this allows for the flow of sodium cations into the cell (Figure 3.1.5) [204, 207]. This causes the inside of the cell to become less negative (depolarise). When this depolarisation reaches a certain threshold, many more sodium channels in that area open, allowing for a greater influx of sodium cations into the cell making the cell positive inside and negative outside (electrical potential can reach up to $\sim +40$ mV), thus triggering an action potential [205, 207].

Once the electrical threshold reaches + 40 mV, the sodium channels are inactivated, and potassium channels are activated [205, 207]. This results in the efflux of potassium ions (which are also positively charged) out of the cell, rendering the cell membrane less positive inside and slowly returning the membrane potential back to its resting level [205]. This sequence of events is passed down onto the next area of the membrane and down the entire length of the axon (transmitting the action potential down the nerve cell) [205, 207].

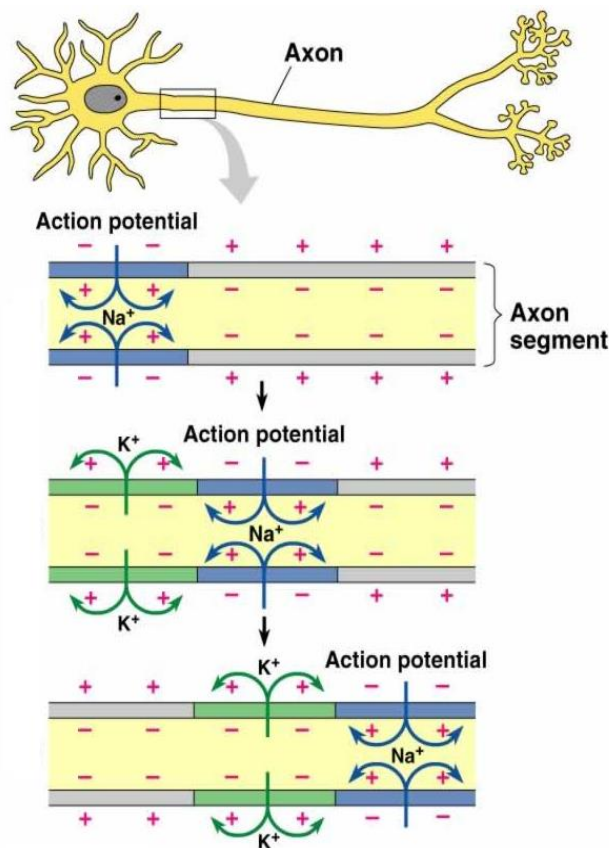


Figure 3.1.5. A schematic diagram showing the flow of a membrane potential as it moves down the length of an axon. Image taken from <http://mikeclaffey.com/psyc170/notes/notes-neurons.html>.

3.1.2.4 The Sciatic Nerve

The sciatic nerve (Figure 3.1.6) is the longest and widest nerve in all vertebrates including humans [12, 13]. It originates from the spinal cord and extends along nearly the entire length of the hind limb [208, 209].

Anatomically, the entire sciatic nerve is composed of individual neurons that are wrapped up in a layer of connective tissue called the endoneurium (Figure 3.1.7). These neurons are bundled together into groups called fascicles, which are further wrapped up by connective tissue called the perineurium. These fascicles are then bundled together to form the sciatic nerve that is further wrapped in connective tissue known as the epineurium [208, 209].



Figure 3.1.6. Picture of a mouse sciatic nerve.

Blood vessels run between the fascicles providing oxygen and nutrients to the neurons. The main function of the sciatic nerve is to provide motor innervation to the muscles of the thigh, hamstring, leg and foot and sensory innervation to the skin of the leg and almost all of the foot (apart from the medial foot section which is innervated by the saphenous nerve). Injury to the sciatic nerve can induce complete motor or sensory loss of the posterior thigh, leg or foot [209].

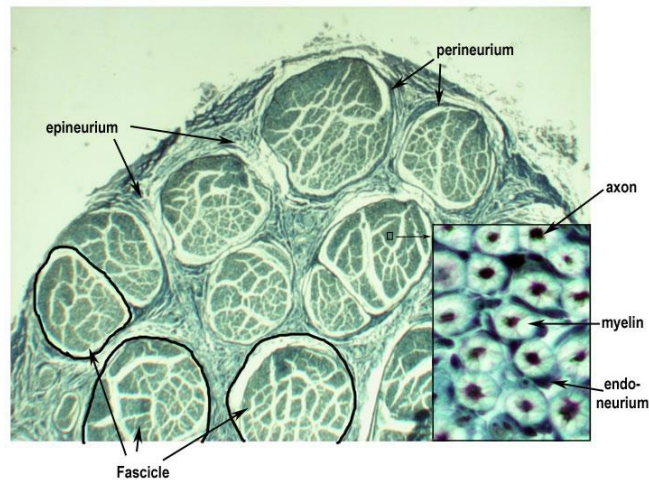


Figure 3.1.7. Histology slide of the sciatic nerve showing the fascicles of nerve fibers, the connective tissue, and the axon and myelin. Image taken from http://missinglink.ucsf.edu/lm/ids_101_histo_resource/nerves_muscle.html.

3.1.2.5 Chemotherapy Induced Neurotoxicity

Chemotherapy induced neurotoxicity is a significant complication in the successful treatment of many cancers [210-212]. Neurotoxicity develops mainly in patients treated with platinum based drugs (cisplatin, oxaliplatin and carboplatin), taxanes (paclitaxel and docetaxel) and vinca alkaloids (vincristine) with the incidence of neurotoxicity influenced by patient age, dose intensity, cumulative dose, the co-administration of other neurotoxic agents and pre-existing conditions such as diabetes and alcohol abuse [210-214].

Chemotherapeutic drugs induce their neurotoxic activity by either causing damage to the peripheral nervous system or the central nervous system and in some cases to both systems [211,214]. Neurotoxicity can be extremely painful and disabling with symptoms occurring either during infusion, shortly after infusion (1-3 hours after drug

administration) or in some rare cases symptoms, can develop months after drug administration [210, 214- 217].

Symptoms of peripheral neurotoxicity include: the loss of sensation in the hands and feet, muscle weakness, muscle paralysis, paraesthesia (tingling, prickling and burning sensation) of the fingers and toes, loss of co-ordination, dysphagia (problems with swallowing) [211, 212, 217, 218]. Symptoms of central neurotoxicity include: ototoxicity (particularly in the high frequency range), coma, seizures, and memory loss [217,218].

Assessment of neurotoxicity is based primarily on clinical examinations and although various neurotoxicity grading scales have been proposed, there is yet no gold standard universal grading system [216, 217, 19]. Neurological examinations include physical evaluation of a patient's response to various external stimuli such as hot and cold temperatures, vibrations (measured by a standard tuning fork placed over bony prominences of the great toe, lateral malleolus, patella, hip, index finger and olecranon), muscle strength (toe extensors, foot extensors and flexors, knee extensors, hip flexors, finger abductors, arm extensors and flexors) and deep tendon reflexes [216, 220]. Clinical electrophysiological motor conduction studies that measure motor nerve potentials (measured by placing surface electrodes and stimulating nerves such as under the head of the fibula and above the ankle) are also used to assess the degree of neurotoxicity [216, 218].

The mechanism of action by which chemotherapeutic drugs induce their neurotoxic effects are very diverse and depend on drug type amongst other factors [212-218]. The methods that have been discovered so far include: damage to neuronal cell bodies by inducing apoptosis, axonal toxicity via transport deficits, and membrane ion channel dysfunction [219-22]. Research in this area is still ongoing, and it is necessary to understand these mechanisms in order to develop successful neuroprotective agents/strategies.

3.1.2.5.1 Etiology and Pathophysiology of Platinum Based Drugs Induced Neurotoxicity

Cisplatin has been shown to predominantly produce sensory neuropathy characterised by severe loss of proprioception, a diminished vibratory sense, paraesthesia and numbness of the feet and high frequency hearing loss [211, 212, 216, 219, 220]. Oxaliplatin induces peripheral neuropathy that is similar to that of cisplatin but can resolve sooner. Another clinical syndrome that is unique to oxaliplatin is that symptoms occur between 30 to 60 minutes after infusion and include cold induced paraesthesia, painful dysesthesia, muscle cramps and muscle spasms [221, 222] .

Over the years, a combination of *in vitro*, *in vivo* and *ex vivo* studies have all contributed significantly to understanding the mechanism of action by which the platinum-based drugs induce their neurotoxic activity. Various *in vitro* cell cytotoxicity, cell morphological and histological studies have shown that the platinum based drugs primarily affect the axons, myelin sheath, neuronal cell body and the glial structures of neurons, with significant high levels of platinum found in the dorsal root ganglia (DRG) leading to shrinking or loss of DRG neurons and a resultant sensory

neuropathy [220-222]. *In vitro* research has demonstrated that the platinum based drugs enter the DRG via metal transporters and that once inside the DRG, form adducts with DNA inducing apoptosis [220-223]. Various *in vitro* and *in vivo* studies have shown that the degree of neurotoxicity is associated with the amount of platinum-DNA adducts formed and that cisplatin is significantly more neurotoxic than oxaliplatin because it produces three times more platinum-DNA adducts in the DRG than equimolar doses of oxaliplatin [219-223]. As well as inducing apoptosis, *in vitro* and *ex vivo* studies have shown that the platinum drugs induce their neurotoxic activity via different pathways including acting on neuronal Na^+ channels and by disrupting the levels of intracellular Ca^{2+} [221-223]. Recent *ex vivo* studies have shown that oxaliplatin can induce hyperexcitability at neuromuscular junctions by prolonging the opening of Na^+ channels which leads to increased neurotransmitter release [221].

3.1.2.5.2 Development of Neuroprotective Agents

A neuroprotective agent should aim to decrease the neurotoxicity associated with chemotherapeutic drugs by providing protection to healthy neuronal tissue without compromising the antitumour efficacy of the anticancer drug [210, 217].

Many strategies have been under investigation as methods of reducing or completely abolishing chemotherapy induced neurotoxicity [210, 218]. Various hypotheses have been tested, however, none thus far have shown complete success. These strategies include: calcium and magnesium infusions, vitamin E, the use of anti-epileptic agents, insulin like growth factor and glutamine [210, 222-227] .

3.1.2.5.2.1 Calcium and Magnesium Infusions

It was hypothesised that the administration of intravenous calcium and magnesium might help reduce or prevent oxaliplatin induced peripheral neuropathy. This hypothesis was made due to studies that showed that an increase in extracellular concentration of calcium facilitated sodium channel closing and thus could decrease hyperexcitability of peripheral neurons induced by oxaliplatin [225-228]. In a non-randomised study involving 161 patients with advanced colorectal cancer, 96 patients received intravenous calcium gluconate and magnesium sulphate before and after oxaliplatin administration. The remaining 65 patients served as a control group. Results showed that only 4% of patients in the CaMg group compared to 31% of the control group had to stop chemotherapy due to neurotoxicity and at the end of the treatment 27% of the CaMg group versus 75% of the control group showed signs of neurotoxicity of any grade [229-230].

3.1.2.5.2.2 Vitamin E

Vitamin E, a fat soluble vitamin classified as an antioxidant, has demonstrated partial neuroprotection in patients receiving cisplatin and paclitaxel [225, 229]. In a recent pilot study, 40 patients receiving either cisplatin, paclitaxel or a combination of these drugs were given vitamin E. Results showed that neurotoxicity occurred in 25% of patients taking vitamin E compared to 73% of patients in the control group [230,].

There is various evidence from a number of small clinical trials that suggest that vitamin E may help to reduce chemotherapy induced neurotoxicity, however, there is a concern that vitamin E may interfere with the efficacy of anticancer agents as it can

interfere with the oxidative breakdown of cellular DNA and cell membranes [231-232].

3.1.2.5.2.3 Anti-epileptic Agents

Anti-epileptic drugs have been suggested as neuroprotective agents against some chemotherapeutic drugs, such as oxaliplatin, because they block sodium channel activity, thereby reducing the hyperexcitability of damaged peripheral nerve [234]. Carbamazepine, gabapentin and pregabalin are all anticonvulsant agents that have been tried in small clinical studies to reduce neurotoxicity in patients treated with oxaliplatin but with no positive results as yet [234].

3.1.2.5.2.4 Insulin Like Growth Factor

Insulin growth factor-1 is involved in regulating body growth and stimulating motor and sensory nerve regeneration. In clinical trials insulin like growth factor prevented the development of paclitaxel induced neuropathy and in animal *in vivo* studies it prevented the development of both vincristine and paclitaxel induced neuropathy [235].

3.1.3 Neuromyopathy (Neuromuscular Toxicity)

Neuromyopathy is defined as a muscular disease of nervous origin. Neuromyopathic agents are referred to as either myotoxins or neurotoxins as they induce muscle damage through direct action on the muscle fibre or indirectly through action on the presynaptic motor neuron.

3.1.3.1 The Neuromuscular Junction

Muscle movement is controlled by the nervous system, particularly by motor neurones (which are the type of neurones that innervate skeletal muscle) [204, 205].

Neuromuscular junctions (Figure 3.1.8) are locations in which the nervous system connects to the muscular system at synaptic clefts [204, 205]. Each neuromuscular junction consists of the axon terminal of a motor neuron and an end plate (the part of the muscle that is in close proximity to the synaptic area) of a muscle fibre.

When an action potential reaches the axons of a motor neuron, voltage-dependent calcium channels embedded at the axonal terminus open up, allowing for the influx of calcium cations into the neuronal membrane (Figure 3.1.9) [204, 205]. This influx results in neurotransmitter filled vesicles to fuse with the axonal terminus membrane and release acetylcholine into the synaptic cleft (neuromuscular junction) [204, 205]. Acetylcholine then binds to ligand gated ion channels (known as nicotinic acetylcholine receptors) found on the membrane of the muscle tissue, inducing these channels to open up and initiating an influx of cations (mainly sodium) into the muscle, generating an endplate depolarisation which leads to muscle contraction [204, 205].

Depolarisation of the muscle endplate results in an action potential propagating along the muscle fiber and down the T tubule membrane [8]. This causes voltage gated calcium ion channels on the sarcoplasmic reticulum to open resulting in an increase in the permeability of the sarcoplasmic reticulum to calcium ions [8,9]. The calcium ions

diffuse into the sarcoplasmic reticulum where it binds to troponin and activates the cross-bridge cycle which is the driving force of muscle contraction [204, 205].

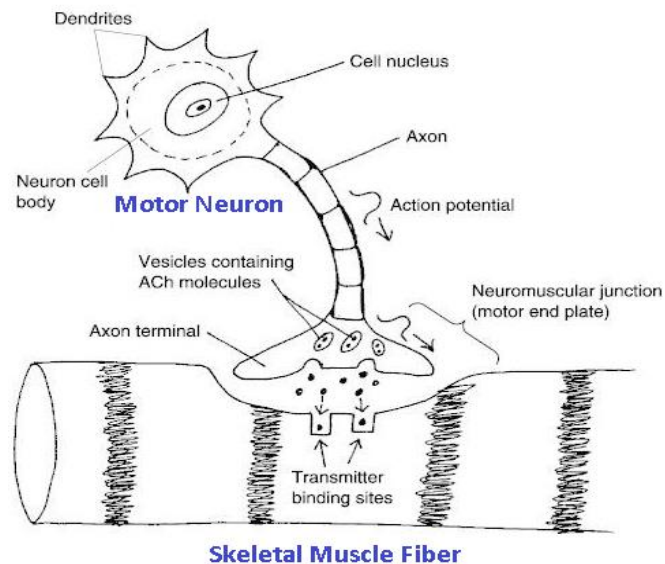


Figure 3.1.8. A schematic diagram of a motor neuron and the neuromuscular junction where the neuron connects with a muscle fiber. Image taken from <http://classconnection.s3.amazonaws.com/334/flashcards/1645334/jpg/nmj1340211926722.jpg>

Acetylcholine is enzymatically broken down into choline and acetate by acetylcholinesterase [8, 9]. Choline is then able to re-enter the motor neuron where with the aid choline acetyltransferase and acetyl-coA, acetylcholine is synthesised [204, 205].

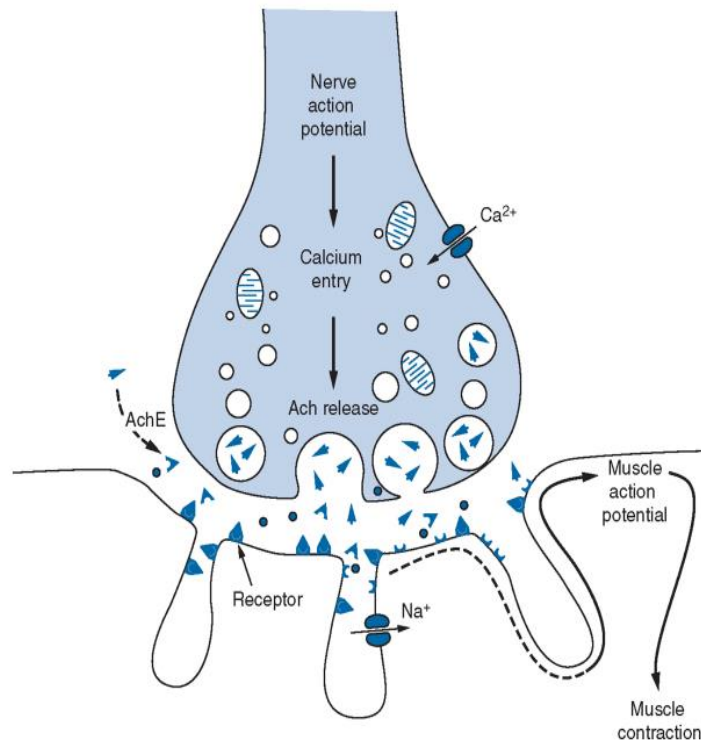


Figure 3.1.9. A schematic diagram of a neuromuscular junction showing the flow of an action potential down the axon, the influx of calcium cations into the axonal terminus followed by the release of acetylcholine (ACh) from the presynaptic neuron and its binding to sodium channels located on the postsynaptic muscular membrane which generates an action potential and ultimately causes muscle contraction. Image taken from http://www.collegepaeds.ac.za/past%20papers/2010-10/FCP1_2010-10.htm.

3.1.3.2 Neuromyopathy Induced by Chemotherapy

It has been shown that various chemotherapeutic drugs induce muscle damage, through indirect action, by disturbing the activity of the presynaptic motor neuron (neuropathy) as discussed above. Symptoms of neuropathy include muscle numbness, muscle

weakness and increased muscle sensitivity [238]. Peripheral neuropathy often affects muscles of the hands, feet and lower legs, and this is because the longer the nerve is, the more vulnerable it is to injury [238].

Anticancer drugs that have been shown to induce the highest incidence of peripheral neuropathy, and thus muscle damage, include: the platinum based drugs (cisplatin, carboplatin and oxaliplatin), the taxanes (docetaxel and paclitaxel) and the vinca alkaloids (vinblastine, vincristine and vindesine) [238, 239].

Although the toxic chemotherapeutic effects induced by platinum drugs, and in particular with cisplatin, are well documented, little is known about the mechanism by which these drugs induce these toxic side effects. Furthermore, very little is known about the toxicity of drug delivery macrocycles such as CB[*n*]s on specific organs and tissues.

3.1.4 Cardiotoxicity

Cardiotoxicity is defined as “toxicity that affects the heart”. Damage to the heart can be due to either electrophysiological dysfunction or/and damage to the heart muscles. These toxic alterations cause the heart to become weaker, which over time can ultimately result in heart failure.

3.1.4.1 The Heart

The heart is a muscular organ about the size of a fist and is located just behind and slightly to the left of the breastbone [240]. It beats between 60-80 beats per minute in a healthy adult and its main function is to pump blood through the cardiovascular

system; a network of arteries and veins [241]. The heart is made up of four chambers: two atrias (left and right) located in the top section of the heart and two ventricles (left and right) located in the bottom end of the heart [240, 241].

The rate at which the heart contracts is controlled by a specialised bundle of neuronal cells located at the top wall of the right atrium known as the sinoatrial node (SA node) [241]. Although all of the heart's cells have the ability to generate action potentials, the SA node normally initiates it. When the SA node generates an action potential, it causes the atrium to contract, sending electrical impulses to the atrioventricular node (AV node) which spreads the electrical impulse to the ventricles. This in turn causes the ventricles to contract, pumping blood to the lungs and the body [241-243].

3.1.4.2 Chemotherapy Induced Cardiotoxicity

Cardiotoxicity has been recognised as a chemotherapeutic induced adverse effect as early as the 1960s were clinical reports of heart failure were common in patients treated with the anthracycline drug doxorubicin [244].

The anthracyclines still remain as the most cardiotoxic chemotherapeutic agents [244]. However, there are a number of other chemotherapeutic agents that also induce cardiotoxic side effects, including: cisplatin, carmustine, mitomycin and cyclophosphamide [248, 250].

Cardiac events associated with chemotherapy may include mild blood pressure changes, arrhythmias (abnormality in the heart's rhythm), myocarditis (inflammation

of the heart tissue), pericarditis (inflammation of the membrane that surrounds the heart), electrocardiographic (ECG) changes, thrombosis (formation of a clot within the heart vessel), myocardial infarction (necrosis of the heart tissue), and congestive heart failure (CHF) [247, 248-250]. These cardiac events associated with chemotherapy may occur acutely (during or shortly after treatment), sub-acutely (within days or weeks after completion of chemotherapy) or chronically (months to years after chemotherapy administration). The level of cardiotoxicity induced depends on the dose administered during each treatment cycle, the total cumulative dose or may be completely independent of the dose [258-260].

There are various techniques that are clinically employed to assess the level of cardiotoxicity induced by chemotherapy and these include: the use of electrocardiograms, chest X-rays and echocardiography to detect pulmonary veins congestion, diastolic and systolic left ventricular dysfunction, and abnormal ventricular abnormal contractility, respectively. Cardiac magnetic resonance imaging can also be used to assess left ventricular systolic function. Measurements of the cardiac enzymes in the plasma are also used in the assessment of chemotherapy induced cardiotoxicity; high levels of B-type peptides correlate with severe congestive heart failure and high levels of troponin may be an indication of myocardial injury.

3.1.4.2.1 Cardiotoxicity Induced by Platinum Based Drugs

Although there are a number of *in vitro* and *ex vivo* studies that demonstrate the cardiotoxic activity of platinum based drugs, and in particular cisplatin, there is still insufficient clinical evidence regarding the cardiotoxicity of these drugs. Clinical

studies have reported that cisplatin induced cardiotoxicity is only observed occasionally in the form of arrhythmia, including: supraventricular tachycardia, bradycardia and conduction abnormalities (electrolyte imbalance) with the majority of these cardiac problems reported to be clinically silent and occurring within hours of drug infusion [259-261]. It has been hypothesised that cisplatin may induce arrhythmias by causing intracellular calcium, potassium and magnesium electrolyte abnormalities as well as by inducing oxidative stress. However these mechanisms have yet to be confirmed.

In a recent clinical study, patient's heart rate, blood pressure, serum electrolyte levels, electrocardiographic and echocardiographic parameters were measured before and after cisplatin infusion and compared. Results showed that two thirds of patients developed either silent atrial or ventricular arrhythmias. The authors hypothesised that because serum electrolyte levels (potassium, magnesium and calcium) were not disturbed, cisplatin arrhythmias may have been due to the effect of the drug on cardiac sodium channels which can lead to increased arrhythmias [261].

There are several experimental *in vitro* studies that support the view that an increase in oxidative stress at the molecular level is implicated in the cardiotoxicity of cisplatin. This is further supported by a recent *in vivo* study which revealed that an administration of a single dose of cisplatin (7 mg/kg) to rats resulted in a significant decrease in both rat heart rate and mean arterial blood pressure and that pre-treatment with apocynin, a specific NADPH oxidase inhibitor, restored the heart rate and blood

pressure to their basal normal values and ameliorated the state of oxidative stress and preserved mitochondrial membrane potential [262].

3.1.5 Aims of This Chapter:

The *in vitro* and *in vivo* toxicity of various anti-cancer drugs and drug delivery systems have been well studied over the years. However, a limitation to these *in vitro* and *in vivo* systemic approaches is that little information can be gathered on the toxicity of drugs to specific organs and the mechanism by which they do so. Therefore, the use of *ex vivo* toxicological models, in which the toxicity of the test compound is determined on intact whole tissue, can provide crucial and reliable predictions of the organ toxicity of drugs and drug delivery systems in the human body. The *ex-vivo* toxicity of the platinum-based drugs and drug delivery macrocycles have never been tested before, therefore the aims of this chapter is to study the following:

- The neurotoxicity of various platinum-based drugs (including: cisplatin, K_2PtCl_4 , 56MESS and PHENEN) and macrocyclic drug delivery systems (including: CB[6], CB[7], Motor2 (cucurbituril derivative) and β -cyclodextrin) were studied using the mouse sciatic nerve preparation.
- The neuromyopathic activity of the platinum-based drugs and macrocyclic drug delivery systems were studied used the chick-biventer nerve-muscle preparation.

- The cardiotoxicity of the platinum-based drugs and macrocyclic drug delivery systems were studied using rat heart atria preparation.
- Furthermore, the effect of the encapsulation of cisplatin by CB[7] on the neurotoxic, neuromyopathic and cardiotoxic effects induced by cisplatin was also examined.

3.2 Materials and Methods

3.2.1 Materials

BALB/C mice and Sprague Dawley rats were obtained from Strathclyde University's in house breeding colonies that were originally sourced from Harlan, UK. Baby chicks were supplied from a breeding hatchery in Scotland (non-schedule 2 supplier).

Cisplatin, potassium tetrachloroplatinate (II) (K_2PtCl_4), β -cyclodextrin and CB[6] were bought from Sigma-Aldrich. Cucurbit[7]uril was bought from Dr Anthony Day, University of New South Wales, Australia. Motor2 was received from Professor Lyle Isaacs, University of Maryland, USA. Pentamer, 56MESS and PHENEN were synthesised within the lab.

3.2.2 Methods

3.2.2.1 Electrophysiological Recordings from Mouse Sciatic Nerve

Balb/c mice weighing between 25-30 g were euthanised with CO₂. The sciatic nerve was carefully dissected out from where it meets the spinal cord to the knee (3-5 cm in length) and immersed in HEPES based physiological salt solution of the following composition: 150 mM NaCl, 5.4 mM KCl, 10 mM HEPES, 12 mM NaHCO₃, 0.38 mM KH₂PO₄, 1.2 mM MgCl₂, 2.5 mM CaCl₂, 10 mM glucose, pH 7.4. The sciatic nerve was then de-sheathed (epineurium connective tissue that surrounds the nerve) under a stereo-microscope and then laid across three inter-connecting chambers with about 70% of the nerve coiled in the middle chamber (Figure 3.2.1). The three chambers were filled with HEPES based physiological salt solution to cover the nerve and electrical isolation between the three chambers was achieved with vaseline.

Electrical connections were made from the central chamber to one of the end chambers by means of Ag/AgCl electrodes. The remaining chamber contained two platinum electrodes connected to a pulse generator. The middle chamber was connected to electrical grounds and the voltage from the third chamber was measured by a high input resistance amplifier. Electrical impulses were supplied to the nerve by a Grass S88 stimulator (0.4 Hz, 0.05 ms duration, 30V) via a SIU 5A stimulus isolation unit (Grass Instrument Co. Quincy, MA, USA).

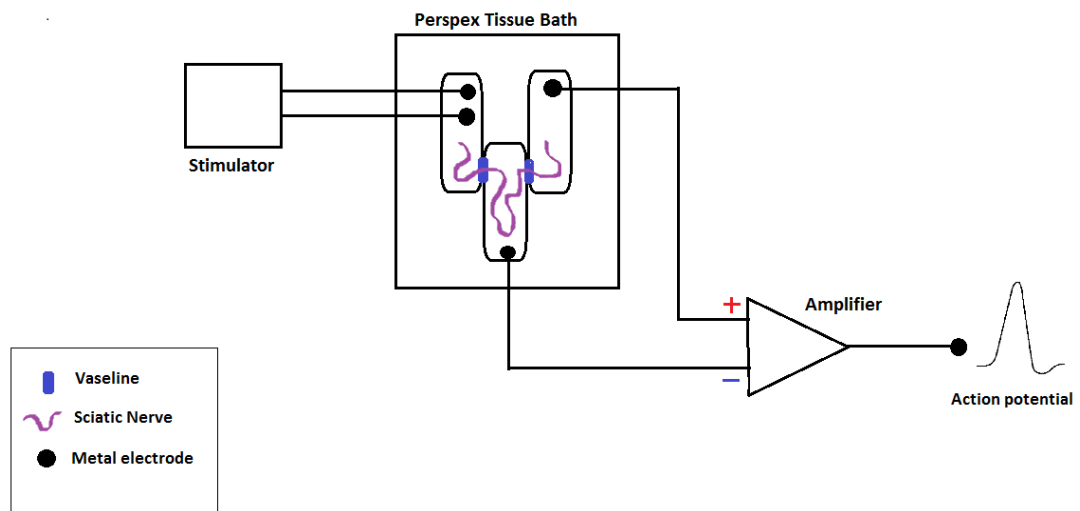


Figure 3.2.1. A schematic diagram of the sciatic nerve bath setup. The sciatic nerve (purple) is laid across three inter-connecting chambers, with each chamber connected to either a stimulator or an amplifier via metal electrodes.

Signals were amplified with a CED 1902 transducer (Cambridge Electronic Design, Cambridge, England), digitised with an analogue digital converter (DigiData 1200 Interface, Axon Instruments, Scotland), and analysed using Microsoft windows based

computer electrophysiological analysis software (WinWCP version 4.5.7; Dempster, 1988).

All experiments were carried out at room temperature and prior to the beginning of each experiment the sciatic nerve was incubated in HEPES based physiological salt buffer for 30 min under constant super-maximal stimulation to demonstrate viability and consistency in the action potential recordings. If the action potential amplitude decreased by 10% the preparation was either remounted in fresh vaseline or discarded. Drugs were added to the middle chamber (1 mM of platinum-based drugs (cisplatin, K_2PtCl_4 , 56MESS, and PHENEN) or 1 mM of macrocyclic drug delivery systems (CB[6], CB[7], β -cyclodextrin, Motor2 and cisplatin@CB[7]). At the end of each experiment tetrodotoxin (TTX; 1 μ g/mL) was added to the central chamber in order to determine the extent of de-sheathing. Sciatic nerves with adequate de-sheathing show a rapid decrease in the amplitude of the action potential when treated with TTX. If the sciatic nerve was not adequately de-sheathed the response to TTX is not as rapid and nerves that portrayed this were discarded and not used in the analysis. Measurements are expressed as the mean \pm SEM (n = 3-5).

3.2.2.2 Isolated Chick Biventer Cervicis Nerve Muscle Preparation

Chicks 3-15 days old were euthanised with CO_2 . The back of their neck was plucked and the skin incised along the midline from the skull to below the base of the neck exposing both of the biventer cervicis muscle lying on either side of the midline. A thread was tied round the upper tendon muscle and a loop was tied at the bottom end of the neck muscle. The muscle was then cut away and kept in buffer solution of the following Krebs-Henseleit physiological salt solution: 118 mM NaCl, 24.9 mM

NaHCO₃, 11.1 mM glucose, 4.69 mM KCl, 1.17 mM MgSO₄, 0.32 mM KH₂PO₄, 2.5 mM CaCl₂ and equilibrated with a gas mixture of 95% O₂, 5% CO₂ to maintain a pH of 7.4. The loop was used to attach the preparation into the organ bath and ring electrodes were placed around the tendon to indirectly stimulate the muscle (Figure 3.2.2).

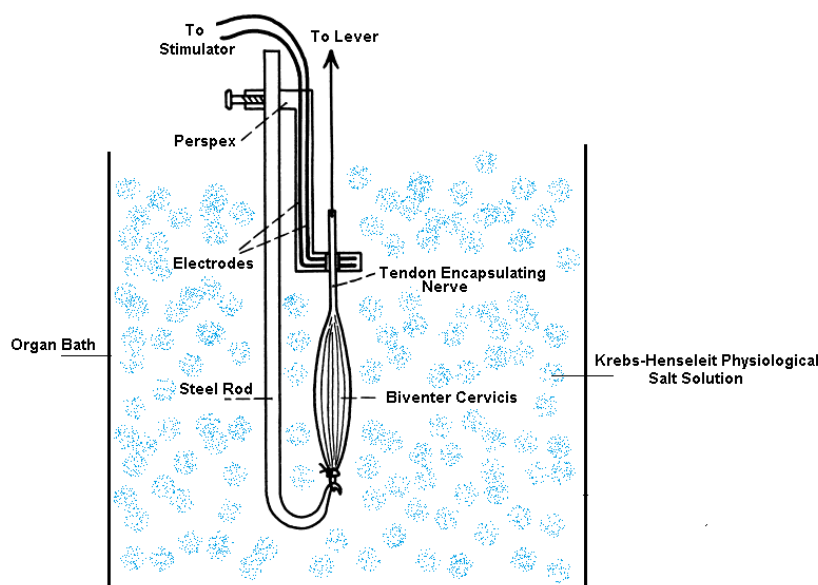


Figure 3.2.2. A schematic diagram showing the biverter cervicis muscle attached to a steel rod via a hoop (tied onto the end of the muscle by silk thread) and an electrode placed around the nerve of the muscle for direct stimulation. Image taken and adapted from <http://www.ncbi.nlm.nih.gov/pmc/articles/PMC1481857/?page=1>.

Prior to the addition of drug, two control responses were obtained: 1 mM ACh (30 s) and 30 mM KCl (30 s), these control drugs were then washed by over flow with drug free Krebs-Henseleit. After the KCl response was obtained, the preparations were allowed to equilibrate for 30 min before the addition 100 μM or 300 μM of platinum based drugs (cisplatin, K₂PtCl₄, 56MESS, and PHENEN) and macrocyclic drug delivery systems (CB[6], CB[7], β-cyclodextrin, Motor2 and cisplatin@CB[7]). At the end of the experiment, the two control responses were repeated to determine the

change in postsynaptic activity. Measurements are expressed as the mean \pm SEM (n = 3-7).

3.2.2.3 Contractile Recordings from Rat Atria

Male Sprague Dawley rats weighing between 250-350 g were killed by cervical dislocation in accordance with the United Kingdom Home Office guidelines. The heart was quickly dissected from the animal and maintained in cold Krebs-Henseleit physiological salt solution of the following composition: 118 mM NaCl, 24.9 mM NaHCO₃, 11.1 mM glucose, 4.69 mM KCl, 1.17 mM MgSO₄, 0.32 mM KH₂PO₄, 2.5 mM CaCl₂, and equilibrated with a gas mixture of 95% O₂, 5% CO₂ to maintain the pH at 7.4. The left and right atria were then carefully removed from the heart under a stereo-microscope and a small loop was tied at one end of both atria and a knot at the other end using a thin thread. The atria were then mounted into separate 10 mL organ baths containing Krebs-Henseleit physiological salt solution and maintained at 37 °C and gassed with 95% O₂, 5% CO₂ throughout the experiment. In the organ bath, one end of the atria was tied to a metal rod and the other end was attached, via a cotton thread, to a grass force displacement transducer model FT03 connected to a powerlab/4SP analogue to digital recording system (AD Instruments) and displayed on a computer running Windows XP (Figure 3.2.3).

The right atria beats spontaneously due to the sinoatrial node, and a contraction was electrically evoked in the left atria by field stimulation (4 Hz, 2 ms duration, 10-15 V strength: Grass S88). A resting tension of 0.5 g was applied to both the left and right atria and maintained throughout the experiment. Prior to the start of each experiment, 10 μ M noradrenaline (NA) was added to the organ bath, and tissue that did not respond

to NA was discarded. With the tissue that did respond, the NA was then washed out and the tissue allowed to equilibrate for 30 min before the addition of drug (100 μM and 300 μM of platinum based drugs (cisplatin, K_2PtCl_4 , 56MESS, and PHENEN) and macrocyclic drug delivery systems (CB[6], CB[7], β -cyclodextrin, Motor 2 and cisplatin@CB[7]). Measurements are expressed as the mean \pm SEM (n = 3-7).

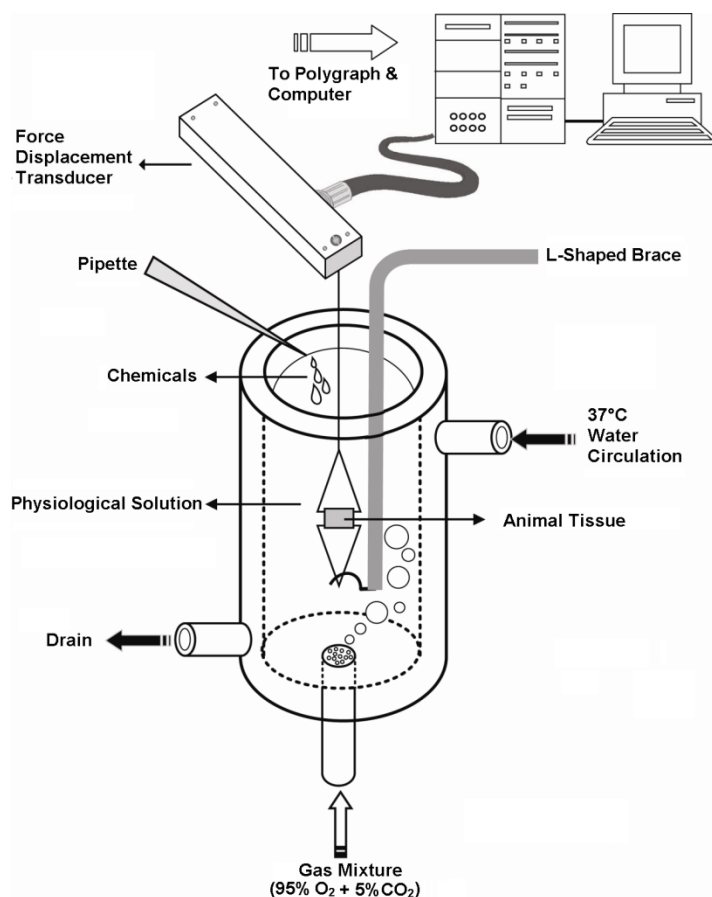


Figure 3.2.3. A schematic diagram showing the setup of the organ bath used for both heart atria preparations. For tissues that were directly stimulated, an electrode was inserted into the organ bath and placed in close proximity to the tissue (not shown). Image taken and adapted from <http://www.intechopen.com/books/artery-bypass/pharmacology-of-arterial-grafts-for-coronary-artery-bypass-surgery>.

3.2.2.4 Statistics

The significance level of individual differences was determined by Student's- t test. A statistical significant difference was deemed to be present when $p < 0.05$.

3.3 Results

3.3.1 Neurotoxicity

3.3.1.1 Viability of the *Ex Vivo* Sciatic Nerve Preparation

To monitor the stability of the desheathed sciatic nerve preparation, the amplitude of the electrically generated nerve compound action potential (nCAP) was measured in volts over a period of two hours. Measurements from multiple experiments were averaged and expressed as means \pm standard error of the mean (S.E.M.), then they were expressed as the percentage of the maximum nCAP over the experimental period; the initial nCAP was considered to be a 100%. A time-response (vitality curve) graph was then plotted using the percentage value at particular time intervals.

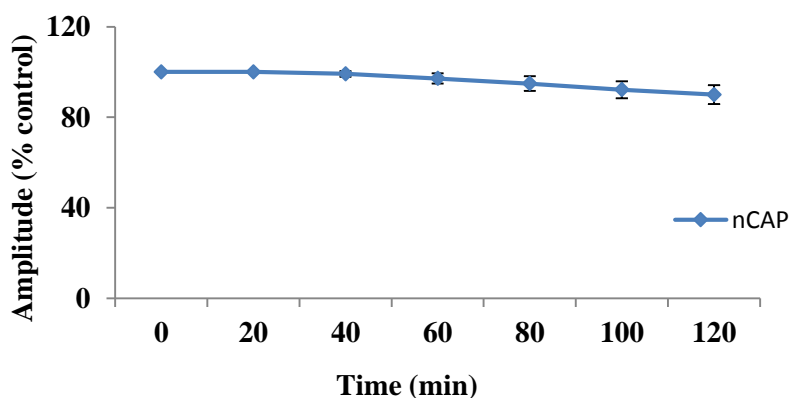


Figure 3.3.1.1. The nCAP amplitude of untreated nerves. Graph showing the change in the amplitude of the nCAP of untreated sciatic nerves over a period of two hours. Results are expressed as the means \pm SEM ($n=3$).

The natural drop-off in nerve conduction was evaluated using a time control study that monitored the stability of the electrically generated nerve compound action potential (nCAP) over a period of two hours. Figure 3.3.1.1 shows that within the

first 40 min the sciatic nerve preparations are still 100% viable with no change in the amplitude of the nCAP. By 80 minutes the amplitude of the nCAP has decreased by only $5 \pm 3.3\%$ but by 120 minutes the sciatic nerve has lost $10 \pm 4.2\%$ of its viability. As a result, the toxicity experiments were carried using macrocycle solutions of 1 mM over a period of 80 minutes to ensure reliability of the results.

3.3.1.2 Neurotoxic Activity of Platinum-Based Drugs

The neurotoxic activity of platinum-based drugs (cisplatin, K_2PtCl_4 , 56MESS and PHENEN), was investigated by treating the desheathed mouse sciatic nerve with 1 mM of drug and by recording any changes made to the amplitude of the nCAP over a period of 80 min.

The results show that all of the platinum-based drugs decreased the nCAP amplitude of the sciatic nerve (Table 2.1). By the end of the experiment, cisplatin had induced a decrease of $13 \pm 4.7\%$ ($p = 0.3$) to the nCAP amplitude of the sciatic nerve, while K_2PtCl_4 had reduced it by $20 \pm 1.5\%$ ($p = 0.01$), 56MESS by $15 \pm 0.6\%$ ($p = 0.02$) and PHENEN by $10 \pm 2.2\%$ ($p = 0.4$). Statistical difference compared to untreated nerve is only observed with K_2PtCl_4 and 56MESS. Therefore only these two drugs can be considered neurotoxic (Figure 3.3.1.2).

Drug	Effect on nCAP	Students paired t-test
Cisplatin	↓ 13 ± 4.7%	<i>p</i> = 0.3
K₂PtCl₄	↓ 20 ± 1.5%	<i>p</i> = 0.01
56MESS	↓ 15 ± 0.6%	<i>p</i> = 0.02
PHENEN	↓ 10 ± 2.2%	<i>p</i> = 0.4

Table 2.1. A summary of the changes induced by each platinum-based drug on the nCAP amplitude of the mouse sciatic nerve after 80 min. The arrows indicate an increase (↑) or decrease (↓) in the nCAP amplitude.

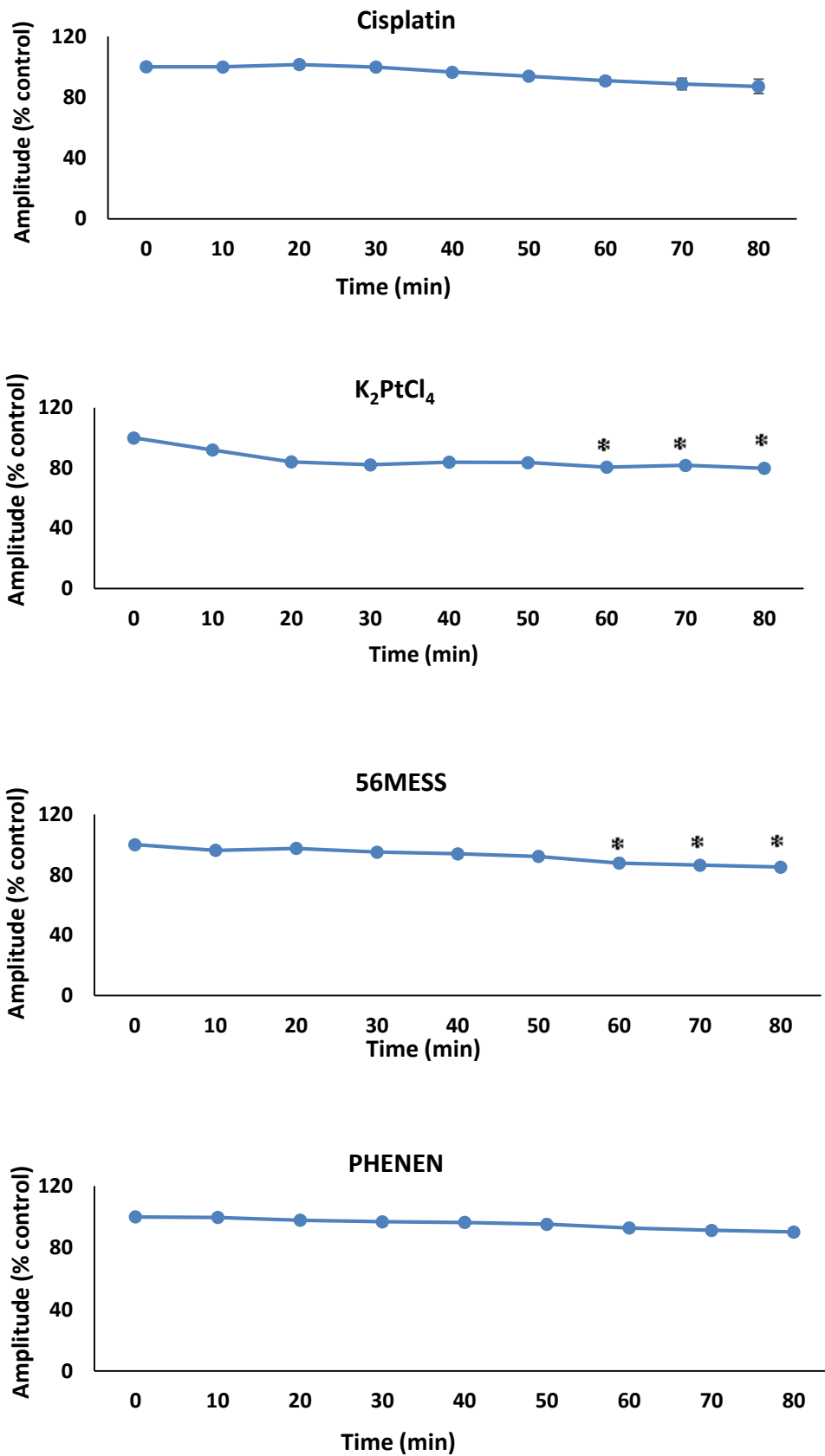


Figure 3.3.1.2. The change in nCAP amplitude of the sciatic nerve after treatment with platinum-based drugs. Graph showing the changes induced in nCAP after treatment with cisplatin, K₂PtCl₄, 56MESS and PHENEN after 80 minutes. Results are expressed as the means ± SEM (*n* = 3). Statistical students paired t-test was performed and significant differences compared to time match control are indicated by * when *p* < 0.05.

3.3.1.3 Neurotoxic Activity of Macrocycles

The neurotoxic activity of the macrocyclic compounds CB[6], CB[7], Motor2 and β -cyclodextrin was investigated by treating the desheathed mouse sciatic nerve with 1 mM of macrocycle and by recording any changes made to the amplitude of the nCAP over a period of 80 min.

The results show that CB[7] and Motor2 induced a decrease in nCAP amplitude by $4 \pm 0.2\%$ ($p = 0.8$) and $13 \pm 1.5\%$ ($p = 0.1$), respectively, while CB[6] and β -cyclodextrin induced an increase in nCAP by $3 \pm 4.6\%$ ($p = 0.3$) and $7 \pm 4.2\%$ ($p = 0.1$), respectively (Figure 3.3.1.3). β -cyclodextrin, which is already used in the clinic, is not known to be neurotoxic, so the similar increase in nCAP by CB[6] implies that the cucurbituril is probably not neurotoxic. The decrease in nCAP by CB[7] is the same magnitude as the natural drop-off in untreated samples indicating it is also not neurotoxic. Whilst Motor2 decreased nCAP by 13% there is no statistical difference compared with untreated nerve, all of the other macrocycles also show no statistical significance to control and therefore all appear to display no neurotoxicity.

Drug	Effect on nCAP	Students paired t-test
CB[6]	$\uparrow 3 \pm 4.6\%$	$p = 0.3$
CB[7]	$\downarrow 4 \pm 0.2\%$	$p = 0.8$
Motor2	$\downarrow 13 \pm 1.5\%$	$p = 0.1$
β-cyclodextrin	$\uparrow 7 \pm 4.2\%$	$p = 0.1$

Table 2.2. A summary of the changes induced by each macrocycle on the nCAP amplitude of the mouse sciatic nerve after 80 min. The arrows indicate an increase (\uparrow) or decrease (\downarrow) in the nCAP amplitude.

The results show that CB[7] and Motor2 induced a decrease in nCAP amplitude by $4 \pm 0.2\%$ ($p = 0.8$) and $13 \pm 1.5\%$ ($p = 0.1$), respectively, while CB[6] and β -cyclodextrin induced an increase in nCAP by $3 \pm 4.6\%$ ($p = 0.3$) and $7 \pm 4.2\%$ ($p = 0.1$), respectively (Figure 3.3.1.3). β -cyclodextrin, which is already used in the clinic, is not known to be neurotoxic, so the similar increase in nCAP by CB[6] implies that the cucurbituril is probably not neurotoxic. The decrease in nCAP by CB[7] is the same magnitude as the natural drop-off in untreated samples indicating it is also not neurotoxic. Whilst Motor2 decreased nCAP by 13% there is no statistical difference compared with untreated nerve, all of the other macrocycles also show no statistical significance to control and therefore all appear to display no neurotoxicity.

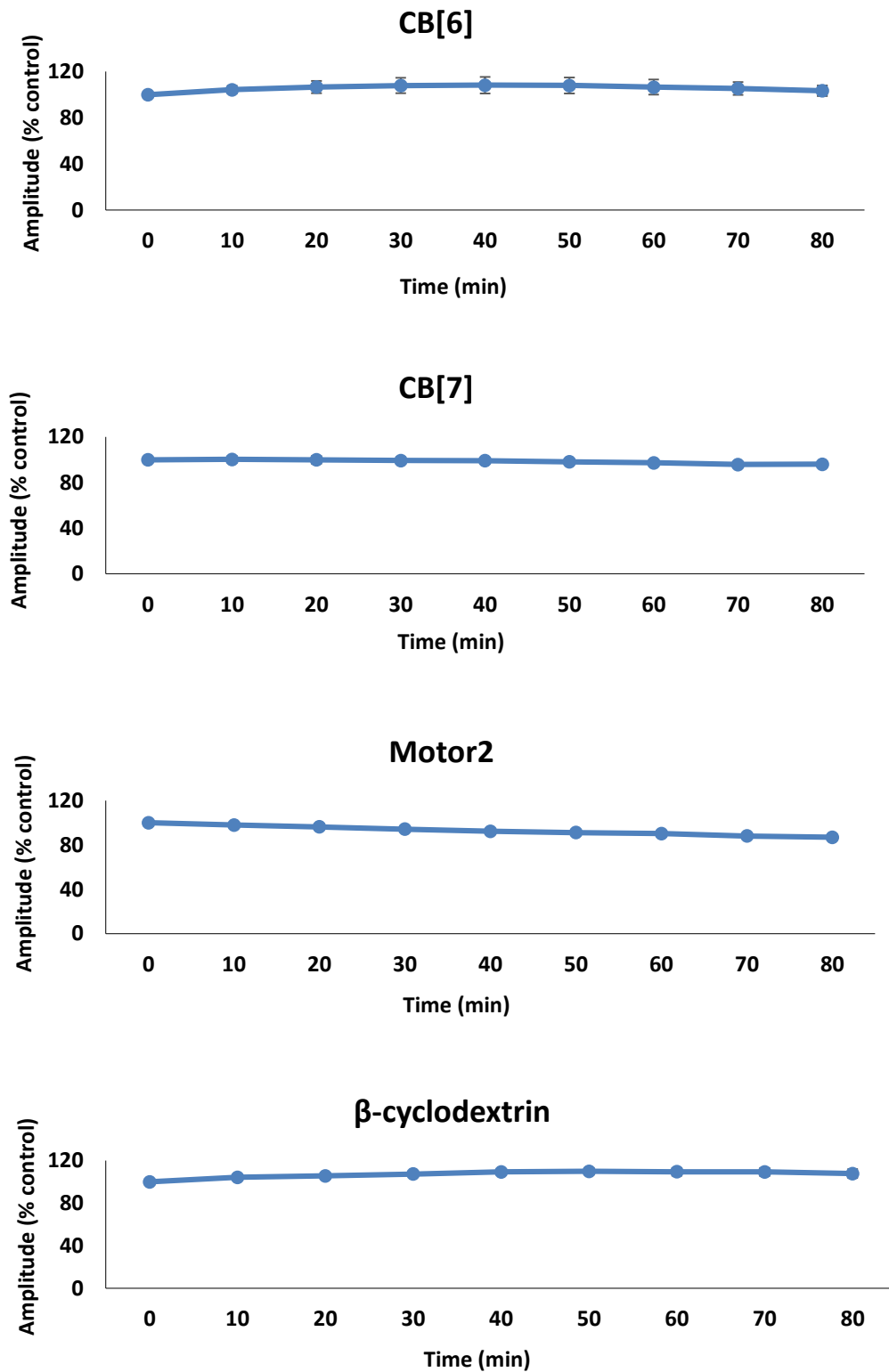


Figure 3.3.1.3. The change in nCAP amplitude of the sciatic nerve after treatment with macrocycles. Graph showing the changes induced in nCAP after treatment with CB[6], CB[7], Motor2 and β -cyclodextrin after 80 minutes. Results are expressed as the means \pm SEM ($n = 3$). Statistical students paired t-test was performed and significant differences compared to time match control are indicated by * when $p < 0.05$.

3.3.1.4 Effect of CB[7] on the Neurotoxicity of Cisplatin

The effect of CB[7] on the neurotoxicity of cisplatin was investigated by analysing and comparing the effect of 1 mM of cisplatin and 1mM of cisplatin@CB[7] on the nCAP amplitude of the desheathed mouse sciatic nerve (Figure 3.3.1.4).

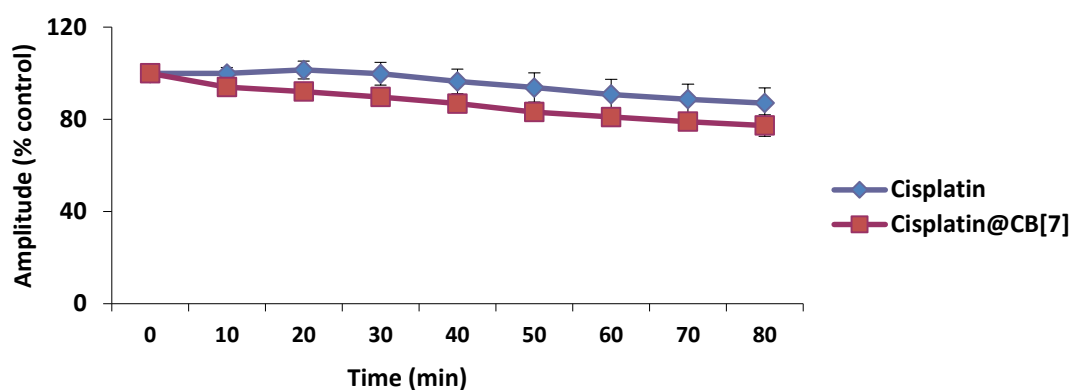


Figure 3.3.1.4. The difference in the change of the nCAP amplitude of the sciatic nerve after treatment with 1 mM of (blue) free cisplatin and (red) cisplatin@CB[7]. Results are expressed as the means \pm SEM ($n=3$). Statistical students paired t-test was performed ($n=3$) and significant differences are indicated by * when $p<0.05$.

Figure 3.3.1.4 show that at 80 min, cisplatin reduced the nCAP amplitude by $13 \pm 4.7\%$ ($p = 0.3$), which shows some neurotoxicity but not at the level normally observed in the clinic. The reason for the lower toxicity is most likely because the sciatic nerve is composed mainly of neuronal axons with smaller amounts of DRG, (which are predominantly located in the spinal cord). Therefore, the small neurotoxicity caused by cisplatin in this experiment is due to the small amounts of DRG. The results for cisplatin@CB[7] are similar to free cisplatin with a decrease in nCAP amplitude of $23 \pm 6.6\%$ ($p = 0.1$). Statistical analysis shows that there is no difference in the

neurotoxicity of cisplatin compared with cisplatin@CB[7]. Therefore indicating that CB[7] does not have a neuro-protective effect on cisplatin.

3.3.2 Neuromyopathy

The neuromyopathy of the drugs and macrocycles were examined using the isolated chick biventer cervicis nerve-muscle preparation. Under *ex vivo* conditions the muscle can be forced to contract using chemical or electrical stimulation. For chemical stimulation, the addition of exogenous acetylcholine (ACh) or KCl results in muscle contraction. The ACh acts by binding to nicotinic receptors located on the muscle membrane causing depolarisation followed by contraction (post-synaptic effect). Potassium chloride causes muscle membrane depolarisation resulting in calcium release into the synaptic cleft. The calcium then binds to neuronal receptors which results in the release of ACh from the neuron ultimately causing muscle contraction (pre-synaptic effect).

Baseline results for the force of muscle contraction was determined using both electrical and chemical stimulation. The nerve-muscle was then exposed to drug/macrocycle and after two hours the force of contraction was determined again. The drugs/macrocycles are neuromyopathic if they demonstrate a statistically significant increase or decrease in the force of muscle contraction compared with baseline results. An increase in force of contraction due to exogenous ACh indicates that the compound tested may have anticholinesterase effect; cholinesterase is an enzyme located in the synaptic cleft that terminates signal transmission by breaking down acetylcholine activity therefore prolonging/increasing the effect of ACh. An

increase in the activity of ACh will synergistically increase/prolong the response to KCl.

3.3.2.1. Viability of the *Ex Vivo* Chick Biventer Cervicis Nerve Muscle Preparation

The viability of the biventer cervicis nerve-muscle preparation was studied by comparing nerve-muscle response to ACh, KCl and the amplitude of the electrically stimulated contraction at the end of the experiment compared to the beginning of the experiment. Figure 3.3.2 shows that after two hours, the untreated nerve-muscles response to ACh, KCl and its electrically stimulated contraction had all decreased by $4 \pm 2\%$ ($p = 0.01$), $18 \pm 5\%$ ($p = 0.1$) and $11 \pm 5\%$ ($p = 0.3$), respectively.

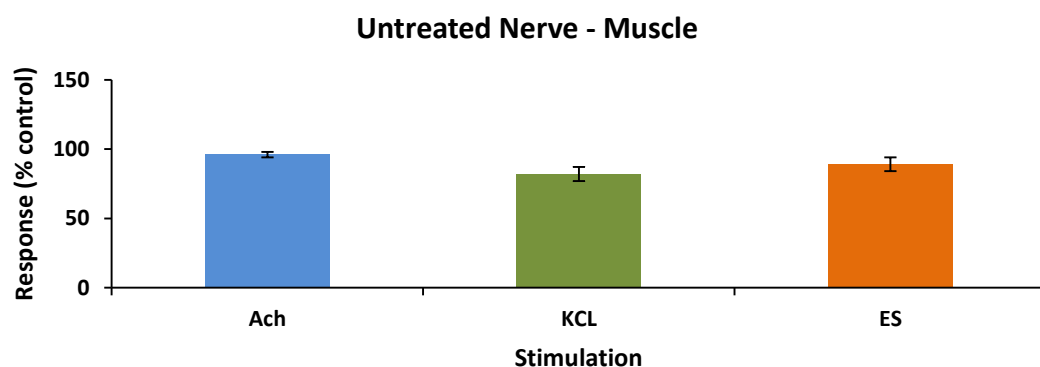


Figure 3.3.2. The percentage change in the response of untreated (control) chick biventer cervicis nerve-muscle to ACh, KCl and to the amplitude of electrically stimulated contraction after two hours incubation. Results are expressed as the means \pm SEM ($n = 3$). Statistical students paired t-test was performed.

3.3.2.2 Neuromyopathic Activity of Platinum Based Drugs

The neuromyopathic activity of various platinum-based drugs (cisplatin, K_2PtCl_4 , PHENEN and 56MESS) were investigated by treating the chick biventer cervicis nerve-muscle with 300 μM of compound for a period of two hours. Before drug exposure, the response of untreated muscle to ACh and KCl as well as the amplitude of the electrically stimulated muscle contraction were recorded. After drug treatment, the response of the muscle to the same agonists and the amplitude of the electrically stimulated contraction were recorded once again and compared to that of pre-treatment (control).

Figure 3.3.2.1 show that all of the platinum drugs tested exhibited neuromyopathic activity. The results show that cisplatin, 56MESS and PHENEN induced muscle toxicity (paralysis) indirectly by interfering with the activity of the presynaptic neuron, whereas K_2PtCl_4 induced muscle toxicity through direct action on the postsynaptic muscle fiber.

At 300 μM , cisplatin induced an increase in nerve-muscle response to ACh and KCl by $96 \pm 32\%$ ($p = 0.005$) and $121 \pm 3\%$ ($p = 0.001$) respectively, whereas it decreased muscle twitch amplitude by $96 \pm 4\%$ ($p = 0.001$). The augmentation of ACh and KCl responses indicates that cisplatin did not interfere with the nicotinic acetylcholine receptors (nAChRs) or with the integrity (depolarisation) of the postsynaptic muscle membrane. Instead, the reduction in muscle twitch amplitude indicates that cisplatin induced neuromyopathy from interfering with activity of the presynaptic nerve terminal. Unlike cisplatin, K_2PtCl_4 decreased nerve-muscle responses to both agonists

as well as the amplitude of the muscle twitch. K_2PtCl_4 decreased nerve-muscle response to ACh by $60 \pm 4.4\%$ ($p = 0.11$), KCl by $90 \pm 2.8\%$ ($p = 0.001$), and twitch amplitude by $82.8 \pm 3.9\%$ ($p = 0.005$). This significant decrease in nerve-muscle response to ACh suggests that K_2PtCl_4 may have blocked the nicotinic receptors on the muscle membrane or the calcium ion channel in the sarcoplasmic reticulum or may have bound to proteins in the muscle fiber that play a role in contraction, therefore indicating that K_2PtCl_4 is acting directly on the postsynaptic muscle fibre. The possibility that K_2PtCl_4 is directly neuromyopathic is further supported by the decrease in the nerve-muscle response to KCl which is an indication that the muscle fibre contractility has been critically impaired.

When treated with $300 \mu M$ of 56MESS, the nerve-muscle response to ACh and KCl were increased by $45 \pm 12\%$ ($p = 0.3$) and $3 \pm 11\%$ ($p = 0.2$) respectively, and a complete blockade in muscle twitch was observed. These results suggest that 56MESS did not induce muscle paralysis by acting on the muscle's nicotinic receptors or with the viability of the membrane, but indirectly via a presynaptic effect at the nervous terminal. This effect is also observed with PHENEN, where an increased nerve-muscle response to ACh and KCl by $77 \pm 7.5\%$ ($p = 0.002$) and $22 \pm 7.2\%$ ($p = 0.2$), respectively was observed as well as a decrease in muscle twitch amplitude by $38\% \pm 1.8\%$ ($p = 0.01$) (Table 3.1 provides a summary of the neuromyopathy results).

	ACh	KCl	Electrical Stimulation
Cisplatin	↑ 96 ± 32% (<i>p</i> = 0.005)	↑ 121 ± 3% (<i>p</i> = 0.001)	↓ 96 ± 4% (<i>p</i> = 0.001)
K₂PtCl₄	↓ 60 ± 4.4% (<i>p</i> = 0.11)	↓ 90 ± 2.8% (<i>p</i> = 0.001)	↓ 82.8 ± 3.9% (<i>p</i> = 0.005)
PHENEN	↑ 77 ± 7.5% (<i>p</i> = 0.02)	↑ 22 ± 7.2% (<i>p</i> = 0.2)	↓ 38 ± 1.8% (<i>p</i> = 0.01)
56MESS	↑ 45 ± 12% (<i>p</i> = 0.3)	↑ 3 ± 11% (<i>p</i> = 0.2)	↓ 100 ± 13% (<i>p</i> = 0.009)

Table 3.1. A summary of the changes induced by each platinum-based drug on the amplitude of the nerve-muscle contraction induced by ACh, KCl and electrical stimulation after two hour incubation. The arrows indicate an increase (↑) or decrease (↓) in nerve-muscle contraction.

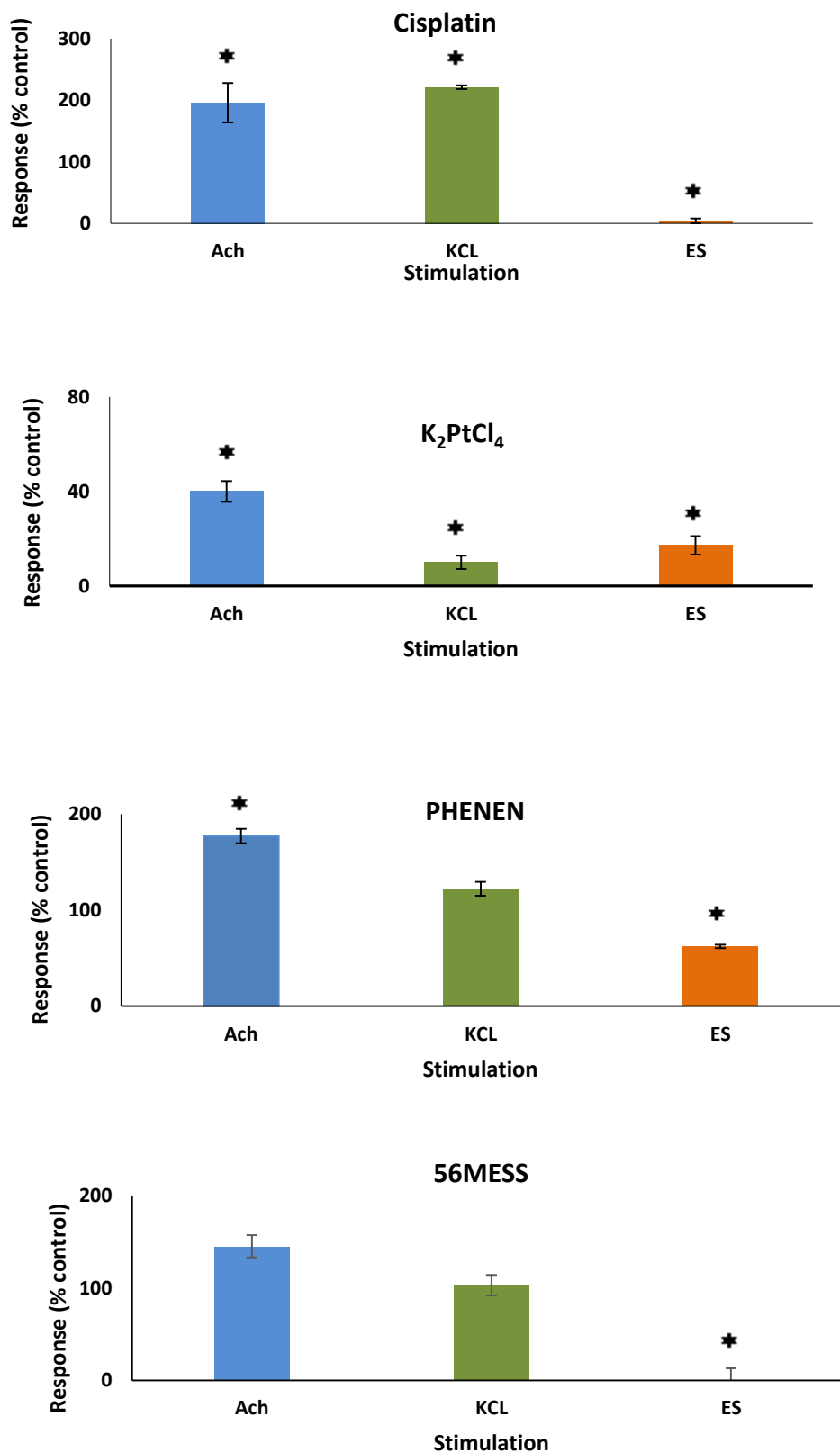


Figure 3.3.2.1. The responses of nerve-muscle to ACh (1 mM, 30 s) KCl (30 mM, 30 s) and electrically stimulated contraction at two hours after exposure to 300µM of platinum-based drugs. Results are expressed as mean ± SEM. For cisplatin; *n* = 4, K₂PtCl₄; *n* = 4, PHENEN; *n* = 3 and 56MESS; *n* = 3. Statistical students paired t-test was performed and significant differences are indicated by * when *p* < 0.05.

3.3.2.3 Neuromyopathic Activity of Drug Delivery Macrocycles

The neuromyopathic of various drug delivery macrocycles (CB[6], CB[7], β -cyclodextrin, and Motor2) were investigated by treating the chick biventer cervicis nerve-muscle with 300 μ M of compound for a period of two hours. Before drug exposure, the response of untreated muscle to ACh and KCl as well as the amplitude of the electrically stimulated muscle contraction were recorded. After drug treatment, the response of the muscle to the same agonists and the amplitude of the electrically stimulated contraction were recorded once again and compared to that of pre-treatment (control).

Figure 3.3.2.2 shows Cucurbit[6]uril increased nerve-muscle response to ACh by $10 \pm 10\%$ ($p = 0.5$), and decreased its response to KCl and electrical stimulated contraction by $24 \pm 17\%$ ($p = 0.5$) and $20 \pm 4\%$ ($p = 0.3$), respectively. Cucurbit[7]uril decreased the nerve-muscle's response to ACh, KCl and the electrically stimulated contraction by $21\% \pm 10\%$ ($p = 0.1$), $51.8 \pm 8\%$ ($p = 0.05$) and $84 \pm 9\%$ ($p = 0.01$), respectively. The cucurbituril-derivative, Motor2, increased nerve-muscle response to both ACh and KCl by $37 \pm 12\%$ ($p = 0.5$) and $2\% \pm 12\%$ ($p = 0.8$), respectively, and decreased its electrically stimulated contraction by $15 \pm 13\%$ ($p = 0.5$). β -Cyclodextrin increased nerve-muscle response to ACh by $20 \pm 7\%$ ($p = .2$), decreased its response to KCl by $15 \pm 9\%$ ($p = 0.2$), and increased its electrical stimulated contraction by $11 \pm 10\%$ ($p = 0.9$).

Overall the largest neuromyopathic effect was observed after nerve muscle exposure to CB[7]. Significant decreases in activity are apparent for KCl ($p = 0.05$) and electrical

stimulation ($p = 0.01$), this indicates that CB[7] may be binding to and blocking the postsynaptic muscle's nicotinic receptors and therefore interfering with the depolarisation ability of the membrane. A small decrease in twitch via electrical stimulation is also observed after exposure to CB[6] ($p = 0.3$) although the decrease is considerably smaller in magnitude compared with CB[7]. Given that β -cyclodextrin also results in a decrease of electrically stimulated contraction ($p = 0.9$), it is not a known neuromyopathic compound, the results may suggest that the electrical stimulation results for CB[6] and CB[7] are statistically decreased, however this may not result in *in vivo* toxicity. Table 3.2 provides a summary of the neuromyopathy results.

	ACh	KCl	ESC
CB[6]	$\uparrow 10 \pm 10\%$ ($p = 0.5$)	$\downarrow 24 \pm 17\%$ ($p = 0.5$)	$\downarrow 20 \pm 4\%$ ($p = 0.3$)
CB[7]	$\downarrow 21 \pm 10\%$ ($p = 0.1$)	$\downarrow 51.8 \pm 8\%$ ($p = 0.05$)	$\downarrow 84 \pm 9\%$ $p = 0.01$
Motor2	$\uparrow 37 \pm 12\%$ ($p = 0.5$)	$\uparrow 2 \pm 12\%$ ($p = 0.8$)	$\downarrow 15 \pm 13\%$ ($p = 0.5$)
β-cyclodextrin	$\uparrow 20 \pm 7\%$ ($p = 0.2$)	$\downarrow 15 \pm 9\%$ ($p = 0.2$)	$\uparrow 11 \pm 10\%$ ($p = 0.9$)

Table 3.2. A summary of the changes induced by each macrocycle on the amplitude of the nerve-muscle contraction induced by ACh, KCl and ES (electrical stimulation) after 120 min. The arrows indicate an increase (\uparrow) or decrease (\downarrow) in nerve-muscle contraction

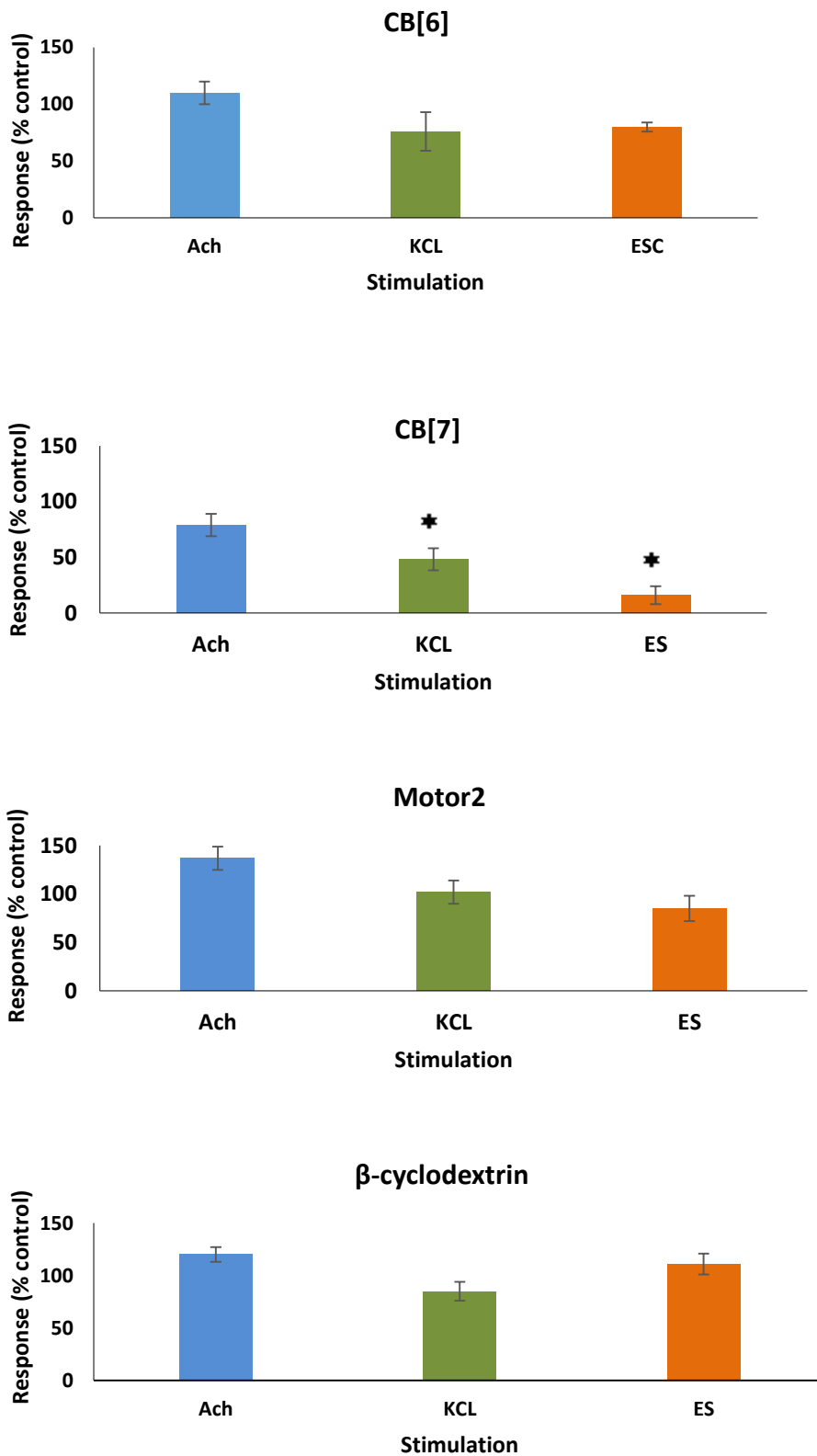


Figure 3.3.2.2. The responses of nerve-muscle to ACh (1 mM, 30 s) KCl (30 mM, 30 s) and electrically stimulated contraction at two hours after exposure to 300 μ M of macrocycle. Results are expressed as mean \pm SEM. For untreated nerves; $n = 3$, CB[6]; $n = 3$, CB[7]; $n = 4$, Motor2; $n = 3$, and β -cyclodextrin; $n = 3$. Statistical students paired t-test was performed and significant differences are indicated by * when $p < 0.05$.

3.3.2.4 Effect of CB[7] on the Neuromyopathy of Cisplatin

The effect of CB[7] on the neuromyopathic activity of cisplatin was investigated by analysing and comparing the effect of 300 μM of cisplatin and 300 μM of cisplatin@CB[7] on the response of the chick biventer cervicis nerve-muscle to chemical and electrical stimulation.

The results show that cisplatin induced significant neuromyopathic activity when measured using both chemical and electrical stimulation (Table 3.3). Figure 3.3.2.3 shows that free cisplatin increased nerve-muscle contraction force to ACh and KCl by $96 \pm 32\%$ ($p = 0.005$) and $121 \pm 3\%$ ($p = 0.001$), respectively, and decreased the force of its electrically stimulated contraction by $96 \pm 4\%$ ($p = 0.001$) which is consistent with the peripheral neuropathy known to occur with cisplatin chemotherapy. The results also suggest that cisplatin may have anticholinesterase activity as demonstrated in previous studies and that this may also contribute in part to the neurotoxic side effects of cisplatin. Encapsulation of cisplatin by CB[7] decreased nerve-muscle response to ACh by $17 \pm 6\%$ ($p = 0.4$), and increased its response to KCl by $59 \pm 27\%$ ($p = 0.2$). Cucurbit[7]uril showed a neuromyopathy-protective effect as cisplatin@CB[7] decreased the electrical stimulated muscle contraction by $36 \pm 12\%$ ($p = 0.04$) only; this is a reduction of the myotoxic activity of free cisplatin by 60%.

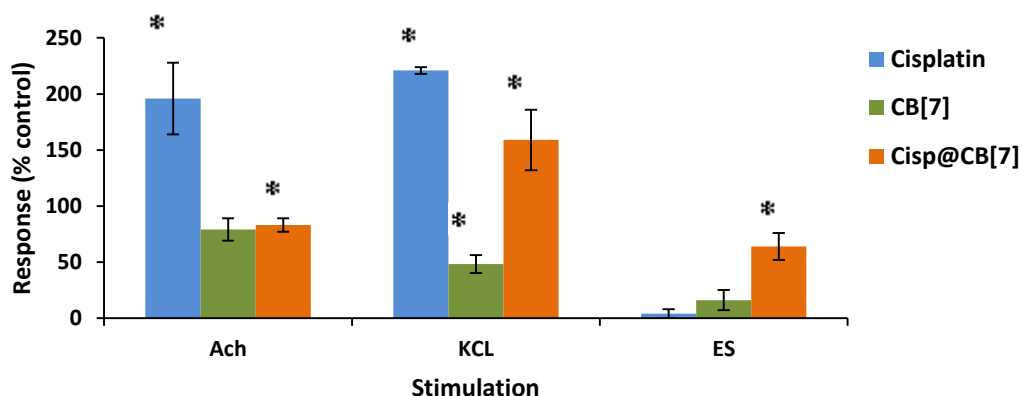


Figure 3.3.2.3. The effect of cisplatin (n = 4), CB[7] (n = 4) and cisplatin@CB[7] (n = 8) on the nerve muscle's response to ACh (grey), KCl (green) and amplitude of its electrically stimulated contraction after two hours of exposure to drug. Results are expressed as mean \pm SEM. Statistical students paired t-test was performed and significant differences are indicated by * when $p < 0.05$.

	ACh	KCl	Electrical Stimulation
Cisplatin	$\uparrow 96 \pm 32\%$ ($p = 0.005$)	$\uparrow 121 \pm 3\%$ ($p = 0.001$)	$\downarrow 96 \pm 4\%$ ($p = 0.001$)
CB[7]	$\downarrow 21 \pm 10\%$ ($p = 0.1$)	$\downarrow 51.8 \pm 8\%$ ($p = 0.05$)	$\downarrow 84 \pm 9\%$ ($p = 0.01$)
Cisplatin@CB[7]	$\downarrow 17 \pm 6\%$ ($p = 0.4$)	$\uparrow 59 \pm 27\%$ ($p = 0.2$)	$\downarrow 36 \pm 12\%$ ($p = 0.04$)

Table 3.3. A summary of the changes induced by free drug and the encapsulated complex on the amplitude of the nerve-muscle contraction induced by ACh, KCl and ES (electrical stimulation) after 120 min. The arrows indicate an increase (\uparrow) or decrease (\downarrow) in nerve-muscle contraction.

3.3.3. Cardiotoxicity

Heart atria from rats were used as a model to study the cardiotoxic activity of the macrocycles. The right atrium contains a natural pacemaker called the sinoatrial (SA) node which causes the atrium to contract naturally; however, such a pacemaker is absent in the left atrium and electrical stimulation is needed to initiate contraction.

3.3.3.1 Viability of the *Ex Vivo* Atria Preparation

The viability of the right and left atria preparation setup was studied by monitoring the rate of atria contraction (beats per minute) and force of contraction (amplitude of contraction) over a period of two hours. A time-response graph was then plotted using the percentage value at particular time intervals (Figure 3.3.3).

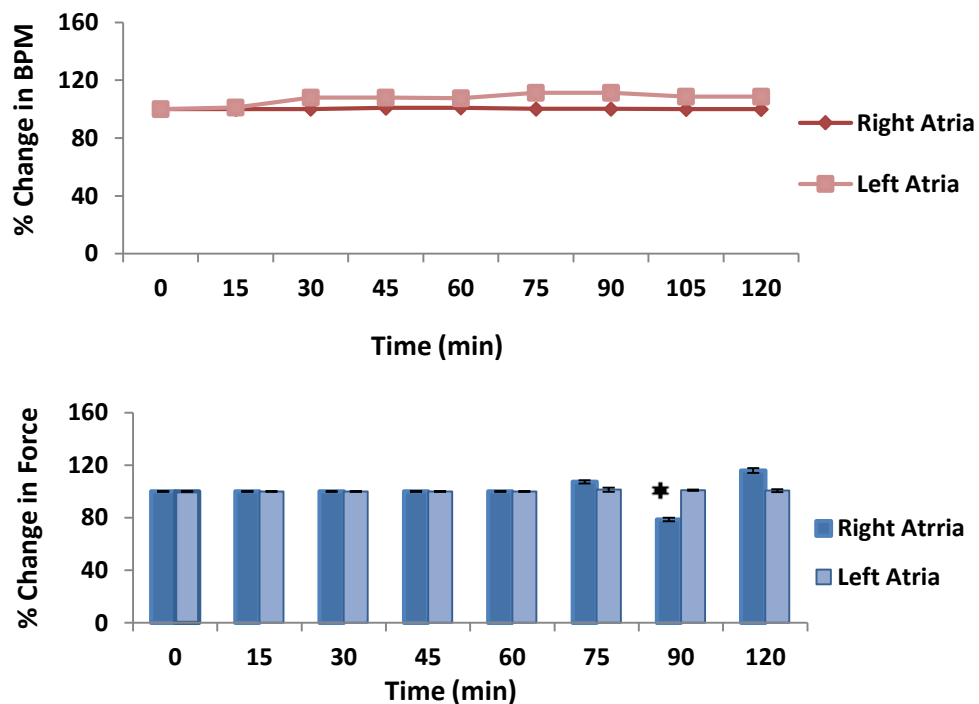


Figure 3.3.3. The change in atria contraction rate (top panel) and force of contraction (bottom panel) in untreated right (dark red, dark blue) and left atria (light red, light blue) over a period of two hours. Results are expressed as the means \pm SEM ($n=3$). Statistical students paired t-test was performed and significant differences compared to time 0 min are indicated by * when $p<0.05$.

Figure 3.3.3 shows that by the end of the experiment, the rate of right atria contraction had increased by of $8 \pm 1\%$ ($p = 0.4$) compared to the rate of contraction at time at 0 min (100%), whereas the left atria remained unchanged at $100 \pm 1\%$. By the end of the experiment, the force of contraction remained at $100 \pm 2\%$ whereas in the left atria it had a statistically significant increase of $16 \pm 1.9\%$ ($p = 0.005$).

3.3.3.2 Cardiotoxic Activity of Platinum-Based Drugs

The cardiotoxic effects of the platinum-based drugs (cisplatin, K_2PtCl_4 , 56MESS and PHENEN) were studied by monitoring changes in the rate of atria contraction and force of contraction over a two hour period in both the right and left atria.

Overall the results show that all of the platinum-based drugs induced a statistically significant change to the rate and/or force of contraction either in the right atria, the left atria or in both.

By the end of the experiment, in the right atria, cisplatin induced a decrease in atria contraction rate by 68.8 ± 8.45 and in the force of contraction by $53.7 \pm 17\%$ ($p = 0.02$). In the left atria, cisplatin decreased contraction rate by $1 \pm 1\%$ ($p = 0.8$) and decreased the force of contraction by $55 \pm 6.1\%$ ($p = 0.02$). When treated with K_2PtCl_4 , the rate of right atria contraction was decreased by $92.7 \pm 4.45\%$ ($p = 0.001$) and the force of its contraction by $99.3 \pm 0.4\%$ ($p = 0.001$), whereas in the left atria, it reduced the rate and force of contraction by $16.2 \pm 3.2\%$ ($p = 0.4$) and $48.4 \pm 9.2\%$ ($p = 0.008$), respectively. In the right atria, 56MESS reduced the rate of contraction by $39.8 \pm 3.4\%$ ($p = 0.04$) and the force of contraction by $26.1 \pm 3.5\%$ ($p = 0.07$), and in the left atria

56MESS reduced the rate of contraction by $7.3 \pm 12.3\%$ ($p = 0.06$) and the force of contraction by $15.1 \pm 7.4\%$ ($p = 0.13$). Finally, PHENEN decreased the rate of right atria contraction by $20.8 \pm 9\%$ ($p = 0.05$) and force of contraction by $22.3 \pm 3.6\%$ ($p = 0.008$) and in the left atria, it increased atria contraction by $0.9 \pm 1.8\%$ ($p = 0.6$) and decreased the force of contraction by $50 \pm 17.5\%$ ($p = 0.02$).

All of the platinum-based drugs displayed cardiotoxic activity. Cisplatin and K_2PtCl_4 were the quickest to induce their toxic activity in both the rate and force of contraction as seen (Figure 3.3.3.2 and 3.3.3.3). Both cisplatin and K_2PtCl_4 induced their toxic effects immediately after exposure, whereas 56MESS induced its toxic activity by 30 minutes and PHENEN by 60 minutes of exposure. Table 3 gives a summary of the effect of each platinum-based drug on the rate and force of atria contraction.

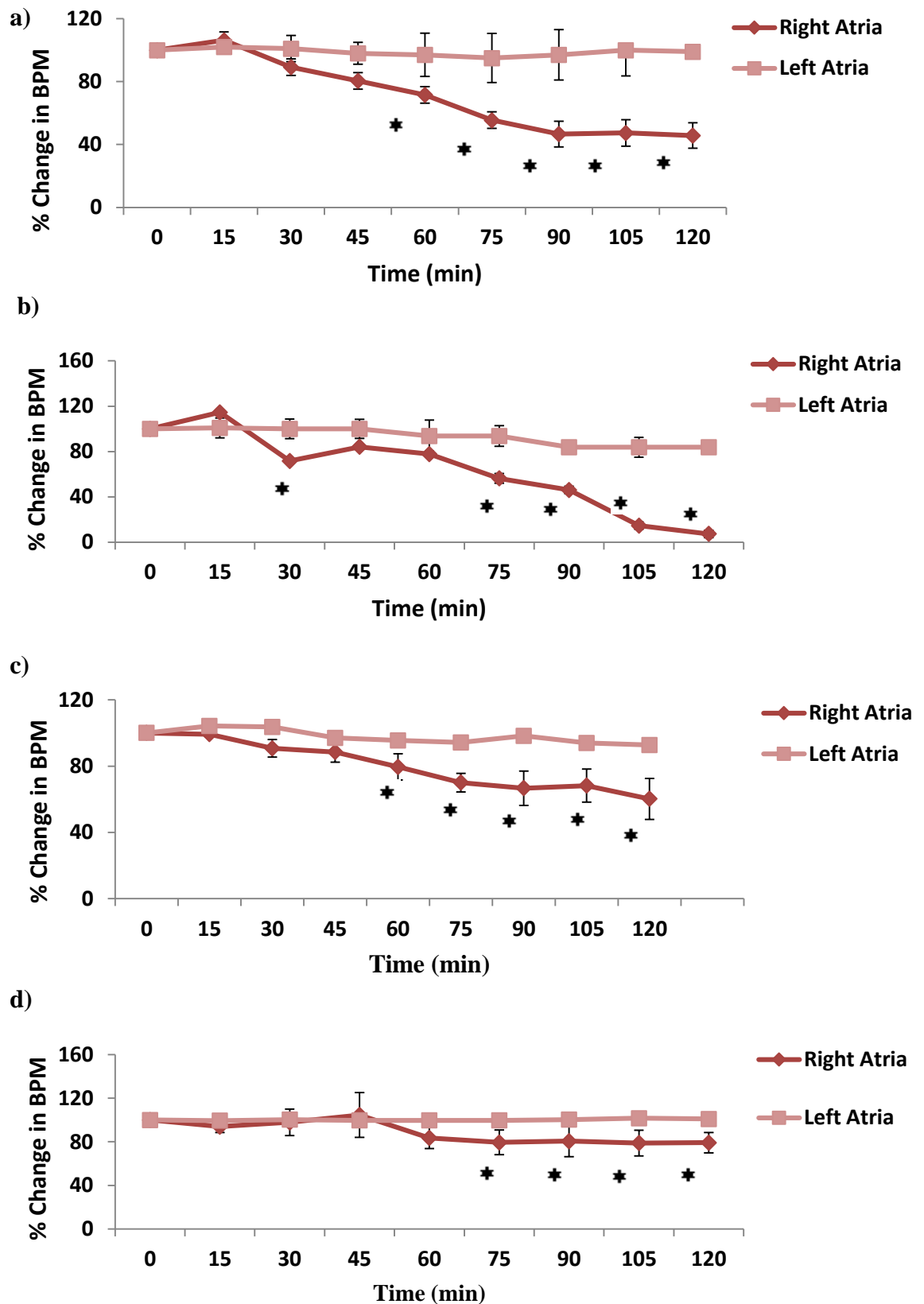


Figure 3.3.3.2. The effect of the platinum-based drugs on atria contraction rate. Graph shows the effect of a) cisplatin, b) K₂PtCl₄, c) 56MESS and d) PHENEN on atria contraction rate. Results are expressed as the means \pm SEM ($n=3$). Statistical students paired t-test was performed and significant differences compared to time match control are indicated by * when $p<0.05$.

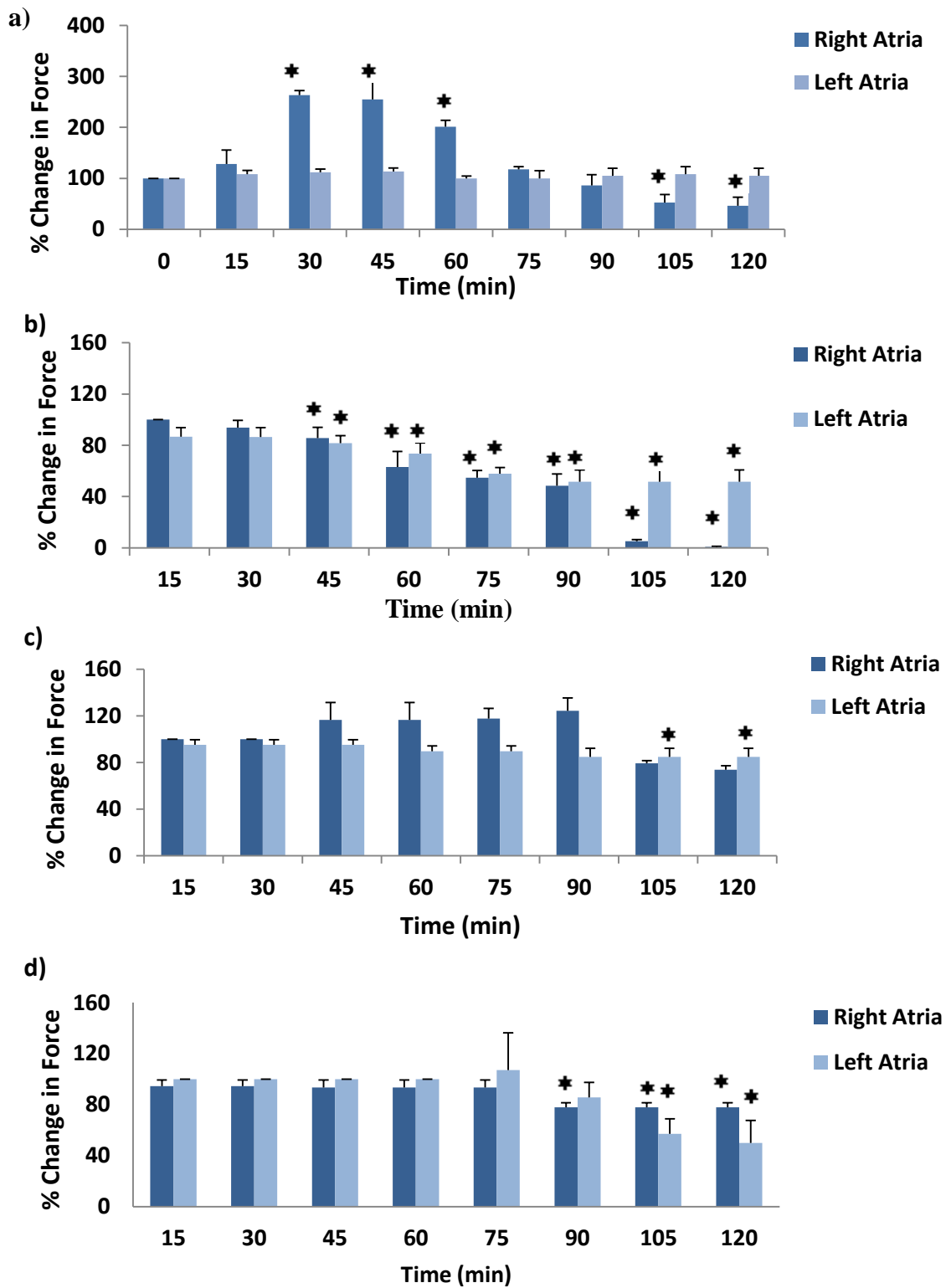


Figure 3.3.3.3. The effect of the platinum-based drugs on atria force of contraction. Graph shows a) cisplatin, b) K₂PtCl₄, c) 56MESS and d) PHENEN on the contraction rate of the right and left atria. Results are expressed as the means \pm SEM ($n = 3$). Statistical students paired t-test was performed and significant differences compared to time match control are indicated by * when $p < 0.05$.

Platinum Drug (300 μ M)	Percent change in rate of contraction		Percent change in force of contraction	
	Right atrium	Left atrium	Right atrium	Left atrium
Cisplatin	$\downarrow 68.8 \pm 1\%$ ($p = 0.001$)	$\downarrow 1 \pm 1\%$ ($p = 0.8$)	$\downarrow 53.7 \pm 17\%$ ($p = 0.02$)	$\downarrow 55 \pm 6.1\%$ ($p = 0.02$)
K₂PtCl₄	$\downarrow 92.7 \pm 4.45$ ($p = 0.001$)	$\downarrow 16.2 \pm 3.2\%$ ($p = 0.4$)	$\downarrow 99.3 \pm 0.4\%$ ($p = 0.001$)	$\downarrow 48.4 \pm 9.25$ ($p = 0.008$)
56MESS	$\downarrow 39.8 \pm 4\%$ ($p = 0.04$)	$\downarrow 7.3 \pm 12.3\%$ ($p = 0.06$)	$\downarrow 26.1 \pm 3.5\%$ ($p = 0.007$)	$\downarrow 15.1 \pm 7.4\%$ ($p = 0.13$)
PHENEN	$\downarrow 20.8 \pm 9\%$ ($p = 0.05$)	$\uparrow 0.9 \pm 1.85$ ($p = 0.6$)	$\downarrow 22.3 \pm 3.6\%$ ($p = 0.008$)	$\downarrow 50 \pm 17.5\%$ ($p = 0.02$)

Table 4.1. A summary of the cardiotoxic changes induced by the platinum-based drugs on the rate and force of contraction in both the right and left atria. Results are expressed as means \pm SEM. ($n = 3$).

3.3.3.3 Cardiotoxic Activity of Macrocyclic Drug Delivery Systems

The cardiotoxic effects of various macrocyclic drug delivery systems (CB[6], CB[7], β -Cyclodextrin, and Motor 2) were studied by monitoring changes in the rate of atria contraction and force of contraction over a two hour period in both the right and left atria.

Overall, the results show that the macrocycles induced greater changes to the force of atria contraction compared to the rate of atria contraction in both the right and left atria. Results shows that by the end of the experiment, in the right atria, CB[6] caused a decrease in the rate of contraction by $12 \pm 6\%$ ($p = 0.3$) and in the force of contraction by $41.7 \pm 20\%$ ($p = 0.06$). Whereas in the left atria, it increased the rate of atria contraction by $3.3 \pm 1.1\%$ ($p = 0.3$) and decreased its force of contraction by $55 \pm 6.1\%$ ($p = 0.001$). CB[7] increased right atria contraction rate by $31 \pm 13.6\%$ ($p = 0.07$) and decreased its force of contraction by $29 \pm 3.4\%$ ($p = 0.04$), and in the left atria, it reduced both the rate and force of contraction by $10 \pm 3.5\%$ ($p = 0.3$) and $18\% \pm 6.8\%$ ($p = 0.1$) respectively. β -cyclodextrin induced an increase in right atria contraction rate by $32 \pm 12\%$ ($p = 0.2$) and increased its force of contraction by $1 \pm 3.3\%$ ($p = 0.6$). In the left atria, β -cyclodextrin increased contraction rate by $3 \pm 3\%$ ($p = 0.8$) and decreased the force of its contraction by $33 \pm 4.1\%$ ($p = 0.002$). Finally, in the right atria, Motor 2 induced an increase in contraction rate by $30 \pm 19\%$ ($p = 0.2$) and reduced its force of contraction by $68.3 \pm 3.1\%$ ($p = 0.001$), and in the left atria, it caused an increase in contraction rate by $15 \pm 3.8\%$ ($p = 0.4$) and a decrease in force of contraction by $60 \pm 5.4\%$ ($p = 0.004$).

These results indicate that all of the macrocycles induced a level of atria cardiotoxicity, with Motor 2 inducing the greatest change in the force of atria contraction in both atrias compared to the other macrocycles. The results also show that in the rate of atria contraction experiments, most of the changes induced by the macrocycles occurred after the first 60 min (Figure 3.3.3.5), whereas in the force of contraction experiments, changes were induced within the first 15 min as seen with Motor2 and CB[7] in the left atria (Figure 3.3.3.6). Table 4 gives a summary of the effect of each macrocycle drug on the rate and force of atria contraction.

Macrocycle (300 μ M)	Percent change in rate of contraction		Percent change in force of contraction	
	Right atrium	Left atrium	Right atrium	Left atrium
CB[6]	$\uparrow 12 \pm 6\%$ ($p = 0.3$)	$\uparrow 3.3 \pm 1\%$ ($p = 0.3$)	$\downarrow 41.7 \pm 20\%$ ($p = 0.06$)	$\downarrow 55 \pm 6.1\%$ ($p = 0.001$)
CB[7]	$\uparrow 31 \pm 13.6\%$ ($p = 0.07$)	$\downarrow 10 \pm 3.5\%$ ($p = 0.3$)	$\downarrow 29 \pm 3.4\%$ ($p = 0.04$)	$\downarrow 18 \pm 6.8\%$ ($p = 0.1$)
Motor2	$\uparrow 30 \pm 19\%$ ($p = 0.2$)	$\uparrow 15 \pm 3.8\%$ ($p = 0.4$)	$\downarrow 68 \pm 3.1\%$ ($p = 0.001$)	$\downarrow 60 \pm 5.4\%$ ($p = 0.004$)
β-cyclodextrin	$\uparrow 32 \pm 12\%$ ($p = 0.2$)	$\uparrow 3 \pm 3\%$ ($p = 0.8$)	$\uparrow 1 \pm 3.3\%$ ($p = 0.4$)	$\downarrow 33 \pm 4.1\%$ ($p = 0.002$)

Table 4.2. A summary of the cardiotoxic changes induced by various macrocycles on the rate and force of contraction in both the right and left atria.

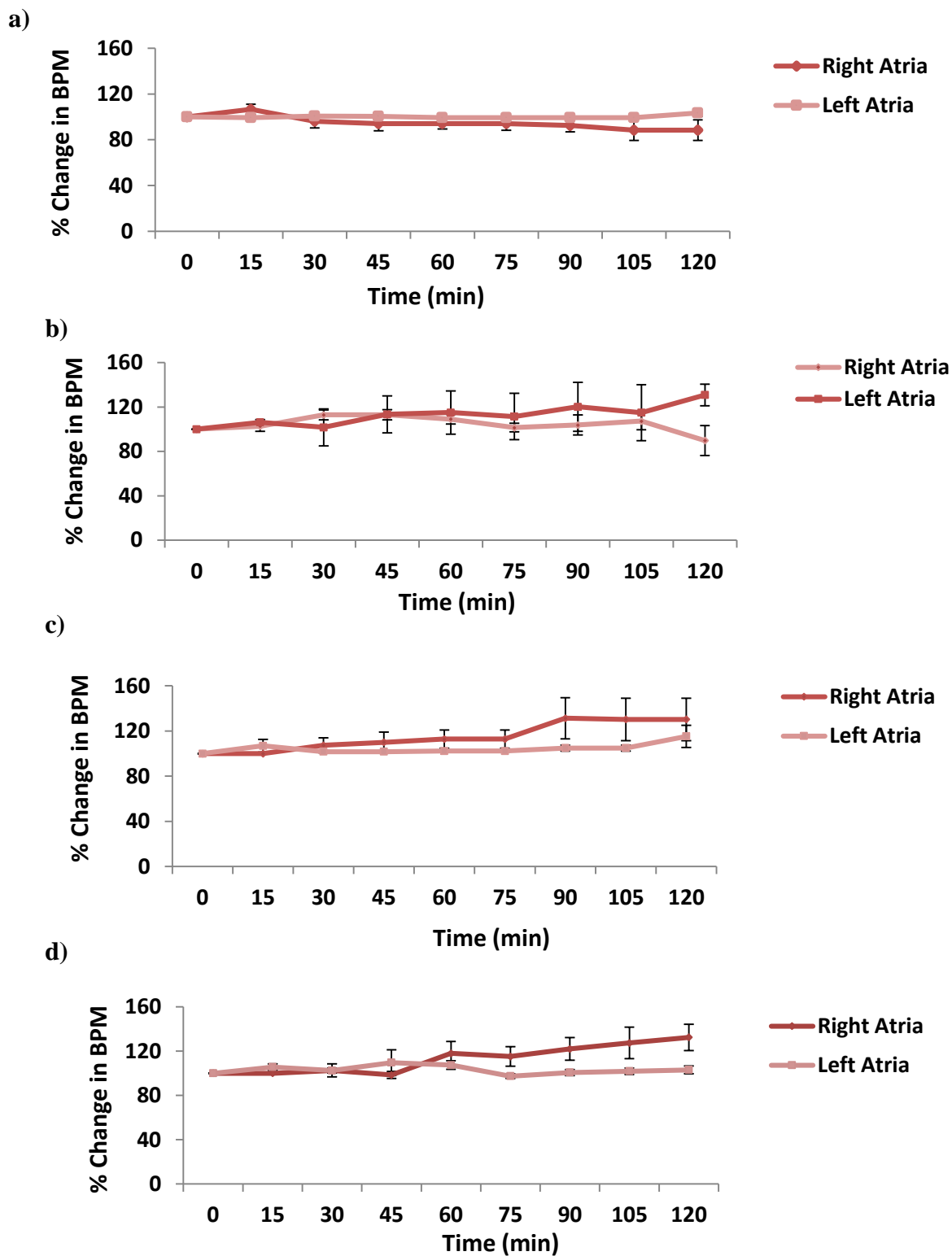


Figure 3.3.3.5. The changes in the rate of atria contraction when treated with 300 μ M of macrocycles. Graph shows (a) CB[6], (b) CB[7], (c) Motor2 and (d) β -cyclodextrin . Results are expressed as the means \pm SEM ($n=3$). Statistical students paired t-test was performed and significant differences compared to time match control are indicated by * when $p < 0.05$.

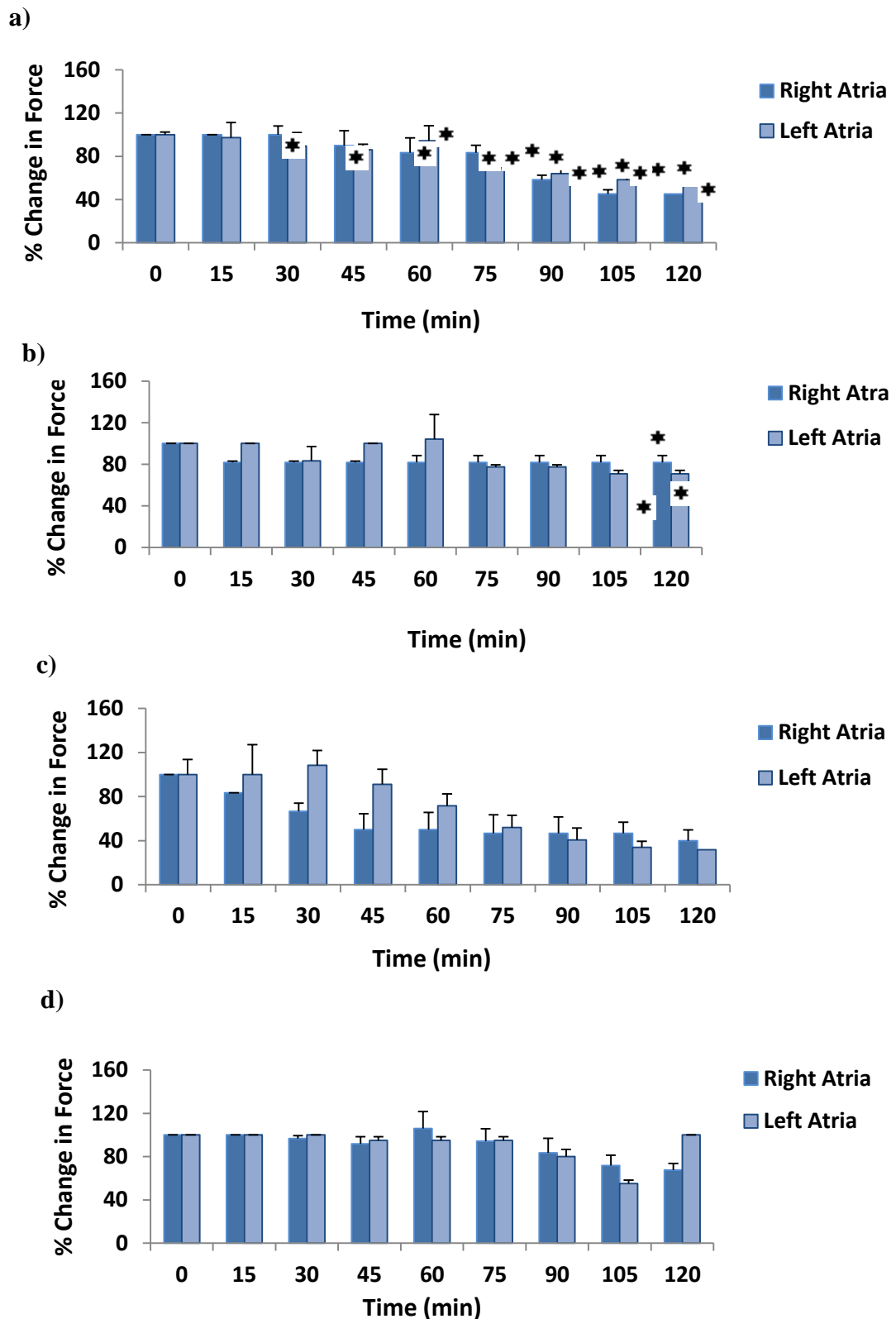


Figure 3.3.3.6. The changes in the force of atria contraction when treated with 300 μ M of macrocycle . Graph shows (a) CB[6], (b) CB[7], (c) Motor2 and (d) β -cyclodextrin. Results are expressed as the means \pm SEM ($n = 3$). Statistical students paired t-test was performed and significant differences compared to time match control are indicated by * when $p < 0.05$.

3.3.3.4 Effect of CB[7] on the Cardiotoxicity of Cisplatin

Although uncommon, there are various clinical studies that have reported cardiotoxic effects of cisplatin. Toxicity occurs in the form of atrial or ventricular arrhythmias, tachycardia, bradycardia and conduction abnormalities. Most of these cardiac problems are reported to be clinically silent and occurring within hours of drug infusion.

The protective effect of CB[7] on the cardiotoxic activity of cisplatin was investigated using free cisplatin and cisplatin@CB[7] in the unpaced right atrium. The right atrium was chosen for this study as cisplatin exhibited less cardiotoxic activity than in the left paced atrium (data not shown (Figure 3.3.3.7)).

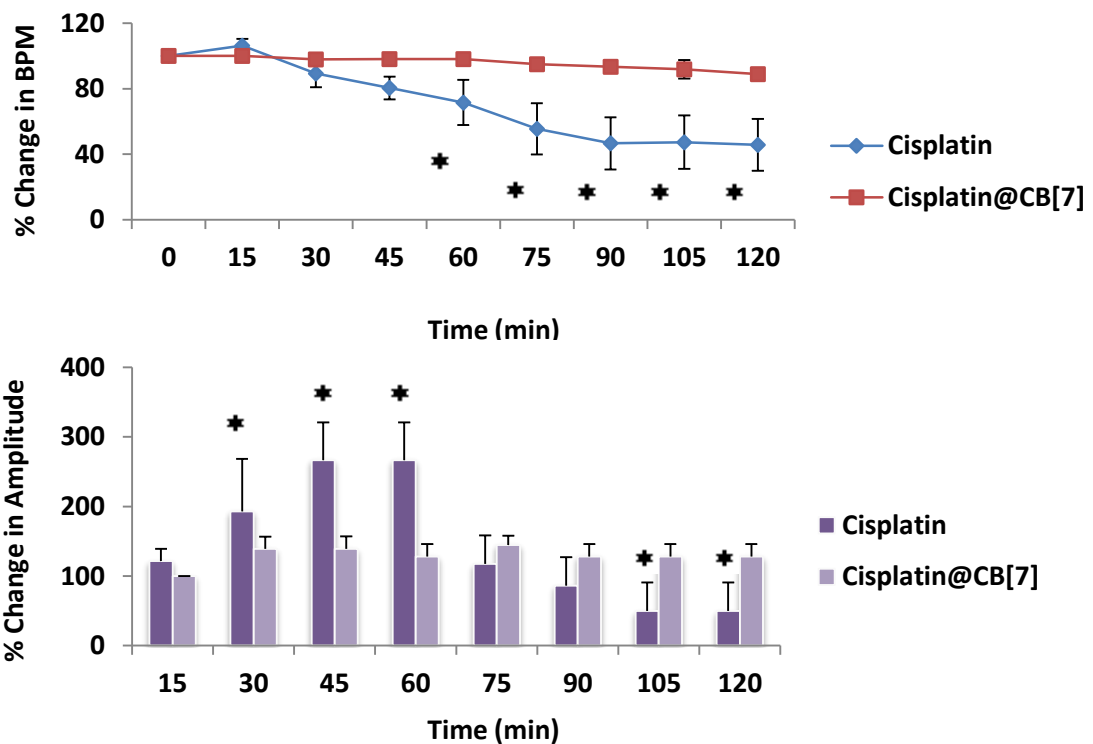


Figure 3.3.3.7. The difference in effects of cisplatin and cisplatin@CB[7] on the rate of contraction (top panel) and force of contraction (bottom panel) of the right atria at specific intervals over a two hour period. Results are expressed as the means \pm SEM ($n = 3$). Statistical students paired t-test was performed significant differences compared to time match control are indicated by * when $p < 0.05$.

Figure 3.3.3.7 shows that cisplatin induced cardiotoxic activity by reducing both the rate and force of contraction by $68.8 \pm 1\%$ ($p = 0.001$) and $53.7 \pm 17.0\%$ ($p = 0.02$), respectively. Furthermore, cisplatin induced a gradual and dramatic increase in the atria's force of contraction by 250% within the first 60 min, after which it was reduced by 54% by the end of the experiment. When encapsulated by CB[7], the cardiotoxic activity of cisplatin was significantly reduced; cisplatin@CB[7] induced only an $11 \pm 5.6\%$ ($p = 0.2$) decrease in the rate of atria contraction, and increased the force of contraction by only $27 \pm 18.0\%$ ($p = 0.2$). As well as reducing the magnitude of change in rate of contraction, CB[7] also stabilised the force of contraction compared to free cisplatin. After 60 min the force of contraction increased by just $27 \pm 18.0\%$ and was maintained at this magnitude throughout the experiment.

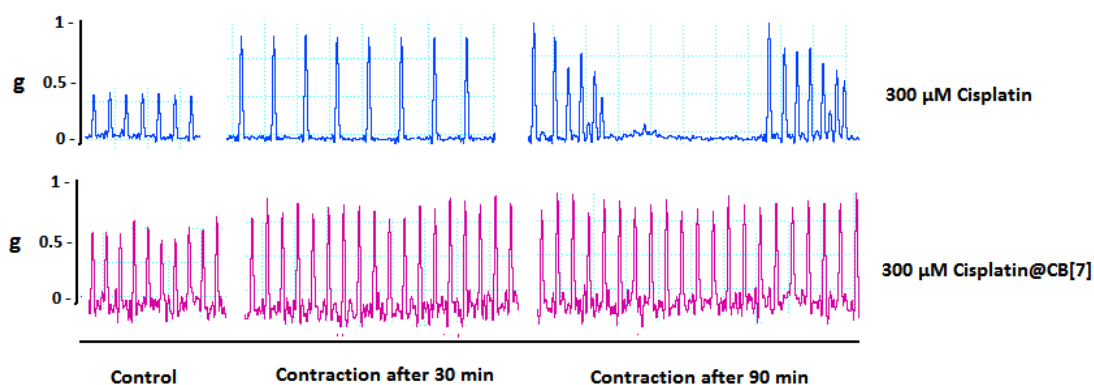


Figure 3.3.3.8. Actual readings of rate and force of contraction of the right heart atria at different time points after treatment with $300 \mu\text{M}$ of cisplatin or $300 \mu\text{M}$ of cisplatin@CB[7].

3.4. Discussion

The platinum-based anticancer agent cisplatin, has been used in the clinic since the early 1970s for the treatment of several kinds of tumours and although it has a 90% cure rate in the treatment of testicular cancer, its use in the clinic is limited not only by the development of cisplatin resistant cancer cells but also by its severe side effects [67-69]. In an attempt to reduce the toxic side effects of cisplatin, second and third generation platinum drugs were synthesised such as carboplatin and lobaplatin which both exhibit lower neurotoxic activity than that associated with cisplatin. Another method that has recently shown promise in reducing the toxic side effects of cisplatin is the use of drug delivery systems such as liposomes and macrocycles [69-71].

In this thesis, *ex-vivo* electrophysiological models were used to study the neurotoxic, neuromyopathic and cardiotoxic activity of cisplatin. Three other platinum-based drugs that have not entered clinical phase trials due to their high cytotoxicity (56MESS, K_2PtCl_4 and PHENEN) were also used in this study for comparison to cisplatin. The effect of drug encapsulation of cisplatin by CB[7] on cisplatin's neurotoxic, neuromyopathic and cardiotoxic activity was also investigated. As well as CB[7], three other macrocycles were used in this study for comparison; the clinically approved β -cyclodextrin, CB[6] and Motor2.

Over the years accumulative data has been provided to show that the platinum-based drugs and specifically cisplatin and oxaliplatin, are highly neurotoxic [40]. Cisplatin has been reported to induce a dose related sensory neuropathy with symptoms that

include numbness, distal paraesthesia (tingling sensation), reduced vibration and joint position sensations and diminished or absent muscle movement [40-43,71]. Recovery from cisplatin induced neuropathy is often incomplete where it can persist for up to 15 years in 55% of patients after treatment has ceased [72].

Studies using both human and rat tissue have shown that cisplatin is preferentially taken up by the dorsal root ganglia where it produces abnormalities in the transcription of ribosomal DNA, a subsequent reduction in protein synthesis and inhibition of axonal growth [251-255]. In a study by McDonald *et al*, cisplatin was shown to bind to neuronal DNA 10-folds higher than it did in pheochromocytoma (PC12) cancer cells in *in vitro* [255]. They also showed that when administered intraperitoneally to adult rats, platinum accumulated to a higher extent in DRG than in multiple other tissues including: liver, brain, muscle and kidney [255]. The authors concluded that this might be due to neuronal cells having increased platinum uptake, decreased platinum efflux, a decrease in platinum detoxification, or decreased DNA adduct repair [255]. Evidence from other studies have suggested that DRG sensory neurons express specific membrane transporters known as organic cation transporters that enhance the transport of cisplatin into the cell at a rate higher than the copper transport proteins expressed in various cancer cells [255]. Levels of glutathione peroxidase which act as a neuro-protective agent have been found to be abolished in neuronal cells treated with cisplatin thus decreasing cellular resistance to cisplatin induced oxidative stress [255-257].

In the neurotoxicity studies in this thesis, the effect of drug on the amplitude of the action potential of the desheathed mouse sciatic nerve over an 80 min period was studied. Results show that cisplatin had slightly reduced the amplitude of the nCAP but did not induce a statistically significant neurotoxic effect. This result is expected as the sciatic nerve does not contain dorsal root ganglia cells compared to the nervous system. In comparison, 56MESS and K_2PtCl_4 both induced a statistically significant neurotoxic effect in the sciatic nerve by inducing a reduction in the amplitude of the nCAP. This suggests that these two platinum-based drugs may induce their neurotoxic effects via a different mechanism to cisplatin. Unfortunately, there are no previous literature studies documented on the neurotoxicity of these drugs for further analysis. However, Oxaliplatin, a second generation platinum-based anticancer drug which is also known to be highly neurotoxic with peripheral neuropathy as its dose limiting side effect has been well studied but often with conflicting results [258, 259]. There is evidence in the literature that suggests that oxaliplatin causes peripheral nerve hyperexcitability by delaying the inactivation of voltage gated sodium channels. However, the use of the anti-epileptic agent carbamazepine which is a sodium channel blocker has failed to significantly reduce the incidence or intensity of oxaliplatin induced neuropathy and instead a Ca^{2+}/Mg^{2+} infusion is currently the gold standard of treatment [258]. This suggests that there may be more than one mechanism by which oxaliplatin induces its neurotoxic activity. In a recent study by Theophilidis *et al*, the electrophysiological effect of oxaliplatin on the rat sciatic nerve was investigated [259]. Their results showed that although oxaliplatin portrayed no significant changes to the amplitude of the nCAP or in the duration of the nCAP depolarisation phase it had drastically elongated the duration of the repolarization phase [77]. Their findings

showed that oxaliplatin had a concentration and a time dependent effects on the firing responses of intra axonal fibers to short stimuli. Three different firing patterns were identified; the first pattern showed high frequency bursting (90 – 130 Hz), the second showed a characteristic plateau with durations ranging from 45 – 140 ms that depended on the exposure time, and the third combined a plateau and a bursting period. These patterns were found to be similar to that of 4-AP, a classical blocker of voltage gated potassium channels in sciatic nerve fibers from young rats [259]. Therefore, Theophilidis *et al* concluded that oxaliplatin may induce its neurotoxic activity by interfering with the activity of potassium channels located on the rat nodal surface, which mediates a slow potassium current that regulate cell excitability [259]. However, in a different study by Vincent *et al* oxaliplatin was reported to have no effect on repolarization phase of the nCAP and that oxaliplatin induced its neurotoxic activity by altering the kinetics of the voltage gated sodium channels. However these differences may be as a result of the different tissues used and therefore there is a difference in the expression of sodium, potassium and calcium channels [260].

Overall the neurotoxicity studies suggest that despite being taken up by neuronal cell bodies, cisplatin's mechanism of neurotoxicity is unlikely due to changes in axonal conduction. A possible explanation for the difference in toxicities of the platinum based drugs is that they are structurally distinct with different leaving groups, this may account for their unique pharmacology.

In the chick biventer-cervicis nerve-muscle experiments all of the platinum-based drugs portrayed significant neuromyopathic activity. Cisplatin induced a large increase in nerve-muscle response to ACh and KCl and decreased the electrically stimulated twitch muscle amplitude suggesting that it induces its neuromyopathic activity by interfering with the activity of acetylcholinesterase or with the presynaptic nerve terminal. In a recent study, Khan *et al* have shown through crystallography and neuro-informatics studies that cisplatin is able to bind with acetylcholinesterase. More interestingly is that cisplatin is able to sit within the “acyl pocket” as well as the “catalytic site” through hydrogen and hydrophobic bonds. These results suggest that cisplatin may induce its neuromyopathic activity by acting as a potent inhibitor of acetylcholinesterase [256]. When encapsulated by CB[7], the extent of cisplatin’s neuromyopathic activity was significantly decreased suggesting that CB[7] may have neuromyo-protective effects and may have implications in the clinic. In comparison, K_2PtCl_4 , which decreased nerve-muscle response to ACh, and KCl may have induced its neuromyopathic activity through a different mechanism by directly acting on the postsynaptic muscle membrane. The possibility that K_2PtCl_4 is directly myopathic is further supported by the decrease in the nerve-muscle response to KCl which is an indication that the muscle fibre contractility has been critically impaired. Both 56MESS and PHENEN showed similar results on the nerve-muscle tissue; they increased the tissues response to Ach and KCl and caused a complete blockade in muscle twitch. These results suggest that both 56MESS and PHENEN may share a similar mechanism of neuromyopathy by acting on the muscle’s nicotinic receptors or with the viability of the membrane, but indirectly via a presynaptic effect at the nervous terminal.

There are only a few studies that have reported cisplatin to be a cardiotoxic agent. These studies have shown that cisplatin can induce arrhythmias, electrocardiographic changes, myocarditis and congestive heart failure. In the clinic these cardiac problems are reported to be clinically silent and can occur either hours after drug infusion, days, months or even years.

In this thesis, the cardiotoxic activity of cisplatin was investigated by monitoring its effect on the rate and force of right and left atria contraction. Results show that cisplatin induced a statistically significant reduction in the rate of contraction in the right atria but not in the left atria, this effect was observed with all the platinum-based drugs tested indicating that they may all share a similar mechanism of cardiotoxic activity, possibly by altering the kinetics of the SA node which is present in the right atria but absent in the left atria. The results from this thesis also showed that cisplatin, 56MESS and PHENEN induced a statistically significant reduction in the force of contraction of the left atria, suggesting that there may be various methods by which these drugs are cardiotoxic.

While there are no published data available on the effects of platinum-based drugs on the SA node, there are studies that have shown cisplatin to induce toxicity to the heart by disturbing its contractility and coronary flow. In a study by Novokmet *et al*, the effect of cisplatin on the perfused isolated rat heart using the lagendorff model was investigated [261]. Their results showed that while cisplatin had no effect on the diastolic blood pressure of the left ventricle it had significantly decreased coronary blood flow in a dose dependent manner, suggesting that cisplatin may not induce its

cardiotoxic activity on cardiac muscle alone, but also on coronary endothelium [261]. Other studies at the molecular level have shown that cisplatin increases the expression of cardiotoxic enzyme biomarkers such as glutathione, GSH lactate dehydrogenase and creatine kinase which in turn cause oxidative stress [261]. This suggests that cisplatin may induce its cardiotoxic activity via lipid peroxidation of cardiac membrane as well as by triggering platelet aggregation and enhancing thromboxane formation causing vascular damage. In a study by Badar *et al* cisplatin was shown to disrupt the enzymatic activity of superoxide dismutase by depleting the levels of zinc and copper in cardiac tissue, this is a similar mechanism of action by which cisplatin induces its nephrotoxic activity [262].

Although there is a lack of information on the precise mechanism of action of the cardiotoxicity of cisplatin and the second generation platinum-based drugs used in the clinic, there is evidence that suggests cisplatin may induce cardiotoxic activity via a number of pathways. It is important that more investigations are carried out in order to provide a mechanism to prevent or treat the cardiotoxicity caused by the platinum-based drugs. Not only have the investigations from this thesis shown that cisplatin is cardiotoxic to the rat heart atria by reducing the rate and force of right atria contraction but that the encapsulation of cisplatin within the macrocycle CB[7] can reduce the cardiotoxic activity induced by cisplatin. More studies at the molecular level need to be performed to explain the precise mechanism by which CB[7] induces its cardioprotective effect.

Chapter 4

Conclusion and Future Studies

4. Conclusion

Cancer is still one of the leading causes of death worldwide and although various anticancer drugs are currently used in the clinic and many more are currently under development their use is greatly limited by their unsuitable pharmacokinetics, toxic side effects, emergence of drug resistance, and poor solubility. A recent method that has shown promise to overcome these problems and increase drug efficacy is the re-formulation of drugs using a range of drug delivery vehicles [263-267]. However, despite these benefits, most drug delivery systems have significant limitations themselves that range from toxic side effects, reproducibility issues, irreversible drug binding, and expensive costs [264-267]]. As such, safer, cheaper and better drug delivery vehicles need to be developed and moved through the pharmaceutical development pipeline [267].

The objective of this thesis was to test the hypothesis that re-formulation of drugs through the use of a drug delivery system can significantly increase the drug's bioavailability and efficacy while reducing the drug's toxic side effects. The thesis has been divided into two sections; in the first section a drug delivery system composed of the platinum-based anticancer drug cisplatin encapsulated within the macrocycle cucurbit[7]uril and further encapsulated within an implantable hydrogel was developed and examined for its *in vitro* and *in vivo* anticancer efficacy and compared to free cisplatin. In this section, the *in vivo* anti-tumour efficacy of free cisplatin towards cisplatin resistant ovarian cells was studied and compared to that of cisplatin encapsulated within cucurbit[7]uril and loaded into an implantable PVA and gelatine based hydrogel. Results showed that the encapsulation of cisplatin@CB[7] within a

2% PVA-gelatine based hydrogel increased the bioavailability of the drug as it overcame cisplatin resistance, furthermore, there was no statistically significant difference in the anticancer effect of a low dose formulation of cisplatin@CB[7] in the 2% PVA hydrogel (30 µg per animal) compared to a high intraperitoneal dose of cisplatin (150 µg per animal). This shows that a lower dose of cisplatin in this CB[7] - hydrogel drug delivery complex can be used to achieve a similar anticancer effect of free cisplatin but with the added benefit of reducing the side effects induced by cisplatin.

In the second section of this thesis, *ex-vivo* electrophysiological models were used to investigate the neurotoxic, neuromyopathic and cardiotoxic activity of free cisplatin compared to cisplatin@CB[7] (amongst other platinum-based drugs and macrocyclic drug delivery systems). The mouse sciatic nerve, chick biventer-cervicis nerve muscle and rat heart atria tissues were used respectively. Results showed that cisplatin did not induce any neurotoxic activity in the sciatic nerve, however had portrayed statistically significant neuromyopathic and cardiotoxic activity. Furthermore when encapsulated by CB[7] these toxicities were reduced, therefore suggesting that CB[7] could have neuromyo- and cardio- protective properties.

Overall, the combined results of this chapter show that the reformulation of cisplatin through using CB[7] and a 2%-PVA gelatine based hydrogel as a drug delivery vehicle can possibly increase the efficacy of cisplatin through a slow release mechanism and by reducing the neuromyopathic and cardiotoxic side effects of cisplatin and thus increasing its bioavailability. The results obtained in this section are in line with those

obtained with other drug delivery systems, for example as explained earlier, although the use of liposomes and macrocycles for the delivery of cisplatin have shown to have no significant anticancer difference compared to free drug, they do have significant lower toxic side effects compared to free drug which could have positive implications on patients life [267-270].

4.1 Future Studies

Although implantable hydrogels could be promising in clinical cancer treatment, they are partially hindered by the time and cost of their surgical procedure. As well as the continued research into tuning drug release rates from implantable hydrogels via better network design and more precise mathematical modelling, scientists have also focused on developing efficient injectable hydrogel models using thermosensitive polymers [270-272].

An injectable hydrogel is one in which the hydrogel polymer matrix is in the aqueous form outside the body, but once injected inside the body, rapidly gels via chemical or physical crosslinking. Injectable hydrogels are an attractive method to bypass the limitations associated with implantable hydrogels; gel formation after an injectable administration avoids an open surgery procedure. This helps facilitate the use of a minimally invasive approach for drug delivery and therefore improving patient's compliance and comfort significantly as well as potentially reducing the cost of therapy [271-274].

Thermosensitive hydrogels are an attractive choice as injectable biomaterials due to their spontaneous gelation in body temperature without the requirement of extra chemical treatment [270, 272]]. Therefore a future direction to this study would be to create an injectable thermosensitive hydrogel containing cisplatin@CB[7] and to compare its efficacy in reducing tumour growth compared to the implantable hydrogel system developed in this study. It would also be of interest to study the effect of the encapsulation of cisplatin within other macrocyclic drug delivery systems such as β -cyclodextrin and to compare its effects with CB[7] in order to develop the most effective and safe slow drug delivery system.

The toxicological experiments described in this thesis illustrate the advantages of using *ex vivo* electrophysiology experiments in understanding and predicting the toxicity induced by different compounds on specific tissue. The fact that the results obtained from these experiments correlate with what is seen in the clinic show that these experimental methods are reliable. To expand this study, it would be of great interest to use other well established toxicological and histological methods to understand the precise mechanisms of action of the platinum-based drugs and especially cisplatin in inducing their cardiotoxic and neuromyopathic activity and the mechanism by which encapsulation by CB[7] reduces these toxicities. Electrophysiological experiments using the diaphragm's phrenic nerve tissue from mice can be employed to measure the quantal content of acetylcholine released from the presynaptic nerve. This can help to identify whether cisplatin's effect on the muscle's contraction rate is an effect of cisplatin acting on the pathway of the production of acetylcholine and its release or by other means. It would also be of

interest to study the toxicity of the platinum-based drugs and other macrocyclic drug delivery compounds on other organ tissues such as kidney, uterus, colon, ileum and bladder this can give a well-rounded understanding of the toxicities induced by these compounds.

Since this study showed that the encapsulation of cisplatin by CB[7] reduced the neuromyopathic and cardiotoxic activity of cisplatin, it would be beneficial to study whether encapsulation of cisplatin by other macrocycles such as β -cyclodextrin portray a similar protective effect. If so, then the use of drug delivery systems would be an interesting option in reducing the toxic side effects induced by anticancer drugs.

References

1. Available from: <http://www.who.int/mediacentre/factsheets/fs297/en/>.
2. Available from :from:<http://www.cancer.org/cancer/>
3. Available from: <http://www.who.int/genomics/public/geneticdiseases/>
4. Nguyen, D.X. and Massague, J, *Genetic determinants of cancer metastasis*. Nat Rev Genet, 2007. **8**(5): p. 341-52.
5. Hunter, K.W., Crawford, N.P and Alsarraj, J, *Mechanisms of metastasis*. Breast Cancer Res, 2008. **10**(1): p. S2.
6. Lodish H, B.A., Zipursky, S.L, et al, *Molecular Cell Biology* 4th ed. 2000, New York W.H.Freeman.
7. Klein, C.A., *Gene expression signatures, cancer cell evolution and metastatic progression*. Cell Cycle, 2004. **3**(1): p. 29-31.
8. Nicolson, G.L., *Molecular mechanisms of cancer metastasis: tumor and host properties and the role of oncogenes and suppressor genes*. Curr Opin Oncol, 1991. **3**(1): p. 75-92.
9. Chial, C., *Proto-oncogenes to Oncogenes to Cancer*. Nature Education, 2007. **1**(1): p.33-34.
10. Duenas, C.V., Camarero, R. and Garcia., S.I., *Function of oncogenes in cancer development: a changing paradigm*. EMBO J, 2013. **32**(11): p.1502-1513.
11. Osborne, C., Wilson, P., and Tripathy, D., *Oncogenes and tumor suppressor genes in breast cancer: potential diagnostic and therapeutic applications*. Oncologist, 2009. **9**(4): p. 361-77.
12. Rajalingam, K., Schreck, R., Rapp, U and Albert, S., *Ras oncogenes and their downstream targets*. BBA, 2007. **1773**(8): p. 1177-95.
13. Goodsell, D., *The Molecular Perspective: The ras Oncogene*. Oncologist, 1999. **4**(3): p. 263-4.
14. Bos, J.L., *Ras oncogenes in human cancer: a review*. Cancer Res, 1990. **49**(17): p. 4682-89.
15. Kim, M.H and Kim, H., *Oncogenes and tumor suppressors regulate glutamine metabolism in cancer cells*. J Cancer Prev, 2013. **18**(3): p221-26.

16. Sanchez-Tapia and Wan, F., *Fastest time to cancer by loss of tumor suppressor genes*. Bull Math Biol, 2014. **76**(11): p2737-84.
17. Sigal, A and Rotter, V., Oncogenic mutations of the p53 tumor suppressor: the demons of the guardian genome. Cancer Res, 2000. **60**(24): p. 6788-6793.
18. Song, H and Xu, Y., *Gain of function of p53 cancer mutants in disrupting critical DNA damage response pathways*. Cell cycle, 2007. **6**(13): p. 1570-73.
19. XU, Y., Induction of genetic instability by gain of function p53 cancer mutants. Oncogene. **27**(25): p. 3501-07.
20. Goodrich, W., *The retinoblastoma tumor-suppressor gene, the exception that proves the rule*. Oncogene, 2006. **25**: p. 5233-48.
21. Knudson, A.G., *Mutation and cancer: statistical study of retinoblastoma*. Proc Natl Acad Sci. **68**(4): p. 820-23.
22. Weinberg, R.A and Hannahan, D., *The Hallmarks of Cancer*. Cell. **100**(1): p. 57-70
23. Weinberg, R.A and Hanahan, D., *Hallmarks of Cancer: The Next Generation*. Cell. **144**(5): p. 646-674
24. Fulda, S., *Evasion of Apoptosis as a Cellular Stress Response in Cancer*. Natl Acad Sci. 2010. **12**(2): p. 2-8
25. Kurokawa, M and Fernald, K., *Evading apoptosis in Cancer*. Trends Cell Biol. **23**(12). P: 620-633
26. Shammas, A.M., *Telomeres, lifestyle, cancer, and aging*. Curr Opin Clin Care. 2011. **14**(1). P: 28-34
27. Alsarraj, J., et al, Mechanisms of metastasis. Breast Cancer Res. 2008. **10**(1). P:25-30.
28. Iruela-Arispe and Ziyad, S., *Molecular mechanisms of tumour angiogenesis*. Genes Cancer. 2011. **2**(12). P: 1085-1096
29. Wolf, S., et al, Chemotherapy-induced peripheral neuropathy: prevention and treatment strategies. Eur J Cancer, 2008. **44**(11): p. 1507-15
30. Boffetta, P., *Environment and cancer risk*. Rev Prat, 2013. **63**(8): p. 1122-5.
31. Palmer, S., *Diet, nutrition, and cancer*. Prog Food Nutr Sci, 1985. **9**(3): p. 283-341.

32. Ames, B.N. and Gold, L.S, *Dietary carcinogens, environmental pollution, and cancer: some misconceptions*. Med Oncol Tumor Pharmacother, 1990. **7**(2): p. 69-85.
33. Gruijl, F.R., *Skin cancer and solar UV radiation*. Eur J Cancer, 1999. **35**(14): p. 2003-9.
34. Rass, K. and Reichrath, J, *UV damage and DNA repair in malignant melanoma and nonmelanoma skin cancer*. Adv Exp Med Biol, 2008. **624**: p. 162-78.
35. Soehnge, H., A. Ouhtit, and Ananthaswamy, O.N, *Mechanisms of induction of skin cancer by UV radiation*. Front Biosci, 1997. **2**: p.538-51.
36. Ananthaswamy, H.N. and Pierceall, W. E, *Molecular mechanisms of ultraviolet radiation carcinogenesis*. Photochem Photobiol, 1990. **52**(6): p. 1119-36.
37. Schlaeffer, F., Tovi, F, and Leiberman, A, *Cisplatin-induced bradycardia*. Drug Intell Clin Pharm, 1983. **17**(12): p. 899-901.
38. Hashimi, L.A., Khalyl, M.F, and Salem, P.A, *Supraventricular tachycardia. A probable complication of platinum treatment*. Oncology, 1984. **41**(3): p. 174-5.
39. Hecht, S.S., *Tobacco smoke carcinogens and lung cancer*. J Natl Cancer Inst, 1999. **91**(14): p. 1194-210.
40. Shopland, D.R., *Tobacco use and its contribution to early cancer mortality with a special emphasis on cigarette smoking*. Environ Health Perspect, 1995. **103**(8): p. 131-42.
41. Pfeifer, G.P. and Hainaut, P, *On the origin of G --> T transversions in lung cancer*. Mutat Res, 2003. **526**(1): p. 39-43.
42. Kode, A., Yang, S.R and Rahman, I, *Differential effects of cigarette smoke on oxidative stress and proinflammatory cytokine release in primary human airway epithelial cells and in a variety of transformed alveolar epithelial cells*. Respiratory Research, 2006. **7**(1): p. 1-20.
43. Church, D.F. and Pryor, W.A, *Free-radical chemistry of cigarette smoke and its toxicological implications*. Environ Health Perspect, 1985. **64**: p. 111-26.
44. Stone, K., et al., *The ESR properties, DNA nicking, and DNA association of aged solutions of catechol versus aqueous extracts of tar from cigarette smoke*. Arch Biochem Biophys, 1995. **319**(1): p. 196-203.

45. Alibek, K., et al., *Role of viruses in the development of breast cancer*. Infect Agent Cancer, 2013. **8**(1): p. 32.
46. Doorbar, J., *Molecular biology of human papillomavirus infection and cervical cancer*. Clin Sci (Lond), 2006. **110**(5): p. 525-41.
47. Ishiji, T., *Molecular mechanism of carcinogenesis by human papillomavirus-16*. J Dermatol, 2000. **27**(2): p. 73-86.
48. Kelly, D.J., *The physiology and metabolism of the human gastric pathogen Helicobacter pylori*. Adv Microb Physiol, 1998. **40**: p. 137-89.
49. Bytzer, P., et al., *Diagnosis and treatment of Helicobacter pylori infection*. Dan Med Bull, 2011. **58**(4): p. 427-33.
50. Kusters, J.G., van Vliet, A.H and Kuipers, E.J, *Pathogenesis of Helicobacter pylori infection*. Clin Microbiol Rev, 2006. **19**(3): p. 449-90.
51. El-Sawalhi, M.M and Ahmed, L.A, *Exploring the protective role of apocynin, a specific NADPH oxidase inhibitor, in cisplatin-induced cardiotoxicity in rats*. Chem Biol Interact, 2014. **207**: p. 58-66.
52. Michielsens, P. and Ho, E, *Viral hepatitis B and hepatocellular carcinoma*. Acta Gastroenterol Belg, 2011. **74**(1): p. 4-8.
53. Cross, D. and Burmester, J.K, *Gene therapy for cancer treatment: past, present and future*. Clin Med Res, 2006. **4**(3): p. 218-27.
54. Miller, M.J., Foy, K.C and Kaumaya, P.T, *Cancer immunotherapy: present status, future perspective, and a new paradigm of peptide immunotherapeutics*. Discov Med, 2013. **15**(82): p. 166-76.
55. Wong, H.H., Lemoine, N.R, and Wang, Y, *Oncolytic Viruses for Cancer Therapy: Overcoming the Obstacles*. Viruses, 2010. **2**(1): p. 78-106.
56. Arrondeau, J., et al., *Development of anti-cancer drugs*. Discov Med, 2010. **10**(53): p. 355-62.
57. Kummar, S., et al., *Phase 0 clinical trials: conceptions and misconceptions*. Cancer J, 2008. **14**(3): p. 133-7.
58. Available from: <http://www.cancerresearchuk.org/about-cancer/cancers-in-general/treatment/surgery/surgery-to-treat-cancer>
59. Ramirez, P.T., Wolf, J.K., and Levenback, C., *Laparoscopic port-site metastases: etiology and prevention*. Gyencol Oncol, 2003. **91**(1): p. 179-189

60. Kolensick, R., et al, *Tumour Response to Radiotherapy Regulated by Endothelial Cell Apoptosis*. Science, 2003. 300: p. 1155-59.
61. Available from: <http://www.macmillan.org.uk/Cancerinformation/Cancertreatment/Treatmenttypes/Radiotherapy/Radiotherapy.aspx>
62. Available from: <http://www.cancercenter.com/treatments/systemic-radiation-therapy/>
63. Available from: <http://www.cancerresearchuk.org/about-cancer/cancers-in-general/treatment/hormone/what-hormone-therapy-is>
64. Available from: <http://www.nationalbreastcancer.org/breast-cancer-hormone-therapy>
65. Bast RC Jr, K.D., Pollock RE et al, *Cancer Medicine*. 5th ed, H.B. Decker. 2000.
66. Better, N.J and Green, M.D, *Anticancer agents and cardiotoxicity*. Semin Oncol, 2006. **33**(1): p. 2-14.
67. Povirk, L.F., and Shuker, D.E, *DNA damage and mutagenesis induced by nitrogen mustards*. Mutat Res, 1994. **318**(3): p. 205-26.
68. Newell, D.R., *Clinical pharmacokinetics of antitumor antifolates*. Semin Oncol, 1999. **26**(6): p. 74-81.
69. Lansiaux, A., *Antimetabolites*. Bull Cancer, 2011. **98**(11): p. 1263-74.
70. Szulawska, A. and Czyz, M, *Molecular mechanisms of anthracyclines action*. Postepy Hig Med Dosw (Online), 2006. **60**: p. 78-100.
71. Arioka, H. and Saijo, N, *Microtubules and antineoplastic drugs*. Gan To Kagaku Ryoho, 1994. **21**(5): p. 583-90.
72. Abal, M., Andreu, J.M and Barasoain, I, *Taxanes: microtubule and centrosome targets, and cell cycle dependent mechanisms of action*. Curr Cancer Drug Targets, 2003. **3**(3): p. 193-203.
73. Boulikas, T. and Vougiouka, M, *Cisplatin and platinum drugs at the molecular level*. Oncol Rep, 2003. **10**(6): p. 1663-82.
74. Wheate, N.J., et al., *The status of platinum anticancer drugs in the clinic and in clinical trials*. Dalton Trans, 2010. **39**(35): p. 8113-27.

75. Zhang, J., et al., *Status of bi- and multi-nuclear platinum anticancer drug development*. *Anticancer Agents Med Chem*, 2010. **10**(4): p. 272-82.
76. Basu B, K.S., *Cellular responses to cisplatin-induced dNA damage*. *Journal of Nucleic Acids*, 2010. 2010: p. 16.
77. McWhinney, S.R., Goldberg, R.M and McLeod, H.L, *Platinum neurotoxicity pharmacogenetics*. *Mol Cancer Ther*, 2009. **8**(1): p. 10-6.
78. Kelland, L., *The resurgence of platinum-based cancer chemotherapy*. *Nat Rev Cancer*, 2007. **7**(8): p. 573-584.
79. Rosenberg, B., Vancamp, L and Krigas, T, *Inhibition of cell division in escherichia coli by electrolysis products from a platinum electrode*. *Nature*, 1965. **205**: p. 698-9.
80. Monneret, C., *Platinum anticancer drugs. From serendipity to rational design*. *Ann Pharm Fr*, 2011. **69**(6): p. 286-95.
81. Hoeschele, J.D., *In remembrance of Barnett Rosenberg*. *Dalton Trans*, 2009(48): p. 10648-50.
82. O'Dwyer, P.J., Stevenson, J.P and Johnson, S.W, *Clinical pharmacokinetics and administration of established platinum drugs*. *Drugs*, 2000. **59**(4) : p. 19-27.
83. Haxton, K.J. and Burt, H.M, *Polymeric drug delivery of platinum-based anticancer agents*. *J Pharm Sci*, 2009. **98**(7): p. 2299-316.
84. Gralla, R.J., et al., *Recommendations for the use of antiemetics: evidence-based, clinical practice guidelines*. *J Clin Oncol*, 1999. **17**(9): p. 2971-94.
85. Basu, A. and Krishnamurthy, S, *Cellular responses to cisplatin-induced DNA damage*. *J Nucleic Acids*, 2010.
86. Holzer, A.K., Manorek, G.H and Howell, S.B, *Contribution of the major copper influx transporter *CTR1* to the cellular accumulation of cisplatin, carboplatin, and oxaliplatin*. *Mol Pharmacol*, 2006. **70**(4): p. 1390-4.
88. Holzer, A.K., et al., *The copper influx transporter human copper transport protein *1* regulates the uptake of cisplatin in human ovarian carcinoma cells*. *Mol Pharmacol*, 2004. **66**(4): p. 817-23.
89. Kelland, L.R., *Preclinical perspectives on platinum resistance*. *Drugs*, 2000. **59**(4): p. 1-8.
90. Eastman, A., *The mechanism of action of cisplatin: from adducts to apoptosis, in cisplatin*. 2006, *Helv Chim Acta*. p. 111-134.

91. Fuertes, M.A., et al., *Cisplatin biochemical mechanism of action: from cytotoxicity to induction of cell death through interconnections between apoptotic and necrotic pathways*. *Curr Med Chem*, 2003. **10**(3): p. 257-66.
92. Mellish, K.J., et al., *Effect of geometric isomerism in dinuclear platinum antitumour complexes on the rate of formation and structure of intrastrand adducts with oligonucleotides*. *Nucl Acids Res*, 1997. **25**(6): p. 1265-71.
93. Kelland, L., *The resurgence of platinum-based cancer chemotherapy*. *Nat Rev Cancer*, 2007. **7**(8): p. 573-84.
94. Siddik, Z.H., *Cisplatin: mode of cytotoxic action and molecular basis of resistance*. *Oncogene*, 2003. **22**(47): p. 7265-79.
95. Dempke, W., et al., *Cisplatin resistance and oncogenes--a review*. *Anticancer Drugs*, 2000. **11**(4): p. 225-36.
96. Chu, G., *Cellular responses to cisplatin. The roles of DNA-binding proteins and DNA repair*. *J Biol Chem*, 1994. **269**(2): p. 787-90.
97. Shen, D.-W., et al., *Cisplatin Resistance: A cellular self-defense mechanism resulting from multiple epigenetic and genetic changes*. *Pharmacological Reviews*, 2012. **64**(3): p. 706-721.
98. Fink, D., Aebi, S and Howell, S.B, *The role of DNA mismatch repair in drug resistance*. *Clin Cancer Res*, 1998. **4**(1): p. 1-6.
99. Duffull, S.B. and Robinson, B.A, *Clinical pharmacokinetics and dose optimisation of carboplatin*. *Clin Pharmacokinet*, 1997. **33**(3): p. 161-83.
100. Hartmann, J.T. and Lipp, H.P, *Toxicity of platinum compounds*. *Expert Opin Pharmacother*, 2003. **4**(6): p. 889-901.
101. McKeage, M.J., *Comparative adverse effect profiles of platinum drugs*. *Drug Saf*, 1995. **13**(4): p. 228-44.
102. Simpson, D., et al., *Oxaliplatin: a review of its use in combination therapy for advanced metastatic colorectal cancer*. *Drugs*, 2003. **63**(19): p. 2127-56.
103. Cersosimo, R.J., *Oxaliplatin-associated neuropathy: a review*. *Ann Pharmacother*, 2005. **39**(1): p. 128-35.
104. Shimada, M., Itamoch, H and Kigawa, J, *Nedaplatin: a cisplatin derivative in cancer chemotherapy*. *Cancer Manag Res*, 2013. **5**: p. 67-76.
105. *Lobaplatin: D 19466*. *Drugs R D*, 2003. **4**(6): p. 369-72.

106. Ahn, J.H., et al., *Nephrotoxicity of heptaplatin: a randomized comparison with cisplatin in advanced gastric cancer*. *Cancer Chemother Pharmacol*, 2002. **50**(2): p. 104-10.
107. Kelland, L.R., *New platinum antitumor complexes*. *Crit Rev Oncol Hematol*, 1993. **15**(3): p. 191-219.
108. Wheate, N.J. and Collins, J.G, *Multi-nuclear platinum drugs: a new paradigm in chemotherapy*. *Curr Med Chem Anticancer Agents*, 2005. **5**(3): p. 267-79.
109. Zhang, G., Zeng, X and Li, P, *Nanomaterials in cancer-therapy drug delivery system*. *J Biomed Nanotechnol*, 2013. **9**(5): p. 741-50.
110. Malam, Y., Loizidou, M and Seifalian, A.M, *Liposomes and nanoparticles: nanosized vehicles for drug delivery in cancer*. *Trends Pharmacol Sci*, 2009. **30**(11): p. 592-9.
111. Hwang, S.-J., et al., *Hydrogels in Cancer Drug Delivery Systems*, in *Drug Delivery Systems in Cancer Therapy*, D. Brown, Editor. 2004, Humana Press. p. 97-115.
112. Fang, J., Nakamura, H and Maeda, H, *The EPR effect: Unique features of tumor blood vessels for drug delivery, factors involved, and limitations and augmentation of the effect*. *Adv Drug Del Rev*, 2011. **63**(3): p. 136-51.
113. Torchilin, V., *Tumor delivery of macromolecular drugs based on the EPR effect*. *Adv Drug Del Rev*, 2011. **63**(3): p. 131-5.
114. Maeda, H., et al., *Vascular permeability enhancement in solid tumor: various factors, mechanisms involved and its implications*. *Int Immunopharmacol*, 2003. **3**(3): p. 319-28.
115. Maeda, H., *Vascular permeability in cancer and infection as related to macromolecular drug delivery, with emphasis on the EPR effect for tumor-selective drug targeting*. *Proc Jpn Acad Ser B Phys Biol Sci*, 2012. **88**(3): p. 53-71.
116. Furuya, M., et al., *Pathophysiology of tumor neovascularization*. *Vasc Health Risk Manag*, 2005. **1**(4): p. 277-90.
117. Maeda, H., et al., *Tumor vascular permeability and the EPR effect in macromolecular therapeutics: a review*. *J Control Rel*, 2000. **65**(1-2): p. 271-84.
118. Greish, K., *Enhanced permeability and retention of macromolecular drugs in solid tumors: a royal gate for targeted anticancer nanomedicines*. *J Drug Target*, 2007. **15**(7-8): p. 457-64.

119. Maeda, H., Sawa, T and Konno, T, *Mechanism of tumor-targeted delivery of macromolecular drugs, including the EPR effect in solid tumor and clinical overview of the prototype polymeric drug SMANCS*. J Control Rel, 2001. **74**(1-3): p. 47-61.
120. Matsumura, Y. and Maeda, H, *A new concept for macromolecular therapeutics in cancer chemotherapy: mechanism of tumoritropic accumulation of proteins and the antitumor agent smancs*. Cancer Res, 1986. **46**(12 Pt 1): p. 6387-92.
121. Maeda, H., *Macromolecular therapeutics in cancer treatment: the EPR effect and beyond*. J Control Rel, 2012. **164**(2): p. 138-44.
122. Gabizon, A. and Martin, F, *Polyethylene glycol-coated (pegylated) liposomal doxorubicin. Rationale for use in solid tumours*. Drugs, 1997. **54**(4): p. 15-21.
123. Maruyama, K., *Intracellular targeting delivery of liposomal drugs to solid tumors based on EPR effects*. Adv Drug Del Rev, 2011. **63**(3): p. 161-9.
124. Vail, D.M., et al., *Pegylated liposomal doxorubicin: proof of principle using preclinical animal models and pharmacokinetic studies*. Semin Oncol, 2004. **31**(6 Suppl 13): p. 16-35.
125. Wheate, N.J., *Improving platinum(II)-based anticancer drug delivery using cucurbit[n]urils*. J Inorg Biochem, 2008. **102**(12): p. 2060-6.
126. Challa, R., et al., *Cyclodextrins in drug delivery: an updated review*. AAPS PharmSciTech, 2005. **6**(2): p. 329-57.
127. Shchepotina, E.G., et al., *Cucurbiturils as containers for medicinal compounds*. Nanotechnologies in Russia, 2011. **6**(11-12): p. 773-779.
128. Allen, T.M and Cullis, P.R., *Liposomal drug delivery systems: From concept to clinical applications*. Adv Drug Deliv, 2013. **65**(1): p. 36-48.
129. Samad, A., Sultana, Y., and Ail, M., *Liposomal drug delivery systems: an update review*. Curr Drug Deliv, 2007. **4**(4): p. 297-305.
130. Mishra, D.N., et al., *Liposomal drug delivery systems - clinical applications*. Acta Pharm, 2005. **55**(1): p. 1-25.
131. Winer, E., et al., *Liposome encapsulated doxorubicin compared with conventional doxorubicin in a randomised multicenter trial as first-line therapy of metastatic breast carcinoma*. Cancer, 2002. **94**(1): p. 25-36
132. Liu., D., et al. *Comparison of safety and toxicity of liposomal doxorubicin vs. conventional anthracyclines: a meta-analysis*. Exp Hematol Oncol, 2012. **23**(1): p. 1-10

133. Boulikas, T., *Low toxicity and anticancer activity of a novel liposomal cisplatin (Lipoplatin) in mouse xenografts*. *Oncol Rep*, 2004. **12**(1): p. 3-12.
134. Stathopoulos, G.P., *Liposomal cisplatin: a new cisplatin formulation*. *Anticancer Drugs*, 2010. **21**(8):p. 732-736
135. Stathopoulos, G.P., Rigatos, S.K and Stathopoulos, J., *Liposomal cisplatin dose escalation for determining the maximum tolerated dose and dose-limiting toxicity: a phase I study*. *Anticancer Res*, 2010. **30**(4): p. 1317-21.
136. Boulikas, T., *Clinical overview on Lipoplatin: a successful liposomal formulation of cisplatin*. *Expert Opin Investig Drugs*, 2009. **18**(8): p. 1197-218.
137. Kanjickal, D.G. and S.T. Lopina, *Modeling of drug release from polymeric delivery systems--a review*. *Crit Rev Ther Drug Carrier Syst*, 2004. **21**(5): p. 345-86.
138. Hoare, T.R. and Kohane, D.S, *Hydrogels in drug delivery: Progress and challenges*. *Polymer*, 2008. **49**(8): p. 1993-2007.
139. Lin, C.C. and Metters, A.T, *Hydrogels in controlled release formulations: network design and mathematical modeling*. *Adv Drug Deliv Rev*, 2006. **58**(12-13): p. 1379-408.
140. Kashyap, N., Kumar, N and Kumar, M.N, *Hydrogels for pharmaceutical and biomedical applications*. *Crit Rev Ther Drug Carrier Syst*, 2005. **22**(2): p. 107-49.
141. Coviello, T., et al., *Polysaccharide hydrogels for modified release formulations*. *J Control Rel*, 2007. **119**(1): p. 5-24.
142. Coviello, T., Matricardi, P and Alhaique, F, *Drug delivery strategies using polysaccharidic gels*. *Expert Opin Drug Deliv*, 2006. **3**(3): p. 395-404.
143. Kim, J.K., et al., *Natural and synthetic biomaterials for controlled drug delivery*. *Arch Pharm Res*, 2013.
144. Chamberlain, M.C., *Treatment of newly diagnosed malignant glioma in the elderly people: new trials that impact therapy*. *Int J Clin Pract*, 2013. **67**(12): p. 1225-7.
145. Panigrahi, M., Das, P.K and Parikh, P.M, *Brain tumor and gliadel wafer treatment*. *Indian J Cancer*, 2011. **48**(1): p. 11-7.
146. Tanase, C.P., et al., *Anti-cancer therapies in high grade gliomas*. *Curr Proteomics*, 2013. **10**(3): p. 246-260.

147. Lin, S.H. and Kleinberg, L.R., *Carmustine wafers: localized delivery of chemotherapeutic agents in CNS malignancies*. *Expert Rev Anticancer Ther*, 2008. **8**(3): p. 343-59.
148. Aoki, T., Hashimoto, N and Matsutani, M, *Management of glioblastoma*. *Expert Opin Pharmacother*, 2007. **8**(18): p. 3133-46.
149. Hart, M.G., et al., *Chemotherapeutic wafers for High Grade Glioma*. *Cochrane Database Syst Rev*, 2008(3): p. 1-23.
150. Fleming, A.B. and Saltzman, W.M, *Pharmacokinetics of the carmustine implant*. *Clin Pharmacokinet*, 2002. **41**(6): p. 403-19.
151. Available from: <http://www.gliadel.com/>.
152. Konishi, M., et al., *In vivo anti-tumor effect through the controlled release of cisplatin from biodegradable gelatin hydrogel*. *J Control Release*, 2003. **92**(3): p. 301-13.
153. Wheate, N.J., Improving platinum (II)-based anticancer drug delivery using cucurbit[n]urils. *J Inorg Biochem*, 2008. **102**(12): p. 2060-6.
154. Challa, R., et al., Cyclodextrins in drug delivery: an updated review. *AAPS PharmSciTech*, 2005. **6**(2): p. 329-57.
155. Shchepotina, E.G., et al., Cucurbiturils as containers for medicinal compounds. *Nanotechnologies in Russia*, 2011. **6**(11): p. 773-79)
156. Lagona, J., et al., *The cucurbit[n]uril family*. *Angew Chem Int Ed*, 2005. **44**(31): p. 4844-70.
157. Isaacs, L., *Cucurbit[n]urils: from mechanism to structure and function*. *Chem Commun*, 2009(6): p. 619-29.
158. Masson, E., et al., *Cucurbituril chemistry: a tale of supramolecular success*. *RSC Advances*, 2012. **2**(4): p. 1213-1247.
159. Hettiarachchi, G., et al., *Toxicology and drug delivery by cucurbit[n]uril type molecular containers*. *PLoS One*, 2010. **5**(5): p. e10514.
160. Walker, S., et al., *The Potential of Cucurbit[n]urils in Drug Delivery*. *Isr. J. Chem*, 2011. **51**(5-6): p. 616-624.
161. Plumb, J.A., et al., *Cucurbit[7]uril encapsulated cisplatin overcomes cisplatin resistance via a pharmacokinetic effect*. *Metallomics*, 2012. **4**(6): p. 561-7.
162. Kemp, S., et al., *Encapsulation of platinum(II)-based DNA intercalators within cucurbit[6,7,8]urils*. *J Biol Inorg Chem*, 2007. **12**(7): p. 969-79.

163. Kennedy, A.R., et al., *A chemical preformulation study of a host-guest complex of cucurbit[7]uril and a multinuclear platinum agent for enhanced anticancer drug delivery*. Dalton Trans, 2009 (37): p. 7695-7700.
164. Uzunova, V.D., et al., *Toxicity of cucurbit[7]uril and cucurbit[8]uril: an exploratory in vitro and in vivo study*. Org Biomol Chem, 2010. **8**(9): p. 2037-42.
165. Hwang, S.-J., et al., *Hydrogels in Cancer Drug Delivery Systems*, in *Drug Delivery Systems in Cancer Therapy*, D. Brown, Editor. 2004, Humana Press. p. 97-115.
166. Blackshear, P.J., *Implantable drug-delivery systems*. Sci Am, 1979. **241**(6): p. 66-73.
167. Lin, C.C. and A.T. Metters, *Hydrogels in controlled release formulations: network design and mathematical modeling*. Adv Drug Del, 2006. **58**(12-13): p. 1379-408.
168. Kanjickal, D.G. and S.T. Lopina, *Modeling of drug release from polymeric delivery systems--a review*. Crit Rev Ther Drug Carrier Syst, 2004. **21**(5): p. 345-86.
169. Hoare, T.R. and Kohane, D.S, *Hydrogels in drug delivery: Progress and challenges*. Polymer, 2008. **49**(8): p. 1993-2007.
170. Lin, C.C. and Metters, A.T, *Hydrogels in controlled release formulations: network design and mathematical modeling*. Adv Drug Deliv Rev, 2006. **58**(12-13): p. 1379-408.
171. Nashyap, N., Kumar, N and Kumar, M.N, *Hydrogels for pharmaceutical and biomedical applications*. Crit Rev Ther Drug Carrier Syst, 2005. **22**(2): p. 107-49.
172. Coviello, T., et al., *Polysaccharide hydrogels for modified release formulations*. J Control Rel, 2007. **119**(1): p. 5-24.
173. Coviello, T., Matricardi, P and Alhaique, F, *Drug delivery strategies using polysaccharidic gels*. Expert Opin Drug Deliv, 2006. **3**(3): p. 395-404.

174. Kim, J.K., et al., *Natural and synthetic biomaterials for controlled drug delivery*. Arch Pharm Res, 2013.
175. Van Tomme, S.R. and Hennink, W.E, *Biodegradable dextran hydrogels for protein delivery applications*. Expert Rev Med Devices, 2007. **4**(2): p. 147-64.
176. Graham, N.B. and McNeill, M.E, *Hydrogels for controlled drug delivery*. Biomaterials, 1984. **5**(1): p. 27-36.
177. Gupta, P., Vermani, K and Garg, S, *Hydrogels: from controlled release to pH-responsive drug delivery*. Drug Discov Today, 2002. **7**(10): p. 569-79.
178. Heller, J., *Controlled release of biologically active compounds from bioerodible polymers*. Biomaterials, 1980. **1**(1): p. 51-7.
179. Ashley, G.W., et al., *Hydrogel drug delivery system with predictable and tunable drug release and degradation rates*. Proc Natl Acad Sci U S A, 2013. **110**(6): p. 2318-23.
180. Heller, J., et al., *Controlled release of water-soluble macromolecules from bioerodible hydrogels*. Biomaterials, 1983. **4**(4): p. 262-6.
181. Kanjickal, D.G. and Lopina, S.T, *Modeling of drug release from polymeric delivery systems--a review*. Crit Rev Ther Drug Carrier Syst, 2004. **21**(5): p. 345-86.
182. Chamberlain, M.C., *Treatment of newly diagnosed malignant glioma in the elderly people: new trials that impact therapy*. Int J Clin Pract, 2013. **67**(12): p. 1225-7.
183. Mecklenburg, L., et al., *The nude mouse skin phenotype: the role of Foxn1 in hair follicle development and cycling*. Exp Mol Pathol, 2001. **71**(2): p. 171-8.
184. Kelland, L.R., *Of mice and men: values and liabilities of the athymic nude mouse model in anticancer drug development*. Eur J Cancer, 2004. **40**(6): p. 827-36.
185. Flanagan, S.P., 'Nude', *a new hairless gene with pleiotropic effects in the mouse*. Genet Res, 1966. **8**(3): p. 295-309.
186. Mecklenburg, L., Tychsen, B and Paus, R, *Learning from nudity: lessons from the nude phenotype*. Exp Dermatol, 2005. **14**(11): p. 797-810.
187. Kopf-Maier, P., Mboneko, V.F and Merker, H.J, *Nude mice are not hairless. A morphological study*. Acta Anat (Basel), 1990. **139**(2): p. 178-90.

188. Hougen, H.P., *The athymic nude rat. Immunobiological characteristics with special reference to establishment of non-antigen-specific T-cell reactivity and induction of antigen-specific immunity.* APMIS Suppl, 1991. **21**: p. 1-39.
189. Pelleitier, M. and Montplaisir, S, *The nude mouse: a model of deficient T-cell function.* Methods Achiev Exp Pathol, 1975. **7**: p. 149-66.
190. Troiani, T., et al., *The use of xenograft models for the selection of cancer treatments with the EGFR as an example.* Crit Rev Oncol Hematol, 2008. **65**(3): p. 200-11.
191. Sharkey, F. and Fogh, J, *Considerations in the use of nude mice for cancer research.* Cancer Metast Rev., 1984. **3**(4): p. 341-360.
192. Sano, D. and Myers, J.N, *Xenograft models of head and neck cancers.* Head Neck Oncol, 2009. **1**: p. 32.
193. Cespedes, M.V., et al., *Mouse models in oncogenesis and cancer therapy.* Clin Transl Oncol, 2006. **8**(5): p. 318-29.
194. Rosol, T.J., et al., *Animal models of bone metastasis.* Cancer, 2003. **97**(3 Suppl): p. 748-57.
195. Choubey, J. and Bajpay, A, K, *In vitro release dynamics of an anticancer drug from swellable gelatin nanoparticles.* J. Appl. Polym. Sci, 2006. 101: p. (2320-32).
196. Naidu, B and Paulson, A. *A new method for the preparation of gelatin nanoparticles: Encapsulation and drug release characteristics.* J. Appl. Polym. Sci, 2010. **21**(6): p. 3495-3500.
197. Ministerrad, N., Tiberg, E and Rad, N, *Development of (eco)toxicity tests.* 1995: Nordic Council of Ministers
198. Gad, S., *Toxicology* 2nd ed, ed. T. Francis. 2000, New York.
199. Barile, F., *Clinical Toxicology. Principles and Mechanisms.* 2nd ed. 2010: Taylor & Francis Inc.
200. Gupta, S.K., *Drug Discovery and Clinical Research* 1st ed. 2011, New Delhi Jaypee Brothers Medical Publishers
201. Barile, F., *Principles of Toxicology Testing* 2nd ed. 2013: Taylor & Francis Ltd.
202. Atterwill, C.K.a.S., C.E., *In vitro methods in toxicology* 1987.

203. Segura-Aguilar, J. and Kostrzewa, R, *Neurotoxins and neurotoxicity mechanisms. an overview*. Neurotoxicity Research, 2006. **10**(3-4): p. 263-285.
204. Sherwood, L., *Introduction To Human Physiology* 8th ed. 2012, California: Brooks/Cole.
205. Widmaier, E., Raff, H., Strang, K. , *Vander's Human Physiology: The Mechanisms of Body Function*. 12th ed. 2010, London: McGraw-Hill Education.
206. Solomon, E.P., *Introduction to Human Anatomy and Physiology* 3rd ed. 2008, Philadelphia Elsevier-Health Sciences Division.
207. Martini F, N.J., and Bartholomew E, *Fundamentals of Anatomy and Physiology*. 8th ed. 2009, San Francisco: Pearson Education.
208. Ferrans, V.J., et al., *Pathogenesis and prevention of doxorubicin cardiomyopathy*. Tsitologiia, 1997. **39**(10): p. 928-37.
209. Fonseca, D.a.M., *The Sciatic Nerve. Blocks, Injuries and Regeneration*. 2012, New York: Nova Science Publishers Inc.
210. Beijers, A.J., Jongen, J.L, and Vreugdenhil, G, *Chemotherapy-induced neurotoxicity: the value of neuroprotective strategies*. Neth J Med, 2012. **70**(1): p. 18-25.
211. Sioka, C. and Kyritsis, A.P, *Central and peripheral nervous system toxicity of common chemotherapeutic agents*. Cancer Chemother Pharmacol, 2009. **63**(5): p. 761-7.
212. Raffa, R.B., et al., *Chemotherapy-induced neuropathic pain* 2013: Taylor & Francis.
213. Argyriou, A.A., et al., *A review on oxaliplatin-induced peripheral nerve damage*. Cancer Treat Rev, 2008. **34**(4): p. 368-77.
214. Quasthoff, S. and Hartung, H.P, *Chemotherapy-induced peripheral neuropathy*. J Neurol, 2002. **249**(1): p. 9-17.
215. Gregg, R.W., et al., *Cisplatin neurotoxicity: the relationship between dosage, time, and platinum concentration in neurologic tissues, and morphologic evidence of toxicity*. J Clin Oncol, 1992. **10**(5): p. 795-803.
216. Park, S.B., et al., *Mechanisms underlying chemotherapy-induced neurotoxicity and the potential for neuroprotective strategies*. Curr Med Chem, 2008. **15**(29): p. 3081-94.

217. O'Connor, A.B, and Dworkin, R.H, *Treatment of neuropathic pain: an overview of recent guidelines*. Am J Med, 2009. **122**(10): p. S22-32.
218. Dworkin, R.H., et al., *Pharmacologic management of neuropathic pain: evidence-based recommendations*. Pain, 2007. **132**(3): p. 237-51.
219. Gamelin, E., et al., *Clinical aspects and molecular basis of oxaliplatin neurotoxicity: current management and development of preventive measures*. Semin Oncol, 2002. **29**(5): p. 21-33.
220. Berger, T., et al., *Neurological monitoring of neurotoxicity induced by paclitaxel/cisplatin chemotherapy*. Eur J Cancer, 1997. **33**(9): p. 1393-9.
221. Wilson, R.H., et al., *Acute oxaliplatin-induced peripheral nerve hyperexcitability*. J Clin Oncol, 2002. **20**(7): p. 1767-74.
222. McWhinney, S.R., Goldberg, R.M, and McLeod, H.L, *Platinum neurotoxicity pharmacogenetics*. Mol Cancer Ther, 2009. **8**(1): p. 10-6.
223. Pasetto, L.M., et al., *Oxaliplatin-related neurotoxicity: how and why?* Crit Rev Oncol Hematol, 2006. **59**(2): p. 159-68.
234. Newton, H.B., *Neurological complications of chemotherapy to the central nervous system*. Handb Clin Neurol, 2012. **105**: p. 903-16.
235. Muto, O., et al., *Reduction of oxaliplatin-related neurotoxicity by calcium and magnesium infusions*. Gan To Kagaku Ryoho, 2007. **34**(4): p. 579-81.
236. De Grandis, D., *Acetyl-L-carnitine for the treatment of chemotherapy-induced peripheral neuropathy: a short review*. CNS Drugs, 2007. **21**(1): p. 39-43; discussion 45-6.
237. Contreras, P.C., et al., *Insulin-like growth factor-I prevents development of a vincristine neuropathy in mice*. Brain Res, 1997. **774**(1-2): p. 20-6.
238. Saif, M.W., *Oral Calcium Ameliorating Oxaliplatin-Induced Peripheral Neuropathy*. J Appl Res, 2004. **4**(4): p. 576-582.
239. Kurniali, P.C., Luo, L.G and Weitberg, A.B, *Role of calcium/magnesium infusion in oxaliplatin-based chemotherapy for colorectal cancer patients*. Oncology (Williston Park), 2010. **24**(3): p. 289-92.
240. Wolf, S., et al., *Chemotherapy-induced peripheral neuropathy: prevention and treatment strategies*. Eur J Cancer, 2008. **44**(11): p. 1507-15.

241. Pace, A., Bove, L and Jandolo, B, *Vitamin E for prophylaxis against chemotherapy-induced neuropathy: a randomized controlled trial*. *Neurology*, 2005. **65**(3): p. 501-2; author reply 501-2.
242. White, H.S., *Comparative anticonvulsant and mechanistic profile of the established and newer antiepileptic drugs*. *Epilepsia*, 1999. **40**(5): p. S2-10.
245. Apfel, S.C., et al., *Nerve growth factor prevents experimental cisplatin neuropathy*. *Ann Neurol*, 1992. **31**(1): p. 76-80.
246. Jaggi, A.S. and Singh, N, *Mechanisms in cancer-chemotherapeutic drugs-induced peripheral neuropathy*. *Toxicology*, 2012. **291**(1-3): p. 1-9.
247. Khakoo, A.Y., et al., *Cardiotoxicity due to cancer therapy*. *Tex Heart Inst J*, 2011. **38**(3): p. 253-6.
248. Geisberg, C.A. and Sawyer, D.B, *Mechanisms of anthracycline cardiotoxicity and strategies to decrease cardiac damage*. *Curr Hypertens Rep*, 2010. **12**(6): p. 404-10.
249. Zhang, J., et al., *Status of bi- and multi-nuclear platinum anticancer drug development*. *Anticancer Agents Med Chem*, 2010. **10**(4): p. 272-82.
250. Basu B, K.S., *Cellular responses to cisplatin-induced dNA damage*. *Journal of Nucleic Acids*, 2010. 2010: p. 16.
251. McWhinney, S.R., Goldberg, R.M and McLeod, H.L, *Platinum neurotoxicity pharmacogenetics*. *Mol Cancer Ther*, 2009. **8**(1): p. 10-6.
252. Wheate, N.J., et al., *The status of platinum anticancer drugs in the clinic and in clinical trials*. *Dalton Trans*, 2010. **39**(35): p. 8113-27.
253. Hartmann, J.T. and Lipp, H.P, *Toxicity of platinum compounds*. *Expert Opin Pharmacother*, 2003. **4**(6): p. 889-901.
254. Carozzi, V.a, Canta, A., Chiorazzi, A., and Cavaletti, G. *Chemotherapy-induced peripheral neuropathy: What do we know about mechanisms?*. *Neurotic Lett*. 2014. **22**(15): p.10-16
255. McDonald, E.S., Randon, K.R., Knight, A., and Windebank, A.J. *Cisplatin preferentially binds to DNA in dorsal root ganglion neurons in vitro and in vivo: a potential mechanism for neurotoxicity*. *Neurobiol. Dis*. 2005. **18**: p. 305-313.
256. Ciarimboli, G., *Membrane transporters as mediators of cisplatin effects and side effects*. *scientific*. 2012. p: 473-479.

257. Lauria, G., et al. *Alpha-lipoic acid prevents mitochondrial damage and neurotoxicity in experimental chemotherapy neuropathy*. 2008. *Exp. Neurol.* 214. p:276-284
258. Kagiava, A., Kosmidis, E.K and Theopohilidis, G, *Oxaliplatin-induced hyperexcitation of rat sciatic nerve fibers: an intra-axonal study*. *Anticancer Agents Med Chem*, 2013. **13**(2): p. 373-9.
259. Vincent, A., et al. *Oxaliplatin induces hyperexcitability at motor and autonomic neuromuscular junctions through effects on voltage-gated sodium channels*. *Br J Pharmacol*. 2005. **146**(7): p. 1027-39.
260. Khan, S., et al. *A neuroinformatics study describing molecular interaction of cisplatin with acetylcholinesterase: a plausible cause for anticancer drug induced neurotoxicity*. *CNS Neurol Disord Drug Targets*. 2014. **13**(2): p. 265-70.
261. Novokmet et al. *Platinum complexes-induced cardiotoxicity of isolated, perfused rat heart: Comparisons of Pt(II) and Pt(IV) analogues versus cisplatin*. *Cardiovasc Toxicol*. 2014. (8): p. 2-9.
262. Radwan, A., et al. *Cisplatin-induced cardiotoxicity: Mechanisms and Cardioprotective Strategies*. *Eur J Pharmacol*. 2011. **650**(1): p. 335-41
263. Winer, E., et al., *Liposome encapsulated doxorubicin compared with conventional doxorubicin in a randomised multicenter trial as first-line therapy of metastatic breast carcinoma*. *Cancer*, 2002. **94**(1): p. 25-36
264. Liu., D., et al. *Comparison of safety and toxicity of liposomal doxorubicin vs. conventional anthracyclines: a meta-analysis*. *Exp Hematol Oncol*, 2012. **23**(1): p. 1-10
265. Boulikas, T., *Low toxicity and anticancer activity of a novel liposomal cisplatin (Lipoplatin) in mouse xenografts*. *Oncol Rep*, 2004. **12**(1): p. 3-12.
266. Wheate, N.J., *Improving platinum (II)-based anticancer drug delivery using cucurbit[n]urils*. *J Inorg Biochem*, 2008. **102**(12): p. 2060-6.
267. Boulikas, T., *Clinical overview on Lipoplatin: a successful liposomal formulation of cisplatin*. *Expert Opin Investig Drugs*, 2009. **18**(8): p. 1197-218.
268. Lin, C.C. and Metters, A.T, *Hydrogels in controlled release formulations: network design and mathematical modeling*. *Adv Drug Deliv Rev*, 2006. **58**(12-13): p. 1379-408.

269. Coviello, T., Matricardi, P and Alhaique, F, *Drug delivery strategies using polysaccharidic gels*. Expert Opin Drug Deliv, 2006. **3**(3): p. 395-404.
270. Chamberlain, M.C., *Treatment of newly diagnosed malignant glioma in the elderly people: new trials that impact therapy*. Int J Clin Pract, 2013. **67**(12): p. 1225-7.
271. Gong, C., et al., *Thermosensitive polymeric hydrogels as drug delivery systems*. Curr Med Chem, 2013. **20**(1): p. 79-94.
272. Nguyen, M.K. and Lee, D.S, *Injectable biodegradable hydrogels*. Macromol Biosci, 2010. **10**(6): p. 563-79.
273. Jeong, B., Kim, S.W and Bae, Y.H, *Thermosensitive sol-gel reversible hydrogels*. Adv Drug Deliv Rev, 2002. **54**(1): p. 37-51.
274. Jeong, B., et al., *Biodegradable block copolymers as injectable drug-delivery systems*. Nature, 1997. **388**(6645): p. 860-2.